การปรับปรุงสมบัติการไหลที่อุณหภูมิต่ำของไบโอดีเซลจากเมล็ดกระบก *Irvingia malayana* Oliv. ex A. Benn.

นางสาวดวงกมล ปาณเล็ก

วิทยานิพนธ์นี้เป็นส่วนหนึ่งของการศึกษาตามหลักสูตรปริญญาวิทยาศาสตรมหาบัณฑิต
สาขาวิชาปิโตรเคมีและวิทยาศาสตร์พอลิเมอร์
คณะวิทยาศาสตร์ จุฬาลงกรณ์มหาวิทยาลัย
ปีการศึกษา 2553

IMPROVING COLD FLOW PROPERTY OF BIODIESEL FROM *Irvingia malayana* Oliv. ex A. Benn. SEEDS

Miss Doungkamol Panlek

A Thesis Submitted in Partial Fulfillment of the Requirements
for the Degree of Master of Science Program in Petrochemistry and Polymer Science
Faculty of Science
Chulalongkorn University
Academic Year 2010

Thesis Title	IMPROVING COLD FLOW PROPERTY OF BIODIESEL FROM *Irvingia malayana* Oliv. ex A. Benn. SEEDS
By	Miss Doungkamol Panlek
Field of Study	Petrochemistry and Polymer Science
Thesis Advisor	Associate Professor Somchai Pengprecha, Ph.D.
Thesis Co-advisor	Kunn Kangvansaichol, Ph.D.

Accepted by the Faculty of Science, Chulalongkorn University in Partial Fulfillment of the Requirements for the Master's Degree

…………………………………………Dean of the Faculty of Science
(Professor Supot Hannongbua, Dr.rer.nat.)

THESIS COMMITTEE

…………………………………………Chairman
(Associate Professor Supawan Tantayanon, Ph.D.)

…………………………………………Thesis Advisor
(Associate Professor Somchai Pengprecha, Ph.D.)

…………………………………………Thesis Co-advisor
(Kunn Kangvansaichol, Ph.D.)

…………………………………………Examiner
(Associate Professor Wimonrat Trakarnpruk, Ph.D.)

…………………………………………External Examiner
(Suchada Butnark, Ph.D.)

ดวงกมล ปาณเล็ก : การปรับปรุงสมบัติการไหลที่อุณหภูมิต่ำของไบโอดีเซลจากเมล็ดกระบก *Irvingia malayana* Oliv. ex A. Benn. (IMPROVING COLD FLOW PROPERTY OF BIODIESEL FROM *Irvingia malayana* Oliv. ex A. Benn. SEEDS) อ.ที่ปรึกษาวิทยานิพนธ์หลัก : รศ.ดร.สมใจ เพ็งปรีชา, อ.ที่ปรึกษาวิทยานิพนธ์ร่วม : ดร.กันย์ กังวานสายชล, 95 หน้า.

งานวิจัยนี้มีจุดมุ่งหมายเพื่อปรับปรุงสมบัติการไหลที่อุณหภูมิต่ำของไบโอดีเซลจากเมล็ดกระบก *Irvingia malayana* Oliv. ex A. Benn. (IM) โดยใช้สารลดจุดไหลเท (PPDs) สังเคราะห์ 4 ชนิด ซึ่งคือ เมทิลลอเรท (ML) เมทิลสเตียเรท (MS) ไอโซโพรพิลลอเรท (IPL) และไอโซโพรพิลสเตียเรท (IPS) และสารเติมแต่งเชิงพาณิชย์ 5 ชนิด ซึ่งคือ CD017, Zenith, Flozol 2251D, Flozol 112 และเคโรซีน ในกลุ่มของสารเติมแต่งเหล่านี้ IPL ให้ผลดีที่สุดในการปรับปรุงสมบัติการไหลที่อุณหภูมิต่ำของไบโอดีเซลจากน้ำมันกระบก (IMME) ซึ่งที่ 500,000 ppm ของ IPL จุดขุ่น (CP) และจุดไหลเท (PP) ของ IMME ลดลง 8.70±1.0 องศาเซลเซียสและ 9.0±1.0 องศาเซลเซียส ตามลำดับ นอกจากนี้ประเภทของสายโซ่ไฮโดรคาร์บอนยังส่งผลต่อสมบัติการไหลที่อุณหภูมิต่ำ ที่ความเข้มข้นเดียวกันของ IPL กับ ML พบว่า แอลกอฮอล์สายโซ่กิ่งให้ผลที่ดีที่สุดต่อการปรับปรุงสมบัติการไหลที่อุณหภูมิต่ำ โดยลดจุดขุ่นและจุดไหลเทของ IMME ได้ 1.55±1.0 องศาเซลเซียส (17.82 เปอร์เซ็นต์) และ 4.0±1.0 องศาเซลเซียส (44.44 เปอร์เซ็นต์) ตามลำดับ ในทางตรงข้ามสมบัติการไหลที่อุณหภูมิต่ำของ IMME ไม่สามารถปรับปรุงโดยใช้ MS และ IPS เนื่องจาก MS และ IPS มีน้ำหนักโมเลกุลสูงกว่า IMME สำหรับสารเติมแต่งเชิงพาณิชย์ เคโรซีนให้ผลดีที่สุดในการลด CP และ PP ของ IMME

สาขาวิชา ปิโตรเคมีและวิทยาศาสตร์พอลิเมอร์ ลายมือชื่อนิสิต..
ปีการศึกษา.............2553.............ลายมือชื่อ อ.ที่ปรึกษาวิทยานิพนธ์หลัก.............
ลายมือชื่อ อ.ที่ปรึกษาวิทยานิพนธ์ร่วม.............

5172289423 : MAJOR PETROCHEMISTRY AND POLYMER SCIENCE
KEYWORDS : BIODIESEL / *Irvingia malayana* Oliv. ex A. Benn. / CLOUD POINT / POUR POINT

DOUNGKAMOL PANLEK: IMPROVING COLD FLOW PROPERTY OF BIODIESEL FROM *Irvingia malayana* Oliv. ex A. Benn. SEEDS. ADVISOR: ASSOC. PROF. SOMCHAI PENGPRECHA, Ph.D., CO-ADVISOR: KUNN KANGVANSAICHOL, Ph.D., 95 pp.

This research aimed to improve the cold flow property of biodiesel from *Irvingia malayana* Oliv. ex A. Benn. (IM) seeds by using four synthesized Pour Point Depressant (PPDs) which were methyl laurate (ML), methyl stearate (MS), *i*-propyl laurate (IPL) and *i*-propyl stearate (IPS) and five commercial additives which were CD017, Zenith, Flozol 2251D, Flozol 112 and kerosene. Among of these additives, IPL gave the best result on improving cold flow property of biodiesel from IM oil (IMME), at which 500,000 ppm of IPL, cloud point (CP) and pour point (PP) of IMME were reduced by 8.70±1.0°C and 9.0±1.0°C, respectively. In addition, the cold flow property could be effected by the types of hydrocarbon chain. At the same concentration of IPL and ML, the branched chain alcohol gave the best result on improving cold flow property by which the CP and PP of IMME were reduced by 1.55±1.0°C (17.82%) and 4.0±1.0°C (44.44%), respectively. On the other hand, the cold flow property of IMME could not be improved by using MS and IPS because of the molecular weight of MS and IPS were higher than that of IMME. For commercial additives, kerosene gave the best result on reducing CP and PP of IMME.

Field of Study : Petrochemistry and Polymer Science Student's Signature........................
Academic Year : 2010 Advisor's Signature……………....
Co-advisor's Signature...................

ACKNOWLEDGEMENTS

I would like to express my deepest appreciation and gratitude to my advisor, Associate Professor Dr. Somchai Pengprecha, and co-advisor, Dr. Kunn Kangvansaichol, for their excellent suggestion, guidance, encouragement and supportiveness throughout the entire period of conducting this thesis. I would also like to extend to Associate Professor Dr. Supawan Tantayanon, Associate Professor Dr. Wimonrat Trakarnpruk and Dr. Suchada Butnark attending as the chairman and members of my thesis committee, respectively, for their kind guidance and valuable suggestions and comments throughout my study.

I thank Center for Petroleum, Petrochemicals, and Advanced Materials and Graduate School of Chulalongkorn University for partial financial support to conduct this research.

Additionally, I would like to thank Excise Department for testing the cold flow property of biodiesel and Miss Budsaya Sriwichan, Mr. Sumetha Issariyanate, Mr. Methawaj Rungsiriworapong, Miss Nisakorn Saengprachum, Miss Piyathida Ruksayot and Miss Kulwadee Kaewprapan in Research Centre for Bioorganic Chemistry for their suggestion, helping and teaching me the experimental techniques throughout this work.

Finally, I would like to express thanks to my family for their care and supports to make my study successful. Thanks are also due to everyone who has contributed suggestions and supports throughout my research.

CONTENTS

Page

ABSTRACT (THAI) iv
ABSTRACT (ENGLISH) v
ACKNOWLEDGEMENTS vi
CONTENTS vii
LIST OF TABLES xi
LIST OF FIGURES xiii
LIST OF ABBREVIATIONS xv

CHAPTER I INTRODUCTION 1
- 1.1 Objectives of the research 2

CHAPTER II THEORY AND LITERATURE REVIEWS 3
- 2.1 Background 3
- 2.2 Vegetable oil chemistry 4
- 2.3 Biodiesel production 8
  - 2.3.1 Direct use and blending 8
  - 2.3.2. Micro-emulsions 8
  - 2.3.3 Pyrolysis 9
  - 2.3.4 Transesterification 9
    - 2.3.4.1 Transesterification kinetics and mechanism 10
- 2.4 Sources of biodiesel 12
  - 2.4.1 *Irvingia malayana* Oliv. ex A. Benn. (IM) 12
- 2.5 Type of catalysts in transesterification 13
  - 2.5.1 Acid-catalyzed processes 13
  - 2.5.2 Alkaline-catalyzed processes 14
  - 2.5.3 Enzyme-catalyzed processes 15
  - 2.5.4 Non-ionic based-catalyzed processes 16
  - 2.5.5 Heterogeneously catalyzed processes 16
  - 2.5.6 Noncatalytic transesterification processes 17

Page

2.6 Transesterification parameters 17
  2.6.1 Moisture content and free fatty acid 17
  2.6.2 Molar ratio of alcohol to oil 18
  2.6.3 Catalyst 18
  2.6.4 Reaction time 18
  2.6.5 Reaction temperature 19
2.7 Biodiesel quality 19
2.8 Cold flow property 22
  2.8.1 The improvement of cold flow property 23
2.9 Pour Point Depressants (PPDs) 24
2.10 Literature reviews 26

CHAPTER III EXPERIMENTAL 29
3.1 Materials and equipments 29
  3.1.1 Raw materials 29
  3.1.2 Chemicals 29
  3.1.3 Equipments 30
3.2 Methods 30
  3.2.1 Solvent extraction of *Irvingia malayana* Oliv. ex A. Benn. (IM) seeds 30
  3.2.2 Determination of properties of IM oil 31
  3.2.3 Synthesis of methyl ester of IM oil (IMME) 31
  3.2.4 Synthesis of Pour Point Depressants (PPDs) 31
    3.2.4.1 Synthesis of methyl laurate and methyl stearate as PPDs 31
    3.2.4.2 Synthesis of *i*-propyl laurate and *i*-propyl stearate as PPDs 32
  3.2.5 Characterization of commercial additives 32
  3.2.6 Determination of cloud point (CP) and pour point (PP) 32
  3.2.7 Characterization and determination of the methyl ester 33
    3.2.7.1 Ester content of IMME 33

Page

3.2.7.1.1 Fourier-Transform NMR spectrometer (FT-NMR) 33
3.2.7.1.2 Gas Chromatography (GC) 33
3.2.7.2 Determination of fatty acid compositions of IMME and PME 33
3.2.7.3 Determination of the properties of IMME and PME 34

CHAPTER IV RESULTS AND DISCUSSION 35
4.1 Solvent extraction of *Irvingia malayana* Oliv. ex A. Benn. (IM) seeds 35
4.2 Determination of properties of IM oil 35
4.3 Synthesis of methyl ester of IM oil (IMME) 35
4.4 Characterization and determination of the methyl ester 36
4.4.1 Ester content of IMME 36
4.4.2 Determination of fatty acid compositions of IMME and PME 36
4.4.3 Determination of the properties of IMME and PME 37
4.5 Synthesis of Pour Point Depressants (PPDs) 38
4.5.1 Synthesis of methyl laurate (ML), methyl stearate (MS), *i*-propyl laurate (IPL) and *i*-propyl stearate (IPS) as PPDs 38
4.5.2 Characterization of commercial additives 39
4.5.2.1 Fourier-Transform Infrared Spectroscopy (FT-IR) 39
4.6 Improvement the cold flow property of methyl ester 41
4.6.1 Using methyl laurate (ML) as PPDs 41
4.6.2 Using methyl stearate (MS) as PPDs 43
4.6.3 Using *i*-propyl laurate (IPL) as PPDs 44
4.6.4 Using *i*-propyl stearate (IPS) as PPDs 45
4.6.5 Using CD017 as PPDs 47
4.6.6 Using Zenith as PPDs 49
4.6.7 Using Flozol 2251D as PPDs 51
4.6.8 Using Flozol 112 as PPDs 52

Page

4.6.9 Using kerosene as PPDs 53

V CONCLUSION AND SUGGESTION 56
5.1 Conclusion 56
5.2 Suggestion 57

REFERENCES 58

APPENDICES 62
Appendix A 63
Appendix B 73
Appendix C 83

VITA 95

LIST OF TABLES

Table **Page**

2.1 Chemical structure of common fatty acids 5
2.2 Chemical composition of vegetable oils 5
2.3 Physical and thermal properties of vegetable oils 6
2.4 Problems and potential solutions for using vegetable oils as engine fuels 7
2.5 Comparison of fuel properties between diesel and biodiesel 20
2.6 Characteristic and quality of biodiesel (methyl ester of fatty acids) in Thailand 21
3.1 Test methods of methyl ester 34
4.1 Comparison of fatty acid compositions of IMME and PME 37
4.2 Some specification for quality of methyl ester 38
4.3 The appearance, percent conversion, percent product yield, acid value and viscosity at 40°C of PPDs 38
4.4 The absorption assignments of commercial additives 39
4.5 Cloud point (CP) and pour point (PP) of IMME, PME and PPDs 40
B1 Values of CP and PP of IMME using ML as PPDs 74
B2 Values of CP and PP of PME using ML as PPDs 74
B3 Values of CP and PP of IMME using MS as PPDs 75
B4 Values of CP and PP of PME using MS as PPDs 75
B5 Values of CP and PP of IMME using IPL as PPDs 76
B6 Values of CP and PP of PME using IPL as PPDs 76
B7 Values of CP and PP of IMME using IPS as PPDs 77
B8 Values of CP and PP of PME using IPS as PPDs 77
B9 Values of CP and PP of IMME using CD017 as PPDs 78
B10 Values of CP and PP of PME using CD017 as PPDs 78
B11 Values of CP and PP of diesel fuel using CD017 as PPDs 78
B12 Values of CP and PP of IMME using Zenith as PPDs 79
B13 Values of CP and PP of PME using Zenith as PPDs 79
B14 Values of CP and PP of diesel fuel using Zenith as PPDs 79

Table **Page**

B15 Values of CP and PP of IMME using Flozol 2251D as PPDs 80
B16 Values of CP and PP of PME using Flozol 2251D as PPDs 80
B17 Values of CP and PP of diesel fuel using Flozol 2251D as PPDs 80
B18 Values of CP and PP of IMME using Flozol 112 as PPDs 81
B19 Values of CP and PP of PME using Flozol 112 as PPDs 81
B20 Values of CP and PP of diesel fuel using Flozol 112 as PPDs 81
B21 Values of CP and PP of IMME using kerosene as PPDs 82
B22 Values of CP and PP of PME using kerosene as PPDs 82
C1 Value of free fatty acid containing in IM oil 91
C2 Saponification number of IM oil 92
C3 Iodine value of IM oil 93
C4 Acid values of IMME, PME and PPDs 94

LIST OF FIGURES

Figure **Page**

2.1 Structure of a triglyceride 4
2.2 Equation for transesterification of vegetable oils 10
2.3 The overall reaction of transesterification 11
2.4 Mechanism of acid-catalyzed transesterification of vegetable oils 14
2.5 Mechanism of alkaline-catalyzed transesterification of vegetable oils 15
2.6 Molecular structures of some non-ionic organic bases 16
2.7 Characteristic structure of the general PPDs polymer additive 25
4.1 TLC of methyl ester of IM oil (IMME) using a mixture of hexane, ethyl acetate and acetic acid (90:10:1 %v/v) as mobile phase 36
4.2 CP and PP of IMME with various concentrations of ML 42
4.3 CP and PP of PME with various concentrations of ML 42
4.4 CP and PP of IMME with various concentrations of MS 43
4.5 CP and PP of PME with various concentrations of MS 44
4.6 CP and PP of IMME with various concentrations of IPL 45
4.7 CP and PP of PME with various concentrations of IPL 45
4.8 CP and PP of IMME with various concentrations of IPS 46
4.9 CP and PP of PME with various concentrations of IPS 47
4.10 CP and PP of IMME with various concentrations of CD017 48
4.11 CP and PP of PME with various concentrations of CD017 48
4.12 CP and PP of diesel fuel with various concentrations of CD017 49
4.13 CP and PP of IMME with various concentrations of Zenith 49
4.14 CP and PP of PME with various concentrations of Zenith 50
4.15 CP and PP of diesel fuel with various concentrations of Zenith 50
4.16 CP and PP of IMME with various concentrations of Flozol 2251D 51
4.17 CP and PP of PME with various concentrations of Flozol 2251D 51
4.18 CP and PP of diesel fuel with various concentrations of Flozol 2251D 52
4.19 CP and PP of IMME with various concentrations of Flozol 112 52
4.20 CP and PP of PME with various concentrations of Flozol 112 53
4.21 CP and PP of diesel fuel with various concentrations of Flozol 112 53

Figure **Page**

4.22 CP and PP of IMME with various concentrations of kerosene 54

4.23 CP and PP of PME with various concentrations of kerosene 54

A1 ^{1}H-NMR spectrum of IM oil 64

A2 ^{1}H-NMR spectrum of IMME 64

A3 ^{1}H-NMR spectrum of ML 65

A4 ^{1}H-NMR spectrum of MS 65

A5 ^{1}H-NMR spectrum of IPL 66

A6 ^{1}H-NMR spectrum of IPS 66

A7 GC chromatogram of 37 FAMEs standard 67

A8 GC chromatogram of IMME 68

A9 GC chromatogram of PME 69

A10 IR spectrum of CD017 70

A11 IR spectrum of Zenith 70

A12 IR spectrum of Flozol 2251D 71

A13 IR spectrum of Flozol 112 71

A14 IR spectrum of kerosene 72

LIST OF ABBREVIATIONS

µl	microliter
µm	micrometer
ASTM	American Standard Test Method
$^{\circ}$C	Degree Celsius
cSt	Centistroke
$^{\circ}$F	Degree
FFA	Free fatty acid
FT-IR	Fourier Transform Infrared Spectroscopy
g	gram
GC	Gas Chromatography
h	hour
NMR	Nuclear Magnetic Resonance Spectroscopy
kg/cm^3	Kilogram per cubic metre
L	Liter
MJ/kg	Millijule per kilogram
min	Minute
mg	Miligram
ml	Milliter
mm	Millimeter
nm	Nanometer
ppm	parts per million
rpm	Revolution per minute
v/v	Volume by volume
w/v	Weight by volume
%wt	percent weight
δ_H	Chemical shift of ^{1}H NMR
CP	Cloud point
IM	*Irvingia malayana* Oliv. ex A. Benn.
IMME	Methyl ester of IM oil
IPL	*i*-propyl laurate
IPS	*i*-propyl stearate

ML	Methyl laurate
MS	Methyl stearate
NaOH	Sodium hydroxide
PME	Methyl ester of palm oil
PP	Pour point
PPDs	Pour Point Depressants

CHAPTER I

INTRODUCTION

Currently, a renewable and environmentally friendly alternative fuel such as biodiesel becomes more attractive due to the contrasts between the increase in world energy requirements and the decrease in petroleum sources. Biodiesel (fatty acid alkyl esters) is typically obtained from transesterification of vegetable oils or animal fats which comprise of triglycerides reacted with an excess alcohol, usually methanol, in the presence of an alkaline catalyst [1]. It has several advantages over petroleum-based diesel because it is biodegradability, improved lubricity, reduced toxicity, lower emissions and it also has a higher flash point [2]. However, there are some significant drawbacks that have limited its application. One of the major problems is unfavorable cold flow properties since it begins to gel at low temperature. The crystallization or thickening of biodiesel at low temperature causes operability problems as solidified materials which can clog fuel lines and filters, mainly due to its high amount of saturated fatty acid alkyl ester components [3].

Irvingia malayana Oliv. ex A. Benn. (IM), known as “krabok” which is available in all regions of Thailand and Southeast Asia. IM oil mainly contains saturated fatty acid especially 42% of lauric acid (C12:0) and 41.8% of myristic acid (C14:0) [4]. These saturated fatty compounds display higher cloud point (CP) and pour point (PP) leading to crystallization at low temperature. The CP is the temperature at which a liquid fatty material becomes cloudy due to formation of crystal and solidification of saturated fatty acid. The PP is the lowest temperature that fluid will flow under standard conditions [5].

To improve the cold flow property of biodiesel, Pour Point Depressants (PPDs) are wildly used as the chemical additives in the industrials because they are designed to control wax crystal formation in oil resulting in lower PP and improved low temperature flow performance [6].

1.1 Objectives of the research:

1. To study the chemical composition of extracted oil from *Irvingia malayana* Oliv. ex A. Benn. (IM) seeds.
2. To synthesize and determine the biodiesel properties according to the specifications of ASTM standards.
3. To study improvement the cold flow property of biodiesel by Pour Point Depressants (PPDs).

CHAPTER II

THEORY AND LITERATURE REVIEWS

2.1 Background

Over the past twenty years, Thailand has had one of the fastest growing economies in the world. The demand for energy was also increased because of the industrial expansion. In 2006, imported energy was increased 16% year on year to a total US$ 21.5 billion. Rising global fuel prices in combination with rising domestic demand led to a 92% increase in the cost of imported refined fuel from 2004-2005. Depend on its massive agricultural base, alternative energy such as biodiesel will play an increasingly important role in Thailand's domestic energy supplies. The government has a target of 4.25 million litres/day of biodiesel, for a 7% consumption substitute of diesel by the year 2011. Palm oil, one of the most readily available inputs for biodiesel production can be found in abundant quantities in Thailand. Its cultivation can produce 5,800 liters of the fuel per hectare (US 580 gallons/acre), making agricultural cultivation of biodiesel incredibly efficient. And, the government is promoting palm oil cultivation to reach 400,000 hectares by 2012 [7].

Biodiesel, a clean-burning alternative fuel, is produced from renewable resources making it biodegradable, nontoxic and essentially free of sulfur and aromatics. Biodiesel is defined as mono-alkyl esters of long chain fatty acids derived from vegetable oils (e.g., soybean, cottonseed, palm, peanut, rapeseed, sunflower, coconut) or animal fats (usually tallow) as well as waste oils (e.g., used frying oils). Depending on the origin and quality of the feedstock, changes to the production process may be necessary. Biodiesel is miscible with petrodiesel in all ratios so it can be blended at any level with petroleum-based diesel or can be used one hundred percent biodiesel with little or no modifications [8].

Biodiesel has several distinct advantages compared with petroleum-based diesel because it was derived from a renewable domestic resource. It can be reduced most exhaust emissions (with the exception of nitrogen oxides, NO_x) and it also has a higher flash point, leading to safer handling and storage. Furthermore, adding biodiesel at low levels (1–2%) can restore the lubricity with the fact that is steadily gaining importance with the advent of low-sulfur petroleum diesel, which have greatly reduced lubricity [9]. However, Biodiesel also has disadvantages because it has storage problems (due to it is biodegradable) and less oxidatively stable than petroleum diesel fuel, hence, old fuel can become acidic and form sediments and varnish. It can cause filter plugging (at low temps, due to polymers, fuel tank deposits, other contaminants). In addition to their feedstock prices, production and processing cost still more expensive than petroleum diesel [10].

2.2 Vegetable oil chemistry

Chemical structure of oils/fats consist of triglyceride molecules of three long chain fatty acids that are ester bonded to a single glycerol molecule. These fatty acids differ by the length of carbon chains, the number, orientation and position of double bonds in these chains as shown in Figure 2.1.

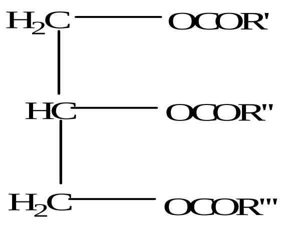

Figure 2.1 Structure of a triglyceride.

Table 2.1 Chemical structure of common fatty acids. [11]

Fatty acid	Systermatic name	Structure	Formular
Lauric	Dodecanoic	12:0	$C_{12}H_{24}O_2$
Myristic	Tetradecanoic	14:0	$C_{14}H_{28}O_2$
Palmitic	Hexadecanoic	16:0	$C_{16}H_{32}O_2$
Stearic	Octadecanoic	18:0	$C_{18}H_{36}O_2$
Arachidic	Eicosanoic	20:0	$C_{20}H_{40}O_2$
Behenic	Docosanoic	22:0	$C_{22}H_{44}O_2$
Lignoceric	Tetracosanoic	24:0	$C_{24}H_{48}O_2$
Oleic	cis-9-Octadecenoic	18:1	$C_{18}H_{34}O_2$
Linoleic	cis-9,cis-12Octadecadienoic	18:2	$C_{18}H_{32}O_2$
Linolenic	cis-9,cis-12,cis-15-Octadecatrienoic	18:3	$C_{18}H_{30}O_2$
Erucic	cis-13-Docosenoic	22:1	$C_{22}H_{42}O_2$

where R’, R’’ and R’’’ represent hydrocarbon chain of fatty acids. Fatty acids vary in carbon chain length and in the number of unsaturated bonds (double bonds). The structures of common fatty acids are given in Table 2.1, and fatty acid compositions of some vegetable oils are given in Table 2.2.

Table 2.2 Chemical composition of vegetable oils. [11]

Vegetable oil	Fatty acid composition (%wt)									
	C14:0	C16:0	C18:0	C20:0	C22:0	C24:0	C18:1	C22:1	C18:2	C18:3
Corn	0	12	2	*Tr*[*]	0	0	25	0	6	*Tr*[*]
Cottonseed	0	28	1	0	0	0	13	0	58	0
Peanut	0	11	2	1	2	1	48	0	32	1
Rapeseed	0	3	1	0	0	0	64	0	22	8
Safflower	0	9	2	0	0	0	12	0	78	0
Soya bean	0	12	3	0	0	0	23	0	55	6
Rice-bran	0.4-0.6	11.7-16.5	1.7-2.5	0.4-0.6	—	0.4-0.9	39.2-43.7	—	26.4-35.1	—
Mahua	—	16-28.2	20-25.1	0.0-3.3	—	—	41.0-51.0	—	8.9-13.7	—
Neem	0.2-0.26	13.6-16.2	14.4-24.1	0.8-3.4	—	—	49.1-61.9	—	2.3-15.8	—
Karanja	—	3.7-7.9	2.4-8.9	—	—	1.1-3.5	44.5-71.3	—	10.8-18.3	—

[*] *Tr : Trace*

Vegetable oils having 10% less heating value than diesel due to the oxygen content in the molecule. In addition, the viscosity of mineral diesel is several times lower than that of vegetable oil due to large molecular weight and complex chemical structure in vegetable oil. The fuel related properties (physical and thermal) of some of the vegetable oils are listed in Table 2.3.

Table 2.3 Physical and thermal properties of vegetable oils. [11]

Vegetable oil	Kinematic viscosity	Cetane number	Heating value (MJ/kg)	Cloud point (°C)	Pour point (°C)	Flash point (°C)	Density (Kg/l)	Carbon residue (wt%)	Ash (wt%)
Corn	34.9	37.6	39.5	−1.1	−40.0	277	0.9095	0.24	0.01
Cotton seed	33.5	41.8	39.5	1.7	−15.0	234	0.9148	0.24	0.01
Cramble	53.6	44.6	40.5	10.0	−12.2	274	0.9044	0.23	0.05
Linseed	22.2	34.6	39.3	1.7	−15.0	241	0.9236	0.22	<0.01
Peanut	39.6	41.8	49.8	12.8	−6.7	271	0.9026	0.24	0.005
Rapeseed	37.0	37.6	39.7	−3.9	−31.7	246	0.9115	0.30	0.054
Safflower	31.3	41.3	39.5	18.3	−6.7	260	0.9114	0.25	0.006
Sesame	35.5	40.2	39.3	−3.9	−9.4	260	0.9133	0.25	<0.01
Soyabean	32.6	37.9	39.6	−3.9	−12.2	254	0.9138	0.27	<0.01
Sunflower	33.9	37.1	39.6	7.2	−15.0	274	0.9161	0.23	<0.01
Palm	39.6	42.0	—	31.0	—	267	0.9180	—	—
Tallow	—	—	40.0	—	—	201	—	6.21	—

Vegetable oils have high viscosity, 35–60 cSt compared to 4 cSt for diesel at 40°C, leads to problem in pumping and spray characteristics. The inefficient mixing of oil with air contributes to incomplete combustion. High flash point attributes to its lower volatility characteristics. This results in high carbon deposit formation, injector coking, piston ring sticking and lubrication oil dilution and oil degradation. The combination of high viscosity and low volatility of vegetable oils cause poor cold starting, misfire and ignition delay.

In Table 2.4 shows probable reasons and potential solutions of the short- and long-term problems associated with utilization of vegetable oils in engine. Polyunsaturated natures of the vegetable oils cause long-term problems such as gum formation, ring sticking etc. Because of these problems, vegetable oils must be chemically modified to a more suitable and compatible fuel for existing engines.

Table 2.4 Problems and potential solutions for using vegetable oils as engine fuels. [11]

Problem	Probable cause	Potential solution
Short-term		
1. Cold weather starting	High viscosity, low cetane, and low flash point of vegetable oils	Preheat fuel prior to injection. Chemically alter fuel to an ester
2. Plugging and gumming of filters, lines and injectors	Natural gums (phosphatides) in vegetable oil	Partially refine the oil to remove gums. Filter to 4 microns
3. Engine knocking	Very low cetane of some oils. Improper injection timing	Adjust injection timing. Preheat fuel prior to injection. Chemically alter fuel to an ester
Long-term		
4. Coking of injectors and carbon deposits on piston and head of engine	High viscosity of vegetable oil, incomplete combustion of fuel. Poor combustion at part load.	Heat fuel prior to injection. Switch engine to diesel when operating at part load. Chemically alter the vegetable oil to an ester
5. Excessive engine wear	High viscosity, incomplete combustion of fuel. Poor combustion at part load. Possibly free fatty acids in vegetable oil. Dilution of engine lubricating oil due to blow-by of vegetable oil.	Heat fuel prior to injection. Switch engine to diesel when operating at part load. Chemically alter the vegetable oil to an ester. Increase lubricating oil changes. Lubricating oil additives to inhibit oxidation.
6. Failure of engine lubricating oil due to polymerization	Collection of poly-unsaturated vegetable oil blow-by in crank-case to the point where polymerization occurs	Same as in 5.

2.3 Biodiesel production [12-14]

Due to vegetable oils are not suitable as fuel for diesel engines; hence they have to be modified to bring their combustion-related properties closer to those of mineral diesel. To diminish the flow and combustion problems, the fuel is modified for reducing its viscosity. Production of biodiesel can be performed four different ways:

- Direct use and blending
- Micro-emulsion
- Pyrolysis (Thermal cracking)
- Transesterification

2.3.1 Direct use and blending

In 1980, Caterpillar (Brazil) used the mixture of 10% vegetable oil to maintain total power without any alterations or adjustments to the engine. At that point, it was not practical to substitute 100% vegetable oil for diesel fuel, but a blend of 20% vegetable oil and 80% mineral diesel was successful. Pramanik et al. [15] found that 50% blend of Jatropha oil can be used in diesel engine without any major operational difficulties but further study is required for the long-term durability of the engine. Direct use of vegetable oils or the use of blends of the oils has generally been considered to be not satisfactory and impractical for both direct and indirect diesel engines. The high viscosity, acid composition, combustion, carbon deposits and lubricating oil free fatty acid content, as well as gum formation due thickening are obvious problems.

2.3.2 Micro-emulsions

To solve the problem of the high viscosity of vegetable oils, micro-emulsions with solvents such as simple alcohols e.g., methanol, ethanol and 1-butanol have been investigated. They are defined as a colloidal equilibrium dispersion of optically isotropic fluid microstructures with dimension generally in the 1–150 nm, formed spontaneously from two normally immiscible liquids. They can improve spray characteristics by explosive vaporization of the low boiling constituents in the micelles. Short-term performance of micro-emulsions of aqueous ethanol in soybean oil was nearly as good as that of no. 2 diesel, in spite of the lower cetane number and energy content.

2.3.3 **Pyrolysis** [16]

Pyrolysis also known as thermal cracking is the conversion of one substance into another by heating in the absence of air or oxygen and cleavage of chemical bonds to yield small molecules with the aid of a catalyst. The pyrolyzed material can be vegetable oils, animal fats, natural fatty acids or methyl esters of fatty acids. The first pyrolysis of vegetable oil was conducted to synthesize petroleum from vegetable oil. Since World War I, many investigators have studied the pyrolysis of vegetable oils to obtain products suitable for fuel. However, the equipment for pyrolysis is expensive for modest throughputs. In addition, while the products are chemically similar to petroleum-derived gasoline and diesel fuel, the removal of oxygen during the thermal processing also removes any environmental benefits of using an oxygenated fuel. It produced some low value materials and, sometimes, more gasoline than diesel fuel.

2.3.4 **Transesterification** [11, 17, 18]

Transesterification, also called alcoholysis, is the most common way to produce biodiesel. In this reaction, triglyceride containing in vegetable oil or animal fat is reacted with an alcohol in the presence of a catalyst to produce fatty acid mono-alkyl esters and glycerol as by product [19-21]. The relation between alcohol and oil is 3:1. However, an excess of alcohol is usually more appropriate to improve the reaction towards the desired product. This process has been widely used to reduce the high viscosity of triglycerides. The transesterification reaction is represented by the equation as seen in Figure 2.2.

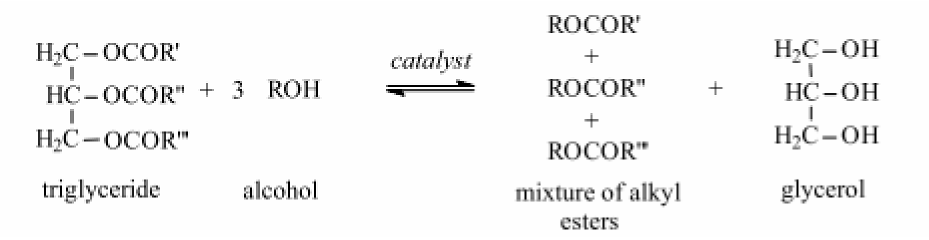

Figure 2.2 Equation for transesterification of vegetable oils.

After the reaction has been completed and glycerol has been removed by gravity settling or centrifugation, some impurities still remain in the fuel. These impurities are glycerol itself, soaps, catalyst, water, methanol, and mono-, di-, and triglycerides. In the usual industrial practice, the impurities are removed by washing with water. Packed washing towers, mixers-settlers, and centrifuges are commonly used with this purpose.

Alcohol that can be used in the transesterification process are methanol, ethanol, propanol, and butanol. Methanol and ethanol are used most frequently, especially methanol because of its low cost and its physical and chemical advantages (polar and shortest chain alcohol). Furthermore, it can quickly react with triglycerides. To complete a transesterification stoichiometrically, a 3:1 molar ratio of alcohol to triglycerides is needed. However, in practice, the ratio needs to be higher to drive the equilibrium to a maximum ester yield. On the other hand, an excessive amount of alcohol makes the recovery of the glycerol difficult, so that the ideal alcohol to oil ratio has to be established empirically, considering each individual process.

A catalyst is usually used to improve the reaction and yield transesterification. The reaction can be catalyzed by acids, alkalis, enzymes, non-ionic base and heterogeneous catalyst. Moreover, noncatalytic process was readily developed to transesterification without using any catalyst.

2.3.4.1 Transesterifcation kinetics and mechanism

Transesterification of triglycerides produce fatty acid alkyl esters and glycerol. The glycerol layer settles down at the bottom of the reaction vessel. Diglycerides and monoglycerides are the intermediates in this process. The mechanism of transesterification is described in Figure 2.3. The first step is the conversion of triglycerides to diglycerides followed by the conversion of diglycerides to monoglycerides and of monoglycerides to glycerol yielding one alkyl ester molecule from each glycerides at each step. The step wise reactions are reversible and a little excess of alcohol is used to shift the equilibrium towards the formation of esters. In presence of excess alcohol, the foreword reaction is pseudo-first order and the reverse reaction is found to be second order. The transesterification reaction can be catalyzed by both homogeneous and heterogeneous catalysts. In turn, the homogeneous catalysts include alkalis and acids. The most commonly used alkali catalysts are sodium hydroxide, sodium methoxide and potassium hydroxide. In this sense, numerous references can be found in the background literature. Sulfuric acid, hydrochloric acid and sulfonic acid are usually preferred as acid catalysts. Finally, the heterogeneous catalysts include enzymes, titanium silicates, alkaline earth metal compounds, anion exchange resins and guanadines heterogenized on organic polymers. The alkali-catalyzed transesterification is much faster than acid–catalyzed transesterification and is most often used commercially.

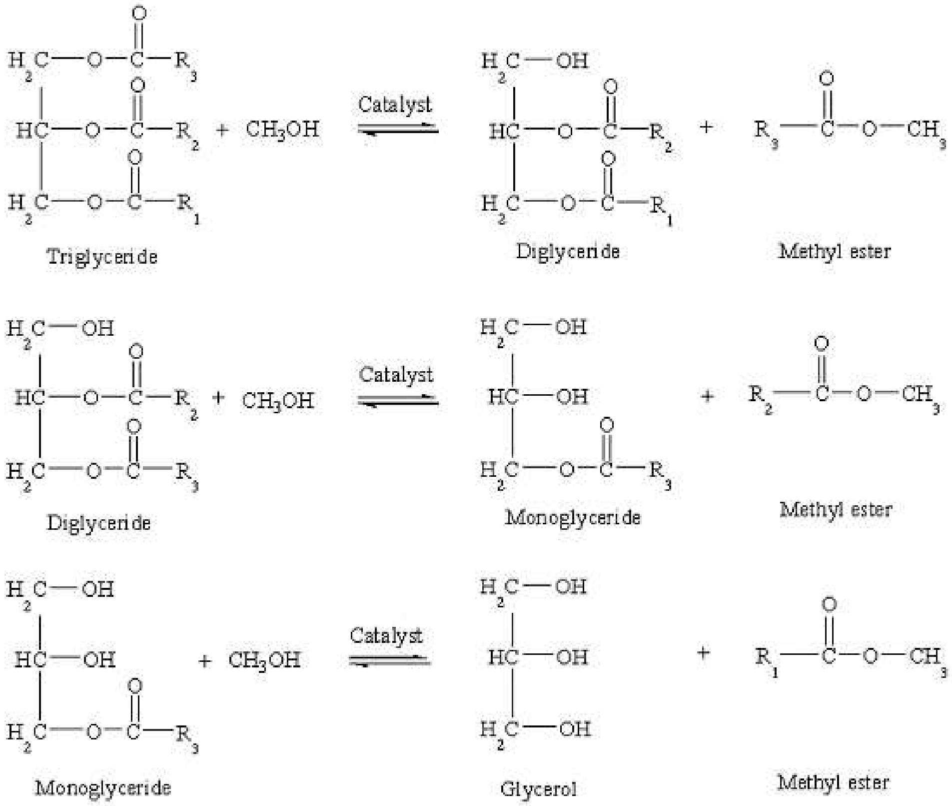

Figure 2.3 The overall reaction of transesterification.

2.4 Sources of biodiesel [22]

There are more than 350 oil-bearing crops identified, among which only soybean, palm, sunflower, safflower, cottonseed, rapeseed and peanut oils are considered as potential alternative fuels for diesel engines. Worldwide consumption of soybean oil is the highest in 2003 (27.9 million metric tons). Vegetable oil is one of the renewable fuels. Concerning about environmental benefits and the fact that these are made from renewable resources vegetable oils have become more attractive. Vegetable oils are a renewable and potentially inexhaustible source of energy with energy content close to diesel fuel. However, extensive use of vegetable oils may cause other significant problems such as starvation in developing countries. The vegetable oil fuels were more expensive than petroleum fuels so they were not acceptable.

In Malaysia and Indonesia palm oil is used as a significant biodiesel source. In Europe, rapeseed is the most common base oil used in biodiesel production. In India and Southeast Asia, the Jatropha tree is used as a significant fuel source. Soybeans are commonly used in the United States for food products which has led to soybean biodiesel becoming the primary source for biodiesel in this country.

2.4.1 *Irvingia malayana* Oliv. ex A. Benn. (IM) [4]

Irvingia malayana Oliv. ex A. Benn. (IM) seeds is produced in Thailand, Cambodia, Malaysia, Laos, Vietnam and Indonesia. This tree is known as the “pauh kijang”, which means “mango of the stags”. It is botanically classified in the family of *Irvingiaceae (Ixonanthaceae)*, sometimes known by the common names Barking Deer’s Mango, wild mango, African mango or bush mango. The Thai name of this nut is “ka bok”, “krabok”, “cha bok”, “tra bok”, “cham-moh”, “saang”, “ma muen”, “ma leun” and “lak-kai”. It produces a popular and inexpensive wood which is rather fragile and light.

Krabok is the fruit of a large, briefly deciduous tree with a straight bole. It grows to as high as 35 meters and has thin buttresses. The grey-brown bark is smooth and sometimes peels off in large pieces. The leaves are elliptic with a shiny upper surface, sized 8-20 cm long and 2.5-9 cm wide. The 5-15 cm long flower clusters are made up of fragrant yellow-white flowers of about 2.5 mm. The fleshy, yellow, oval fruit resembles a small mango, measuring 2-6 cm x 1.5-4 cm, which sticky juicy flesh and a light brown seed.

The seeds of this tree are roasted and their inner part served as a snack. In Vietnam, the white-yellow oil from krabok seeds is used to make wax, soap and a cocoa substitute. When the sweet and fragrant fruit ripens and falls, it is a favourite with wild animals and can also be eaten by humans. The wood is increasingly being used to make furniture and high quality charcoal. The tree propagates naturally by seed, with forest animals such as wild pigs and deer distributing the seed by eating the fruit. Saplings grow under the light shade of other trees. Coppicing is possible. The fatty acid compositions of oil was found to contain 96.2 %wt of saturated fatty acids which were primarily lauric acid (C12:0) and myristic acid (C14:0). The advantages of IM are charcoal, firewood, indoor-construction material, magarine, soap and candle.

2.5 Type of catalysts in transesterification

2.5.1 Acid-catalyzed processes [16]

Transesterification of triglycerides containing high free fatty acid can be preferable catalyzed by using acid catalyst such as sulfonic and sulfuric acids. These catalysts give very high yield, however, they require very high temperatures and long reaction time. In general, a 1%mol of sulfuric acid is a good amount for a conversion of 99% in 50 h. The mechanism of the acid-catalyzed transesterification of vegetable oils is shown in Figure 2.4. The protonation of the carbonyl group of the ester leads to the carbocation, which after a nucleophilic attack of the alcohol, produces the tetrahedral intermediate, which eliminates glycerol to form the new ester, and to regenerate the catalyst. Acid-catalyzed transesterification should be carried out in the absence of water, in order to avoid the competitive formation of carboxylic acids which reduce the yields of alkyl esters.

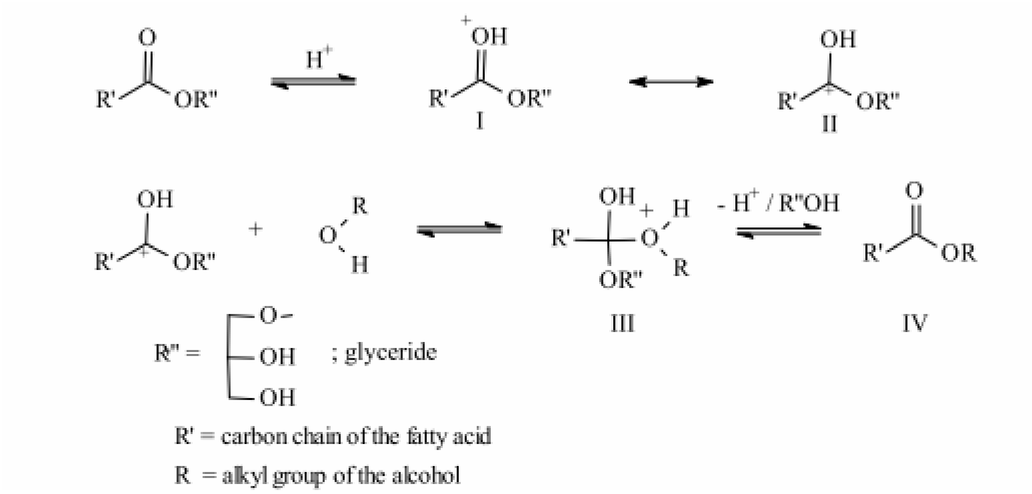

Figure 2.4 Mechanism of acid-catalyzed transesterification of vegetable oils.

2.5.2 Alkaline-catalyzed processes

Alkaline-catalyzed transesterification process is wildly used to synthesize biodiesel because it is faster than acid-catalyzed process and less corrosive to industrial equipment than acidic catalyst. Sodium hydroxide, sodium methoxide and potassium hydroxide are the most commonly used as alkali catalysts. The alkaline catalyst concentrations in the range of 0.5–1 %wt and 94–99% conversion of vegetable oils into esters. However, even if a water-free alcohol to oil mixture is used, some water is produced in the system by the reaction of the hydroxide with the alcohol. The presence of water gives rise to hydrolysis of some of the produced ester, with consequent soap formation. This saponification reaction reduces the ester yields and considerably difficults the recovery of the glycerol due to the formation of emulsions.

The mechanism of alkali-catalyzed transesterification is described in Figure 2.5. The first step involves the attack of the alkoxide ion to the carbonyl carbon of the triglyceride molecule, resulting in the formation of a tetrahedral intermediate. The reaction of this intermediate with an alcohol produces the alkoxide ion in the second step. In the last step the rearrangement of the tetrahedral intermediate gives rise to an ester and a diglyceride.

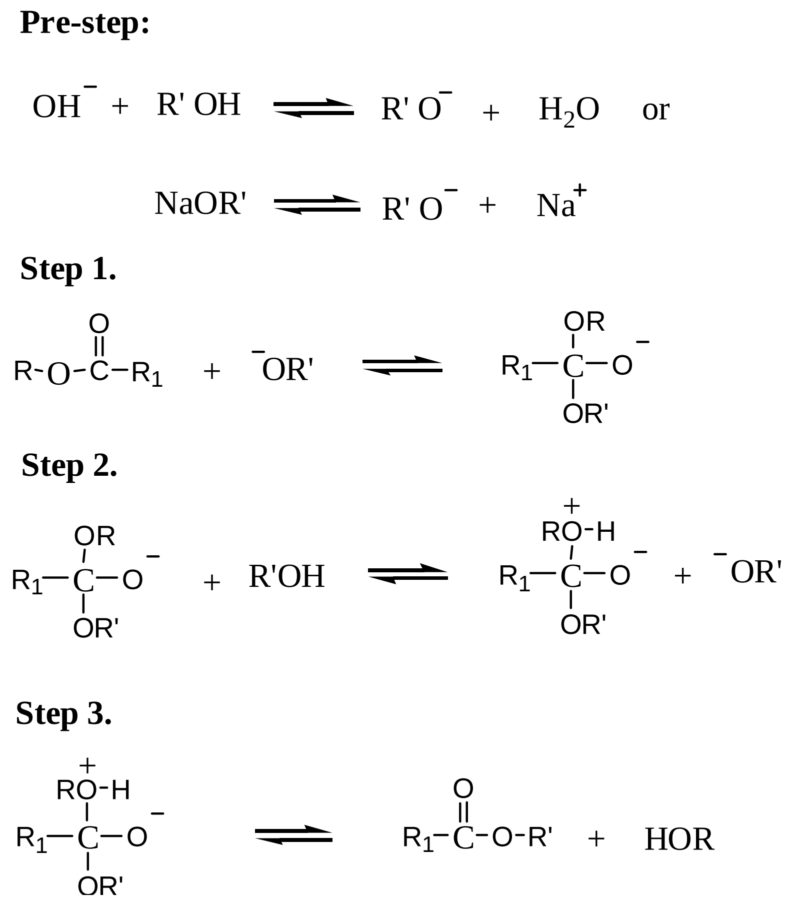

Figure 2.5 Mechanism of alkaline-catalyzed transesterification of vegetable oils.

2.5.3 Enzyme-catalyzed processes

Transesterification with alkaline as a catalyst has several disadvantages due to the problem of free fatty acid and water interference, the difficulty of glycerol recovery and requiring alkaline wastewater treatment. To solve these problems, the enzyme is chosen to replace conventional catalyst because the glycerol from enzymatic transesterification process can be easily recovered without any complex process and free fatty acids contained in waste oils and fats can be completely converted to methyl esters.

The most favorable enzyme which can be used as catalyst for tranesterification and esterification is lipase due to its biocompatibility, biodegradability and environmental acceptability of the biotechnical procedure. The extra cellular and the intracellular lipases are also able to catalyze the transesterification of triglycerides effectively. However, it still unfavorable when compared with alkaline-catalyzed process because the production cost is very high.

2.5.4 Non-ionic based-catalyzed processes

To obtain milder reaction condition and simplify manipulations of the factors involved in increasing the yield of the alkyl ester, organic bases has been developed and used as catalyst for organic synthesis. Bases such as amines were used in this process for example 1,2,2,6,6-pentamethylpiperidine, 2,6-di-tert-butylpyridinep and 4-dimethyl-aminopyridine(DMAP). Moreover, amidines such as 1,8 diazabicyclo [5.4.0]undec-7-ene (DBU) and 1,5-diazabicyclo[4.3.0]non-5-ene (DBN); guanidines such as 1,5,7 triazabicyclo[4.4.0]dec-5-ene (TBD) are frequently used in organic synthesis.

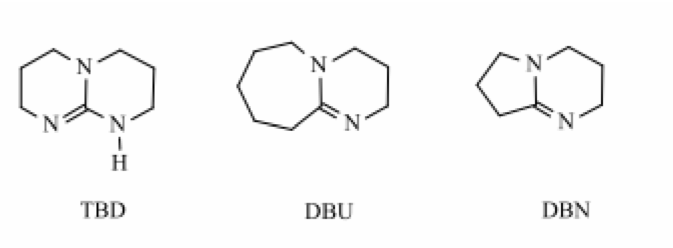

Figure 2.6 Molecular structures of some non-ionic organic bases.

2.5.5 Heterogeneously catalyzed processes

Heterogeneous catalysts are very useful for biodiesel production with the ability to achieve high yields of biodiesel esters without the need to neutralize and wash the biodiesel products. The example for heterogeneous catalysts are alkali earth or transition metal oxides such as CaO, MgO, BaO, and ZnO/Al_2O_3, alkaline metal oxides supported on zeolites and MCM-41, ion exchange resins such as clay minerals with acidic reaction sites and sulfated metal oxides such as ferric sulfate ($Fe_2(SO_4)_3$). The advantages of heterogeneous catalyst are reusable and do not form soaps, more tolerant to water and free fatty acids in the feedstock, improve product yield and purity, simpler purification process for glycerol and ease of separating biodiesel product. It also has several drawbacks because it require high temperatures and pressures to work well, those on solid support tend to show less activity than the active species in solution and there is the possibility of leaching which might contaminate the biodiesel.

2.5.6 Noncatalytic transesterification processes

Supercritical alcohol**,** especially methanol, is used for transesterification of vegetable oil without using any catalyst. Due to its nature, hydrophobic with a lower dielectric constant, non-polar triglycerides can be well solvated with supercritical methanol to form a single phase oil to methanol mixture. However, liquid methanol is a polar solvent and has hydrogen bondings between OH oxygen and OH hydrogen to form methanol clusters. Thus, the oil to methyl ester conversion rate was found to increase dramatically in the supercritical state. Free fatty acids contained in crude oils and fats could also be converted efficiently to methyl esters in supercritical methanol, leading to increase of the total yield of methyl esters from used oils [23]. In addition, because the process is non-catalytic, the purification of products after the transesterification reaction is much simpler and more environmentally friendly compared with the alkali-catalyzed process in which all the catalyst and saponified products have to be removed to obtain biodiesel fuel. On the other hand, high temperature and pressure is required in this process and large amount of methanol is necessary to perform the reaction. Therefore, production process such as continuous operation, production cost and scale up has to further investigate.

2.6 Transesterification parameters

2.6.1 Moisture content and free fatty acid

Vegetable oil with free fatty acid (FFA) value lower than 3%, the base-catalyzed reaction is chosen to complete the reaction. If the FFA of the starting oil is high, it must be refined by saponification using NaOH solution to remove free fatty acids. The two-step esterification process is required for this oil. Initially the FFA can be converted to fatty acid alkyl esters by an acid-catalyzed pretreatment and in the second step transesterification is completed by using alkaline-catalyst to complete the reaction.

2.6.2 Molar ratio of alcohol to oil

Molar ratio of alcohol to triglyceride is one of the most important variables affecting the yield of ester. When 100% excess methanol is used, the reaction rate is at its highest. The ratio for transesterification requires three moles of alcohol and one mole of triglyceride to yield three moles of fatty acid ester and one mole of glycerol. Higher molar ratios result in greater ester conversion in a shorter time. A molar ratio of 6:1 is normally used in industrial processes to obtain fatty acid alkyl ester yields higher than 98% by weight.

2.6.3 Catalyst

Alkali-catalyzed transesterification is faster than acid-catalyzed. However, if oil contains high FFA and more water, acid-catalyzed transesterification is more suitable [24]. The acids could be sulfuric acid, or organic sulfonic acid. Sodium hydroxide was chosen to catalyze the transesterifications because it is cheaper and is used widely in large-scale processing. More recently, an immobilized lipase was employed to catalyze the methanolysis of corn oil in flowing supercritical carbon dioxide with an ester conversion of >98%.

2.6.4 Reaction time

The conversion rate of transesterification increases with reaction time. Effect of reaction time on transesterification of beef tallow with methanol was studied [25]. During the first minute, the reaction was very slow due to the mixing and dispersion of methanol into beef tallow. However, from one to five min, the reaction proceeded very fast and the yield of methyl ester was increased from 1 to 38%. At about 15 min, the production of beef tallow slowed down and reached the maximum value. Freedman et al. (1984) transesterified peanut, cotton seed, sunflower and soybean oils under the condition of methanol to oil ratio of 6:1, 0.5 %wt sodium methoxide catalyst and 60°C. An approximate yield of 80% was observed after 1 min for soybean and sunflower oils. After 1 h, the conversions were almost the same for all four oils (93±98%).

2.6.5 Reaction temperature

Transesterification can occur at different temperatures, depending on the oil used. For the transesterification of refined soybean oil with methanol (6:1) using 1% NaOH, three different temperatures were used [27]. After 6 min, ester yields were 94, 87 and 64% for 60, 45 and 32°C, respectively. After 1 h, ester formation was identical for the 60 and 45°C runs and only slightly lower for the 32°C run. Temperature clearly influenced the reaction rate and yield of esters.

2.7 Biodiesel quality

The characteristics of biodiesel are close to petroleum diesel, hence, biodiesel is needed to replace mineral diesel. Biodiesel has viscosity close to mineral diesel because the conversion of triglycerides into methyl or ethyl esters through the transesterification process reduces the molecular weight to one-thirds that of the triglycerides. These vegetable oil esters contain 10–11% oxygen by weight, which may encourage combustion than hydrocarbon-based diesel in an engine. The cetane number of biodiesel is around 50. Biodiesel has lower volumetric heating values (about 10%) than mineral diesel but has a high cetane number and flash point. The esters have cloud point and pour points that are 15–25°C higher than those of mineral diesel. The properties of biodiesel from different oils and diesel fuels are compared in Table 2.5.

Table 2.5 Comparison of fuel properties between diesel and biodiesel. [26]

Fuel property	Diesel	Biodiesel
Fuel standard	ASTM D975	ASTM PS 121
Fuel composition	C10-C21 HC	C12-C22 FAME
Lower heating value, Btu/gal	131,295	117,093
Viscosity, at 40° C	1.3-4.1	1.9-6.0
Specific gravity kg/l at 60° F	0.85	0.88
Density, lb/gal at 15° C	7.079	7.328
Water, ppm by wt	161	0.05% max
Carbon, wt %	87	77
Hydrogen, wt %	13	12
Oxygen, by dif. wt %	0	11
Sulfur, wt %	0.05 max	0.0 - 0.0024
Boiling point (°C)	188-343	182-338
Flash point (°C)	60-80	100-170
Cloud point (°C)	-15 to 5	-3 to 12
Pour point (°C)	-35 to -15	-15 to 10
Cetane number	40-55	48-65
Stoichiometric air/fuel ratio wt./wt.	15	13.8
BOCLE Scuff, grams	3,600	>7,000

For Thailand, it has set legislative assembly characteristic and quality of biodiesel as shown in Table 2.6.

Table 2.6 Characteristic and quality of biodiesel (methyl ester of fatty acids) in Thailand. [27]

Characteristic	**Value**	**Method of standard**
Methyl ester, %wt.	>96.5	EN 14103
Density at 15^{o}C, kg/m^{3}	860-900	ASTM D 1298
Viscosity at 40^{o}C, cSt	3.5-5.0	ASTM D445
Flash point, ^{o}C	>120	ASTM D 93
Carbon residue, on 10% distillation residue, %wt	<0.30	ASTM D 4530
Cetane number	>51	ASTM D 613
Sulfur, %wt.	<0.0010	ASTM D 2622
Sulfated ash, %wt.	<0.02	ASTM D 874
Water, %wt.	<0.050	ASTM D 2709
Total contaminate, %wt.	<0.0024	ASTM D 5452
Copper strip corrosion	<96.5	ASTM D 130
Oxidation stability at 110^{o}C, h	>6	EN 14112
Acid value, mg KOH/g	<0.50	ASTM D 664
Iodine value, g Iodine/100 g	<120	EN 14111
Linolenic acid methyl ester, %wt.	<12.0	EN 14103
Methanol, %wt.	<0.20	EN 14110
Monoglyceride, %wt.	<0.80	EN 14105
Diglyceride, %wt.	<0.20	EN 14105
Triglyceride, %wt.	<0.20	EN 14105
Free glycerin, %wt.	<0.02	EN 14105
Total glycerin, %wt.	<0.25	EN 14105
Group I metals (Na+K)	<5.0	EN 14108 and EN 14109
Group II metals (Ca+Mg)	<5.0	EN 14538
Phosphorus, %wt.	<0.0010	ASTM D 4951

2.8 Cold flow property [3, 5, 6, 28]

Cold flow property is one of the major problems associated with the use of biodiesel as the diet of diesel engines. Cold flow properties of fuel are usually characterized by the following four temperature measures.

1. Cloud point (CP)

The cloud point (CP) is the temperature of a liquid specimen when the smallest observable cluster of wax crystals first appears upon cooling under described conditions (ASTM, 2002a). ASTM D6749-02 is the standard automatic test method for cloud point of petroleum products.

2. Pour point (PP)

The pour point (PP) is the lowest temperature at which movement of the test specimen is observed under the prescribed conditions. ASTM D6749-02 is the standard method for detecting the pour point of petroleum product using an automatic air pressure method.

3. Cold filter plugging point (CFPP)

The cold filter plugging point (CFPP) is the highest temperature, expressed in the multiples of 1°C, at which a given volume of fuel fails to pass through a standardized filtration device in a specified time when cooled under the conditions prescribed in test method (ASTM, 1999).

4. Low temperature flow test (LTFT)

The low temperature flow test (LTFT) is a minimum pass temperature, expressed as a multiple of 1°C, at which a test fail can be filtered in 60 seconds or less (ASTM D4539-03).

The high amount of saturated fatty acid methyl ester components cause operability problems such as clog fuel lines and filters because it was crystallization or thickening of biodiesel at low temperatures. If the biodiesel has large amount of saturated fatty compounds, the higher cloud point and pour point are found. Normally, the cloud point usually occurs at a higher temperature than the pour point. The cloud point is the temperature at which a liquid fatty material becomes cloudy due to the formation of crystals and solidification of saturated. With decreasing temperature, more solids form and material approaches the pour point at which the lowest temperature that can flow.

If the temperature drop is large enough to achieve the saturation temperature of any of the fatty acid methyl ester components, these precipitate in the liquid mixture in the form of microscopic. At further decrease of temperature the submicrometer crystals grow further, they become visible. This temperature is then denoted as the cloud point. With further decrease of temperature the saturation temperatures of other components are achieved, the crystals gradually grow until they can be seen, and they start to coalesce into sizeable agglomerates. Gradually the whole system ceases to be liquid, which is referred to as the pour point. Agglomeration of crystals occluded by the liquid phase hinders the flow of fuels through the fuel pipe and blocks the fuel filter.

2.8.1 The improvement of cold flow property [5, 6, 29]

To solve the problems of fuels at low-temperatures, five methods were purposed.

1. **Blending of fatty acid methyl/ ethyl ester with conventional diesel fuel**

The most wildly used method of improvement cold flow property is blending of fatty acid methyl/ ethyl ester with fossil. Fossil fuel in blended fuels acts at low temperatures as a solvent of precipitated crystals, which is reflected in improved low temperature characteristics of the fuel. The advantage of this method is preparation of the mixture by simple blending of the components.

2. **Winterization**

Winterization has been used to reduce the cloud point and pour point of biodiesel by lowering its saturated fatty acid methyl ester components. The solid fraction of fuels are removed by cooling of esters. The problem of this method is given low yield due to large obstruction of crystals with the liquid making winterization less acceptable.

3. Preparation of fatty esters with branched chain

The cold flow property of fuels could be improved by using branched chain of ester such as *i*-propyl, *i*-butyl and 2-butyl instead of the methyl esters. Branched esters have lower melting point in the neat diesel form. In 1995, the esters based on these alcohols and soybean oil-based FFA exhibit the onset temperatures from DSC (differential scanning calorimetry) measurements by 7–11°C and 12–14°C lower for iso-propyl and 2-butyl esters, respectively. The cloud point and pour point were decreased simultaneously.

4. Preparation of esters with bulky substituents in the chain

The synthesis of esters with a bulky substituent into the chain influences the cold flow property of fuels. The bulky substituent disrupts the harmony during the solid phase formation, and the orientation in one direction.

5. Use of chemical additives

The most convenient method to improve the cold flow property of fuels is using the chemical additives. By adding the additives, the cloud point and pour point of fuels can be decreased. This technology is also very attractive in the industry considering the problems encountered with other methods.

2.9 Pour Point Depressants (PPDs) [6, 29-32]

Pour point depressants are also called cold flow improvers, paraffin inhibitors or wax modifiers. The advantages of this method are simplicity and economy reason. The main attraction is its relative cheapness and variability of dosage. Any PPDs should be soluble in oil and have an ability to co-crystallize with the growing wax crystals from the oil below its cloud point.

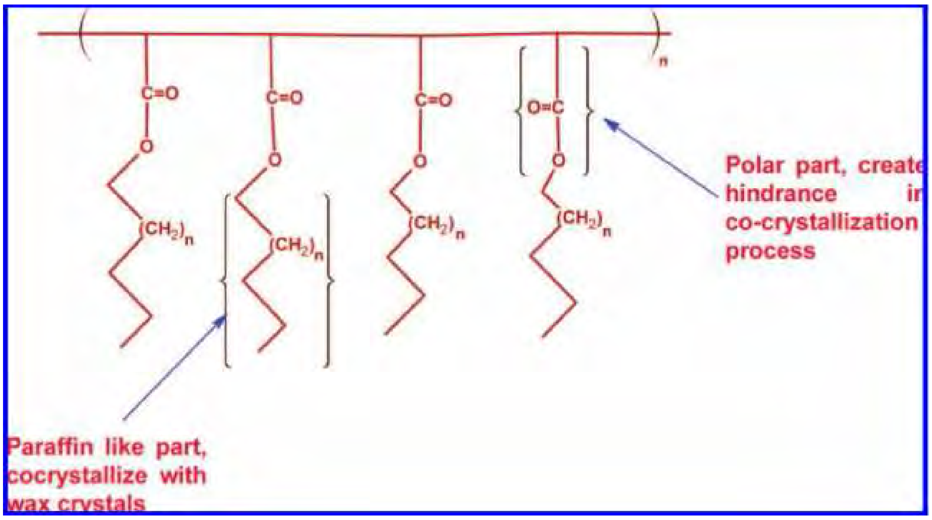

Figure 2.7 Characteristic structure of the general PPDs polymer additive.

All pour point depressants are separated into two parts which are paraffin like part (non-polar part) and polar part. Generally, at or below the cloud point, the paraffin like part of pendant chains of the PPDs provides nucleation site and co-crystallizes with wax crystals, while the polar part creates a barrier to the formation of interlocking wax network as shown in Figure 2.7 and it also prevents the crystal growth and agglomeration of wax crystal. The shape and size of the wax crystals will reduce and avoid the formation of interlocking networks, which results in the lowering of the pour point.

The nature of wax crystals that precipitated from oil and cohesive forces between the wax crystals has been changed and destroyed due to the function of these PPDs. Hence, the tendency of the wax crystals are decreased to interlock and set into gel.

Some additives (PPDs) improving the cold flow property are developed for diesel fuel are effective also for biodiesel. They are applied at low concentrations between 0.05 and 0.2 wt%. The PPDs influence the size and morphology of crystals, and the rate of their growth. The cloud point value is therefore altered only slightly, but the pour point decrease significantly. These additives crystallize together with that component of the fuel, which is first to nucleate. The molecules of additives contain function groups, which prevent the crystal growth and agglomeration. This lead to formation of a large number of small compact needle-like particles, which form a porous filtration cake on the filter, and do not hinder the passage of the liquid phase through the filter.

2.10 Literature reviews

In 2003, Kumar *et al*. [33] studied the transesterification for producing biodiesel from vegetable oils and animal fats by using sodium hydroxide and sulfuric acid as catalysts. The result showed that the mode of the reaction, molar ratio of the glycerides to alcohol, type and quality of catalyst, reaction time, reaction temperature and purity of oil and fats had an affect on the transesterification. Under the best condition (1:6 molar ratio of the glycerides to alcohol, 1 %wt of sodium hydroxide, 1.5 h and 70°C), high yield of biodiesel was obtained.

In 2004, Chuang-Weu *et al*. [32] studied the performance of additives for improving the cold flow properties of higher blend ratios of soybean biodiesel. Neat biodiesel and its blends with kerosene (D#1) and low sulfur diesel fuel (LSD #2) were treated with the cold flow improver additives. The cold flow properties of biodiesel (B100) and 80% (B80) to 90% biodiesel in kerosene were evaluated with pour point depressants, to identify approaches to transport and mix biodiesel with diesel in cold climates. Two additives significantly decreased the pour points of soybean biodiesel blends, but all the four additives had little effect on cloud points. A mixture of 0.2% additive, 79.8% biodiesel, and 20% kerosene reduced the pour point of B100 by 27°C.

In 2005, Meher *et al*. [34] studied the transesterification of Karanja oil with methanol for the production of biodiesel. The optimum reaction conditions such as catalyst concentration, alcohol to oil molar ratio, temperature, and rate of mixing were investigated. The result showed that 85% yield was obtained in 15 min and reaction was almost complete in two hours with 97–98 %yield of methyl esters by using 1% KOH as catalyst, methanol to oil molar ratio 6:1, at 65°C with rate of mixing 360 rpm for a period 3 h. In addition, the reaction could be completed within 1 h by using 12:1 molar ratio of methanol to oil or higher. In contrast, with a low rate of stirring at 180 rpm, the reaction was incomplete whereas stirring at high rpm was a time efficient process.

In 2005, Nascimento *et al*. [35] studied the synthesis of additives to reduce the crystallization temperature (T_{CO}) of methyl hexadecanoate (PalMe). These additives were esters of carboxylic acids with linear or branched alkyl chains of up to 16 carbon atoms with alcohols having cyclic or branched alkyl chains or an alkoxy group. They reported that the crystallization temperature of PalMe could be decreased by 10°C depending on the molecular mass, molecular structure and concentration of the additive. The best result was the hexadecanoic acid either with cyclohexanol or 2-ethylhexanol.

In 2006, Soriano *et al*. [29] studied the use of ozonized vegetable oils as pour point depressant for neat biodiesel. The result showed that biodiesel derived from sunflower oil, soybean oil and rapeseed oil were effected by ozonized vegetable oils (1-1.5% by weight) in reducing the pour point to -24, -12 and -30°C, respectively but unaffected on cloud point. On the other hand, ozonized vegetable oils effected on palm oil biodiesel by decreasing in cloud point but not in pour point. The most significant reduction in pour point was obtained when the biodiesel and ozonized samples were prepared from the same vegetable oil.

In 2009, Al-Sabagh *et al*. [30] studied the synthesis of pour point depressants from styrene-maleic anhydride copolymer reacted with alcohol which contain carbon 8, 12, 16 and 18 atoms to reduce pour point of waxy crude oil. The result showed that efficiency of pour point depressants depend on branched chain length of alcohol. Long-branched chain (C18) gave maximum reduction (27°C to -3°C) while short-branched chain (C8) gave minimum reduction (27°C to 6°C) at the same concentration (10,000 ppm).

In 2009, Smith *et al*. [36] studied the alkoxylation of the unsaturated portion of biodiesel for reducing cloud point without compromising ignition quality or oxidation stability. They synthesized the alkoxylated biodiesel under mild conditions, using renewable feedstocks, with reasonable residence times and without the use of organic solvents. Canola oil was transesterified with methanol, ethanol and butanol. The result showed that the cloud point for methyl and ethyl biodiesel increased slightly, while a reduction of 1 K was achieved for butyl biodiesel. The presence of by-products negated much of the expected improvement in cloud point for butoxy butyl biodiesel.

In 2009, Purnanand *et al*. [28] studied the effect of ethanol, kerosene and commercial additive on cold flow properties of Mahua Methyl Ester (MME) fuel obtained from *Madhuca indica*, one of the important species in India. The result showed that the cold flow properties of MME were improved by using ethanol and kerosene as pour point depressants (PPDs) at the concentration up to 20%. At the concentration of 20% of kerosene and 20% of ethanol, cloud points of MME were reduced from 291 K (18°C) to 278 K (5°C) and from 291 K (18°C) to 281 K (8°C). In addition, the reduction in pour points of MME was from 280 K (7°C) to 265 K (-8°C) when using 20% of kerosene and up to 269 K (-4°C) when using 20% of ethanol as same as using 2% Lubrizol additive as PPDs.

CHAPTER III

EXPERIMENTAL

3.1 Materials and equipments

3.1.1 Raw materials

1. *Irvingia malayana* Oliv. ex A. Benn. (IM) seeds was purchased from Chanthaburi Province
2. Palm biodiesel was provided by Verasuwan Co., Ltd. Samut Sakhon Province

3.1.2 Chemicals

1. Chloroform-D: NMR spectroscopy grade; Merck
2. Cyclohexane: analytical grade; Merck
3. Dodecanoic acid: analytical grade; Sigma-Aldrich
4. Ethanol: analytical grade; Merck
5. Ethyl acetate: analytical grade; Lab-Scan
6. Glacial acetic acid: analytical grade; Merck
7. Heptane: analytical grade; Merck
8. Hexane: analytical grade; Lab-Scan
9. Hydrochloric acid: analytical grade; Merck
10. Methanol: analytical grade; Merck
11. Methyl heptadecanoate: analytical grade; Fluka
12. Octadecanoic acid: analytical grade; Sigma-Aldrich
13. Phenopthalein indicator: analytical grade; Merck
14. Potassium dichromate: analytical grade; Lab-Scan
15. Potassium hydrogen phthalate: analytical grade; Merck
16. Potassium hydroxide: analytical grade; Lab-Scan
17. Potassium iodide: analytical grade; Lab-Scan
18. Sodium hydroxide: analytical grade; ACS

19. Sodium thiosulfate: analytical grade; Lab-Scan
20. Sulfuric acid: analytical grade; Carlo Erba
21. Toluene: analytical grade; Merck
22. Wijs solution: analytical grade; Merck
23. 37 Component FAMEs standard; Supleco
24. 2-Propanol: analytical grade; Merck
25. Flozol 112: commercial additive; The Lubrizol Corporation
26. Flozol 2251D: commercial additive; The Lubrizol Corporation
27. CD017: commercial additive
28. Zenith: commercial additive
29. Kerosene

3.1.3 Equipments

1. Fourier-Transform NMR Spectrometer: Mercury (400MHz); Varian
2. Viscometer: W. Herzog GmbH; HVU48x/490/HVM472
3. Gas Chromatograph: Varian CP-3800
4. Fourier-Transform Infrared Spectroscopy: Nicolet
5. Mini Flash: FLA; Grabner instruments
6. Rotary evaporator: Buchi R-200
7. Mini Cloud/Pour Point Tester: MPC 240L

3.2 Methods

3.2.1 Solvent extraction of *Irvingia malayana* Oliv. ex A. Benn. (IM) seeds

500 ml of hexane was added to 500 g of the crushed kernel in 2000 ml Erlenmeyer flask and allowed to shake overnight. The organic extract was filtered and evaporated to dryness by rotary evaporator. The percentage of extracted IM oil was determined. The properties of IM oil were determined according to section 3.2.2.

3.2.2 Determination of properties of IM oil

The % free fatty acid (FFA), saponification number (SN) and iodine value (IV) of IM oil were determined according to ASTM D 5555, ASTM D 5558 and ASTM D 5554 standards, respectively.

3.2.3 Synthesis of methyl ester of IM oil (IMME)

500 g of IM oil was added into 1000 ml of round bottom flask equipped with condenser. After the oil was heated to 65°C, the solution of sodium hydroxide (5.0 g) in methanol (290 ml, 12:1 molar ratio of methanol to oil) was slowly added into the reaction and then the mixture was heated to 65°C for 1.5 h. The reaction mixture was monitored by TLC developed by hexane: ethyl acetate: acetic acid (90:10:1 %v/v) and visualized by vanillin solution. The reaction mixture was transferred to a separatory funnel and allowed glycerin to separate. The IMME layer (upper layer) was washed with warm deionized water until the IMME layer was cleared. The residue water was removed by rotary evaporator. The ester content and fatty acid compositions of IMME were analyzed by NMR and gas chromatography technique, respectively. The product yield of IMME was calculated by:

$$\text{Product yield (\% wt)} = \frac{\text{Weight of IMME}}{\text{Weight of IM oil}} \times 100$$

3.2.4 Synthesis of Pour Point Depressants (PPDs)

3.2.4.1 Synthesis of methyl laurate and methyl stearate as PPDs

50 g of lauric/stearic acid was added into 1000 ml of round bottom flask equipped with condenser. After the lauric/stearic acid was heated to 65°C, methanol (363/266 ml, 40:1 molar ratio of methanol to acid) and conc. H_2SO_4 (0.54 ml, 2 %wt of acid) were slowly added into the reaction and then the mixture was heated to 65°C for 10 h. The reaction mixture was monitored by TLC developed by hexane: ethyl acetate: acetic acid (90:10:1 %v/v) and visualized by vanillin solution.

The reaction mixture was transferred to a separatory funnel and washed with warm deionized water. The unreacted lauric/stearic acid was removed by using 5M sodium hydroxide solution. The methyl laurate (ML) and methyl stearate (MS) were washed several times with warm deionized water until the ML and MS were cleared. The residued water was removed by rotary evaporator. The percent conversion of ML and MS was analyzed by NMR technique. The acid value of ML and MS was determined according to ASTM D 974 standard. The product yield of ML and MS was calculated by:

$$\text{Product yield (\% wt)} = \frac{\text{Weight of PPDs}}{\text{Weight of acid}} \times 100$$

3.2.4.2 Synthesis of *i*-propyl laurate and *i*-propyl stearate as PPDs

Following the procedure as described in section 3.2.4.1, using *i*-propanol instead of methanol at 83°C, *i*-propyl laurate (IPL) and *i*-propyl stearate (IPS) were obtained.

3.2.5 Characterization of commercial additives

Five commercial additives (CD017, Zenith, Flozol 2251D, Flozol 112 and kerosene) were characterized for functional groups by using Fourier-Transform Infrared Spectroscopy (FT-IR).

3.2.6 Determination of cloud point (CP) and pour point (PP)

Methyl ester of IM oil (IMME) and palm oil (PME) were mixed thoroughly with synthesized PPDs (ML, MS, IPL and IPS) and commercial additives (CD017, Zenith, Flozol 2251D, Flozol 112 and kerosene) at various concentrations. The CP and PP of the mixtures were determined according to ASTM D 6749 standard.

3.2.7 Characterization and determination of the methyl ester

3.2.7.1 Ester content of IMME

3.2.7.1.1 Fourier-Transform NMR Spectrometer (FT-NMR)

The ester content of IMME was calculated by comparing the peak area of methoxy proton (signal at δ_H 3.7 ppm) and methylene proton (signal at δ_H 2.3 ppm) using the following equation:

$$\boxed{\%\ \text{Ester content} \quad = \quad [(2I_{OCH3}) / (3I_{CH2})] \times 100}$$

3.2.7.1.2 Gas Chromatography (GC)

The ester content of IMME was determined by using methyl heptadecanoate as an internal standard. The ester content of IMME was calculated by the following equation:

$$C = \left(\frac{\sum A - Ai}{Ai} \right) \times \left(\frac{Ci \times Vi}{m} \right) \times 100$$

C = Methyl ester content

$\sum A$ = Total area of fatty acid methyl esters

Ai = Area of methyl heptadecanoate

Ci = Concentration of methyl heptadecanoate solution

Vi = Volume of methyl heptadecanoate solution

m = Mass of the sample

3.2.7.2 Determination of fatty acid compositions of IMME and PME

The fatty acid compositions of IMME and PME were determined by using standard 37 fatty acid methyl esters.

3.2.7.3 Determination of the properties of IMME and PME

The properties of IMME and PME were determined according to the test methods shown in Table 3.1.

Table 3.1 Test methods of methyl ester

Property	Method
Viscosity at 40°C (cSt)	ASTM D 445
Flash point (°C)	ASTM D 93
Density @15°C (g/cm^3)	ASTM D 4052
Acid number (mg KOH/g)	ASTM D 974

CHAPTER IV

RESULTS AND DISCUSSION

4.1 Solvent extraction of *Irvingia malayana* Oliv. ex A. Benn. (IM) seeds

The oil was extracted from the kernel or seed using hexane as a solvent. The percentage of extracted IM oil was 76 %wt. It contained a high percentage of oil which may be a new source of raw materials for biodiesel production.

4.2 Determination of properties of IM oil

The properties of IM oil including % free fatty acid (FFA), saponification number (SN) and iodine value (IV) were investigated. The results indicated that it had 2.49 %wt of FFA, saponification number of 237.92 mg KOH/g and iodine value of 5.22 mg I_2/g, respectively. These properties will be discussed later in sections 4.3 and 4.4.2.

4.3 Synthesis of methyl ester of IM oil (IMME)

Due to % free fatty acid of IM oil was lower than 3 % (according to section 4.2), this oil was subjected to transesterification reaction and the reaction was monitored by Thin Layer Chromatography (TLC). As can be seen in Figure 4.1, IM oil was almost completely converted to methyl ester (biodiesel). There was a trace of diglyceride and monoglyceride in IM oil due to three steps of conversion of triglyceride to methyl ester. The product yield of IMME was 93 %. The appearance of IMME was yellow liquid.

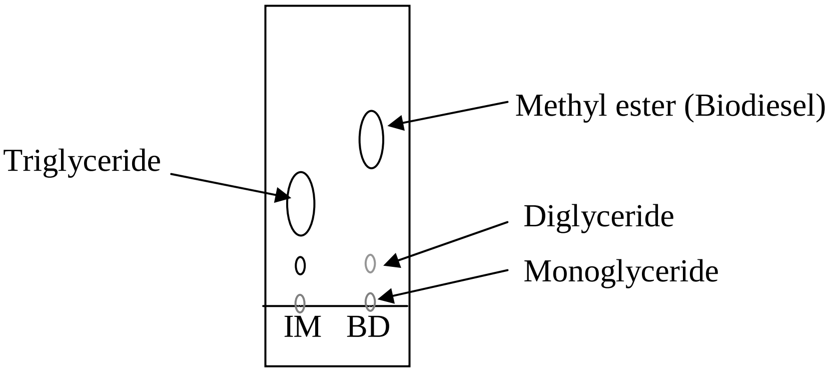

Figure 4.1 TLC of methyl ester of IM oil (IMME) using a mixture of hexane, ethyl acetate and acetic acid (90:10:1 %v/v) as mobile phase.

4.4 Characterization and determination of the methyl ester

4.4.1 Ester content of IMME

The ester content of IMME could be calculated from NMR and GC. The NMR spectrum of IM oil and IMME were shown in Figures A1-A2 and GC chromatogram of IMME was shown in Figure A4, respectively. It could be seen that both techniques gave similar values of the ester content which were 97.87 % (NMR) and 96.13% (GC), respectively.

According to EN 14103 standard, ester content should be higher than 96.5 %wt. Therefore, IMME could fulfill the specification of methyl ester standards.

4.4.2 Determination of fatty acid compositions of IMME and PME

To determine the fatty acid compositions, the methyl ester of IM oil (IMME) and palm oil (PME) were investigated by GC. The results were shown in Table 4.1.

Table 4.1 Comparison of fatty acid compositions of IMME and PME.

Fatty acid compositions	**IMME**[a] **(%wt)**	**PME**[b] **(%wt)**
C10:0 (Capric acid)	2.43	-
C12:0 (Lauric acid)	46.25	0.32
C14:0 (Myristic acid)	43.83	0.94
C16:0 (Palmitic acid)	3.96	37.46
C16:1 (Palmitoleic acid)	0.56	-
C18:0 (Stearic acid)	0.33	3.87
C18:1n9c (Oleic acid)	2.31	45.91
C18:2n6c (Linoleic acid)	0.33	11.17
C20:0 (Arachidic acid)	-	0.33

Remark : a = Methyl ester of IM oil
b = Methyl ester of palm oil

As can be seen in Table 4.1, IMME mostly consisted of lauric acid (46.25%) and myristic acid (43.83%). This fatty acid compositions were relevant to saponification number and iodine value (according to section 4.2). It could be concluded that IM oil mostly consisted of low molecular weight saturated fatty acids as compared to that of palm oil.

4.4.3 Determination of the properties of IMME and PME

The properties of methyl ester such as viscosity, flash point, density and acid value were determined according to ASTM standards. The values of these properties of IMME and PME were shown in Table 4.2.

Table 4.2 Some specification for quality of methyl ester.

Property	Standard Value	IMME	PME	Standard method
Viscosity at 40°C[a] (cSt)	3-5	2.87	4.44	ASTM D 445
Flash point (°C)	>120	130	>120	ASTM D 93
Density @15°C (g/cm^3)	860-900	872.52	880.14	ASTM D 4052
Acid value (mg KOH/g)	< 0.5	0.14	0.42	ASTM D 974

Remark : a = Measured by W-Herzog GmbH

From Table 4.2, the results showed that IMME had properties within the range of standard values except viscosity at 40°C of IMME was slightly lower than standard value.

4.5 Synthesis of Pour Point Depressants (PPDs)

4.5.1 Synthesis of methyl laurate (ML), methyl stearate (MS), *i*-propyl laurate (IPL) and *i*-propyl stearate (IPS) as PPDs

The appearance, percent conversion, percent product yield, acid value and viscosity of PPDs were shown in Table 4.3.

Table 4.3 The appearance, percent conversion, percent product yield, acid value and viscosity at 40°C of PPDs.

PPDs	Appearance	% Conversion[a]	% Product yield	Acid value (mg KOH/ g oil)	Viscosity at 40°C[b] (cSt)
Methyl laurate (ML)	Colorless oil	98.48	87.49	0	2.39
Methyl stearate (MS)	White plate	97.55	84.15	0	-[c]
i-propyl laurate (IPL)	Colorless oil	96.51	88.12	0	2.88
i-propyl stearate (IPS)	Colorless oil	96.05	87.83	0	2.95

Remark : a = Measured by ^{1}H-NMR
b = Measured by W-Herzog GmbH
c = Solid at room temperature

From Table 4.3, it could be seen that the appearance of ML, IPL and IPS were colorless oil, in contrast, MS was an white plate which could be changed into liquid when heated. The percent conversion and product yield of PPDs were in the range of 96.05-98.48 % and 84.15-88.12 %, respectively. The acid value of all PPDs were 0 mg KOH/g oil which refered to the unreacted lauric/stearic acid was completely removed from synthesized PPDs. The viscosity at 40°C of ML, IPL and IPS were 2.39, 2.88 and 2.95, respectively.

4.5.2 Characterization of commercial additives

4.5.2.1 Fourier-Transform Infrared Spectroscopy (FT-IR)

Five commercial additives (CD017, Zenith, Flozol 2251D, Flozol 112 and kerosene) were characterized for functional groups by using FT-IR spectroscopy. The IR spectra of five commercial additives were shown in Figures A10-A14.

Table 4.4 The absorption assignments of commercial additives.

Wave number (cm^{-1})					Assignments
CD017	Zenith	Flozol 2251D	Flozol 112	Kerosene	
-	-	-	-	1378	C-H Bending (CH_3)
1239, 1369	1163, 1239	1163	1157	-	C-O Stretching
1736	1736	1735	1735	-	C=O Stretching
2851, 2920	2850, 2918	2850, 2918	2850, 2918	2855, 2925, 2956	C-H Aliphatic stretching
-	3027	-	-	-	=C-H Stretching of aromatic

According to their absorption bands, in Table 4.4, the spectra of CD017, Zenith, Flozol 2251D and Flozol 112 indicated the C=O stretching peak of the carbonyl group of ester at 1735-1736 cm^{-1} and C-O stretching peak of ester at 1157-1369 cm^{-1}. The C-H aliphatic stretching of four additives were shown at 2850-

2920 cm^{-1}. In addition, Zenith had an adsorption peak of =C-H stretching at 3027 cm^{-1} and C=C stretching at 1375-1492 cm^{-1} indicating aromatic ring. On the other hand, kerosene was found only the peak of C-H aliphatic stretching at 2855-2956 cm^{-1} which referred to the hydrocarbon in the structure.

Table 4.5 Cloud point (CP) and pour point (PP) of IMME, PME and PPDs.

IMME, PME and PPDs	CP_{ave} (°C)	PP_{ave} (°C)
IMME	3.40 ± 1.0	-2.0 ± 1.0
PME	18.30 ± 1.0	18.0 ± 1.0
Methyl laurate (ML)	2.30 ± 1.0	3.0 ± 1.0
Methyl stearate (MS)	36.55 ± 1.0	36.0 ± 1.0
i-propyl laurate (IPL)	-15.15 ± 1.0	-13.0 ± 1.0
i-propyl stearate (IPS)	24.50 ± 1.0	24.0 ± 1.0
CD017	31.70 ± 1.0	9.0 ± 1.0
Zenith	21.20 ± 1.0	18.0 ± 1.0
Flozol 2251D	22.55 ± 1.0	20.0 ± 1.0
Flozol 112	23.70 ± 1.0	22.0 ± 1.0
Kerosene	< -50.00 ± 1.0	-

From Table 4.5, the results showed that CP and PP of IMME were lower than PME by 14.90±1.0°C and 20.0±1.0°C, respectively. This result could be described by chain length of fatty acid. According to fatty acid compositions from Table 4.1, IMME mostly consisted of lauric acid (46.25 %wt, C12:0) and myristic acid (43.83 %wt, C14:0), while oleic acid was the main component in PME (45.91 %wt, C18:1n9c).

The same explanation could be applied to the value of ML and MS, the ΔCP and ΔPP were 34.25±1.0°C and 33.0±1.0°C, respectively. For IPL, it had the value of CP and PP equal to -15.15±1.0°C and -13.0±1.0°C and gave ΔCP and ΔPP values equal to -17.45±1.0°C and -16.0±1.0°C when compared to ML. This result could be explained by the packing of ML and IPL molecules. ML was a crystalline having regular arrangement which had no empty site to trap the wax crystals of oil resulting in the growth and agglomeration of wax. Conversely, IPL was an amorphous having more space to combine with wax crystal of oil retarding the growth and agglomeration of wax. The same explanation could be applied to the value of IPS when compare to MS.

From Figures A10-A14, ratio of polarity calculating from peak area of carbonyl group and aliphatic hydrocarbon were 0.28, 0.28, 0.22 and 0.22 for CD017, Zenith, Flozol 2251D and Flozol 112, respectively. The higher ratio indicated the higher polarity in the structure preventing the crystal growth and agglomeration which will hinder the solidification of oil. From Table 4.5, CD017 had the highest cloud point (31.70±1.0°C) because of its high molecular weight. It was found that Flozol 2251D and Flozol 112 had similar cloud point and pour point due to their similar molecular weight. Furthermore, IR spectrum of kerosene in Figure 4.6 indicated that it had only hydrocarbon in the structure so it could not calculated the ratio of polarity.

4.6 Improvement the cold flow property of methyl ester

4.6.1 Using methyl laurate (ML) as PPDs

From Figures 4.2 and 4.3, the CP and PP of IMME were decreased from 3.40°C to -3.75°C (ΔCP = 7.15°C) and from -2.0°C to -7.0°C (ΔPP = 5.0°C) when using 500,000 ppm of ML. At the same concentration as IMME, the CP and PP of PME were also decreased from 18.30°C to 8.05°C (ΔCP = 10.25°C) and from 18.0°C to 8.0°C (ΔPP = 10.0°C).

The cold flow property of IMME and PME could be improved by adding ML at the higher concentration. The CP and PP of PME were decreased 30.24% and 50%, respectively when compared with IMME. Moreover, ML had a greater effect on palm oil because PME contains less amount of short chain fatty acids than IMME (see Table 4.1). Besides, the CP of ML (2.30±1.0°C) was similar to the CP of IMME because IMME mainly consisted of lauric acid.

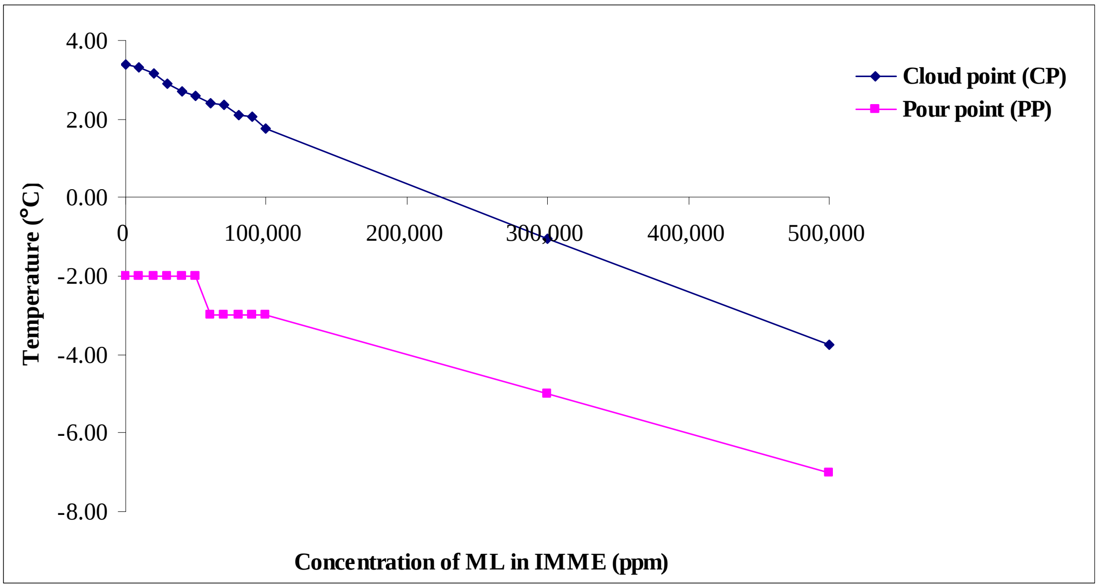

Figure 4.2 CP and PP of IMME with various concentrations of ML.

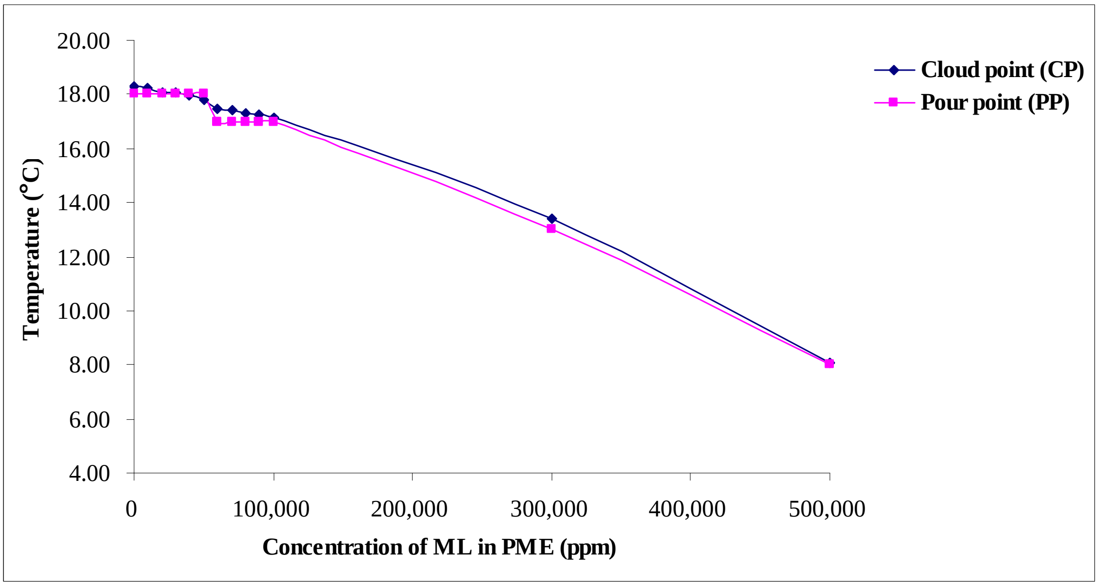

Figure 4.3 CP and PP of PME with various concentrations of ML.

4.6.2 Using methyl stearate (MS) as PPDs

From Figure 4.4, the result showed that the cold flow property of IMME could not be improved by using MS as PPDs because the CP and PP of MS (36.55±1.0°C and 36.0±1.0 °C) were higher than IMME. The PP of IMME still remained at -2.0°C and the PP would be increased if the addition of MS was higher than 20,000 ppm. Due to the chain length of fatty acids, MS had a higher molecular weight than IMME. Therefore, the CP and PP of IMME were increased when using the higher concentration of MS.

From Figure 4.5, it could be seen that CP and PP of PME were improved by using MS as PPDs. At the concentration 30,000 ppm, the CP was decreased from 18.30°C to 17.85°C (ΔCP = 0.45°C). The CP would be increased if the addition of MS was higher than 40,000 ppm. The PP of PME still remained at 18.0°C when using MS in the range of 0-20,000 ppm. At the concentration 30,000-70,000 ppm, the PP was decreased 1.0°C and the PP was increased when the concentration of MS was higher than 70,000 ppm.

It could be concluded that ML was more effective than MS because the ML had a shorter hydrocarbon chain and more polar than MS. The functions of polarity part in PPDs are to prevent the crystal growth and agglomeration which will hinder the solidification of oil.

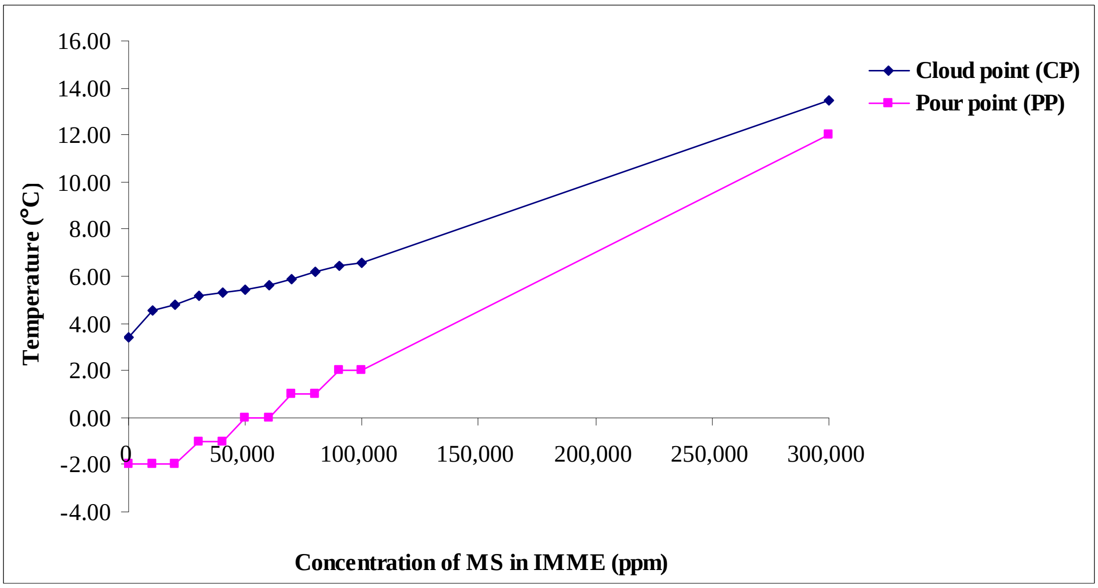

Figure 4.4 CP and PP of IMME with various concentrations of MS.

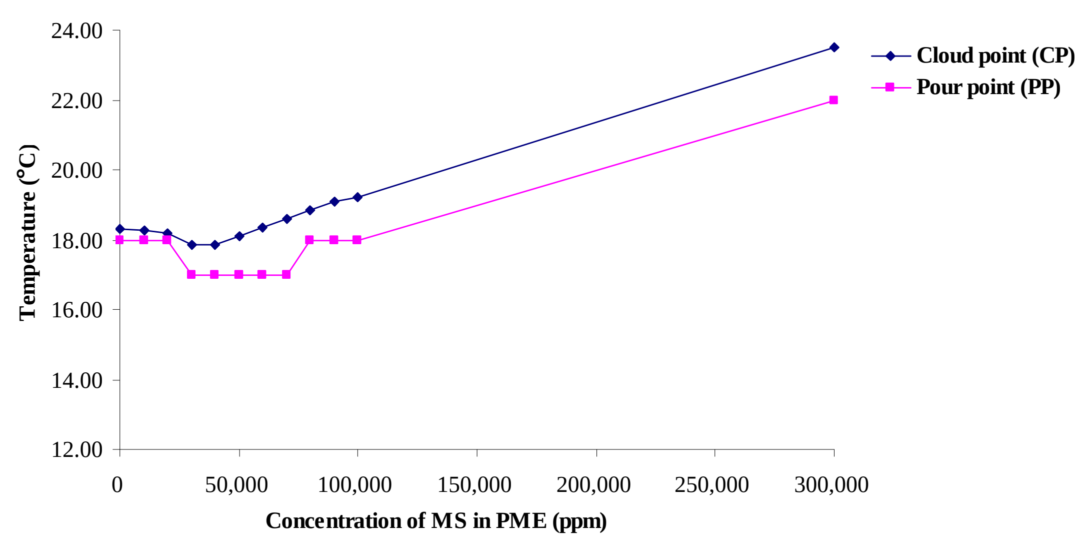

Figure 4.5 CP and PP of PME with various concentrations of MS.

4.6.3 Using *i*-propyl laurate (IPL) as PPDs

As can be seen in Figures 4.6 and 4.7, the CP and PP of IMME were decreased from 3.40°C to -5.30°C (ΔCP = 8.70°C) and from -2.0°C to -11.0°C (ΔPP = 9.0°C) when using 500,000 ppm of IPL. At the same concentration as IMME, the CP and PP of PME were also decreased from 18.30°C to 5.75°C (ΔCP = 12.55°C) and from 18.0°C to 6.0°C (ΔPP = 12.0°C).

It could be seen that the cold flow property of IMME and PME could be improved by adding IPL at the higher concentration. Furthermore, IPL had a greater effect on palm oil because PME contains less amount of short chain fatty acids than IMME (see Table 4.1). The CP and PP of PME were decreased 30.68% and 25%, respectively when compared with IMME.

From the experiment, the cold flow property of IMME and PME could be improved by both ML and IPL. In addition, IPL was more effective PPDs than ML due to the effect of branched chain ester. IPL was synthesized by iso-propanol which was branched chain alcohol, whereas, ML was synthesized by methanol which was straight chain alcohol. The branched chain will hinder the packing of wax crystals to avoid the solidification of oil. Thus, when using IPL as PPDs, the CP and PP of methyl ester were decreased in a large amount when compared with ML.

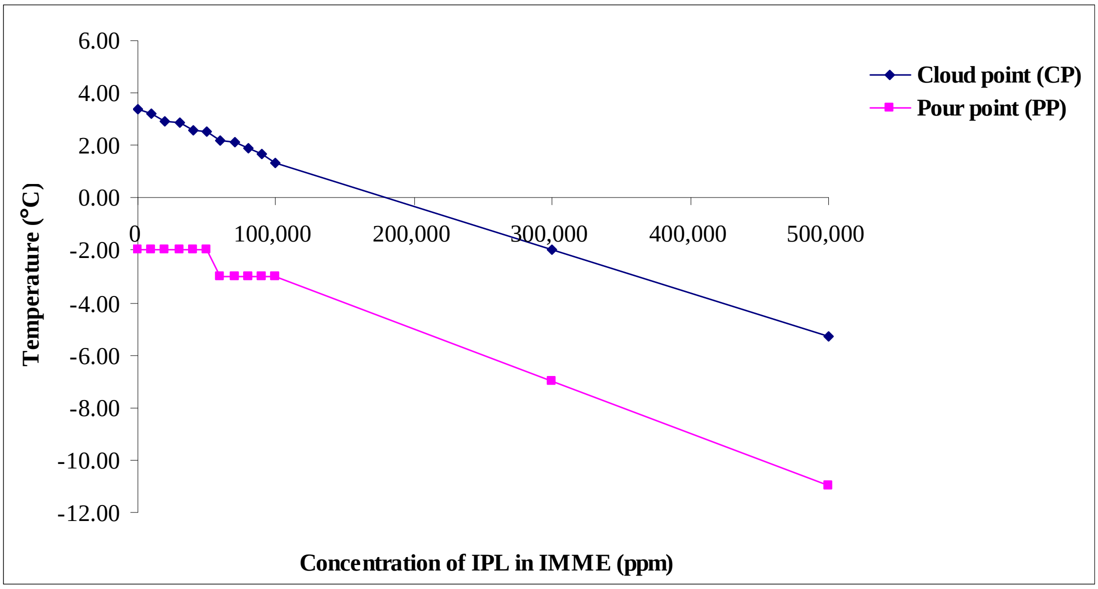

Figure 4.6 CP and PP of IMME with various concentrations of IPL.

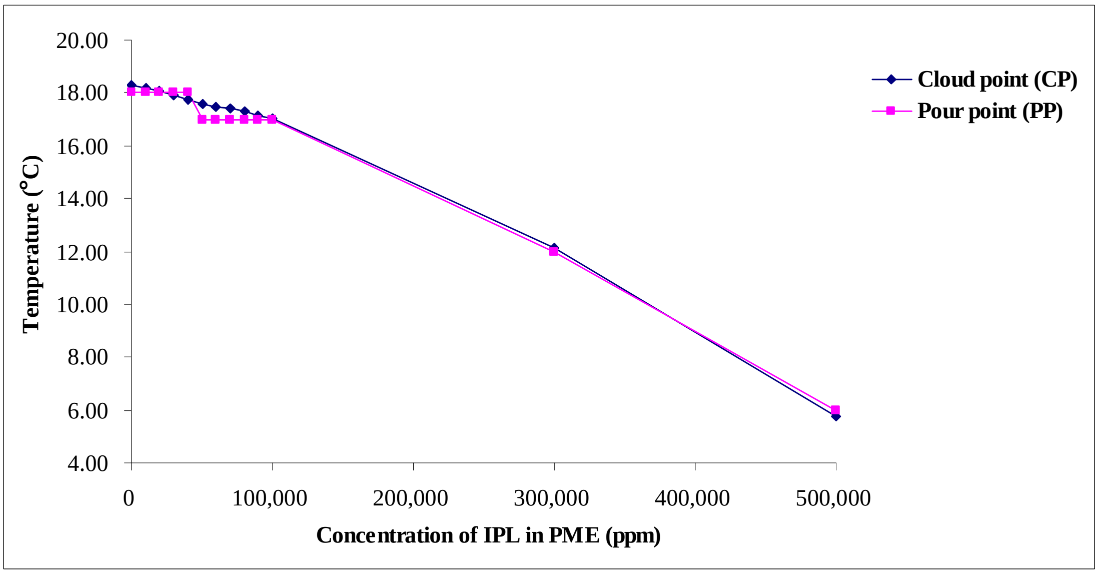

Figure 4.7 CP and PP of PME with various concentrations of IPL.

4.6.4 Using *i*-propyl stearate (IPS) as PPDs

From Figure 4.8, the CP and PP of IMME could not be improved by using IPS with any concentrations because the CP and PP of IPS (24.50±1.0°C and 24.0±1.0°C °C) were higher than IMME. The CP of IMME was increased when using the higher concentration of IPS. The PP of IMME still remained at -2.0°C, however, the PP would be increased if the addition of MS was higher than 60,000 ppm. Due to the chain length of fatty acids, IPS had a higher molecular weight than IMME. Therefore, the CP and PP of IMME were increased when using the higher concentration of IPS.

From Figure 4.9, the CP and PP of PME were improved by using IPS as PPDs and they were better than using MS as PPDs. At 40,000 ppm of IPS, the CP of PME was decreased from 18.30°C to 17.40°C (ΔCP = 0.90°C). The CP was increased when using IPS higher than 40,000 ppm. In addition, the PP of PME could be decreased to 2.0°C when using 30,000-70,000 ppm of IPS.

Similarly to the ML comparing with MS, IPL was also more effective than IPS because the IPL had a shorter hydrocarbon chain and more polar than IPS. The functions of polarity part in PPDs are to prevent the crystal growth and agglomeration which will hinder the solidification of oil.

It could be concluded that the cold flow property of IMME could not be improved by using MS and IPS because the chain length of IMME was shorter than MS and IPS. Moreover, the CP and PP of IMME were lower than MS and IPS (see Table 4.5). When compared with MS, it was found that IPS was more effective than MS with the same reason as the comparison between ML and IPL in section 4.6.3.

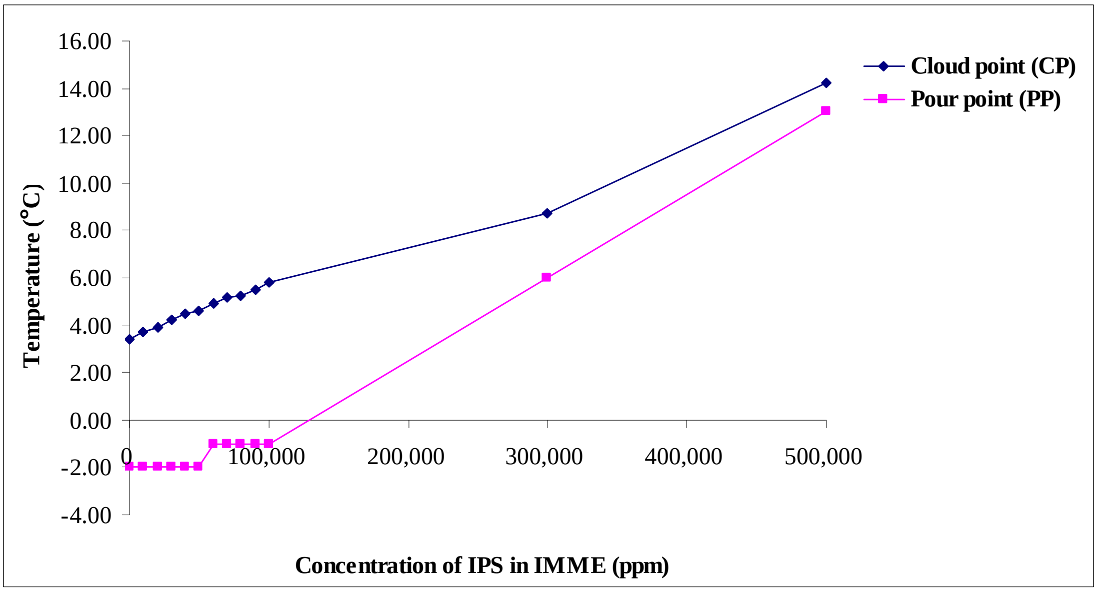

Figure 4.8 CP and PP of IMME with various concentrations of IPS.

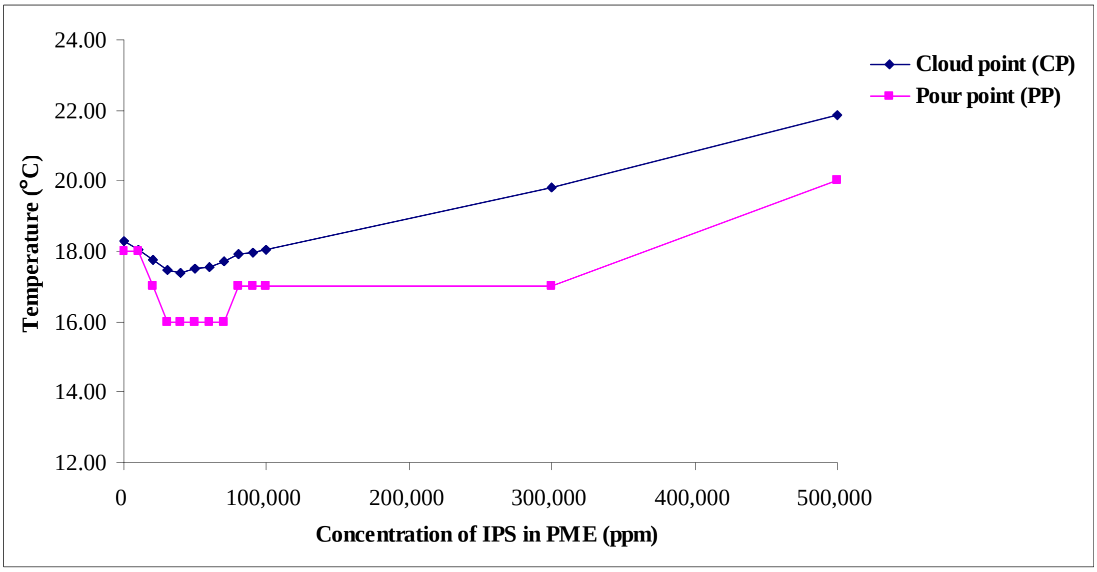

Figure 4.9 CP and PP of PME with various concentrations of IPS.

4.6.5 Using CD017 as PPDs

From Figures 4.10 and 4.11, the CP of IMME was decreased from 3.40°C to 1.40°C. The maximum reduction of CP was achieved by using CD017 at 100 ppm. In contrast, the CP was increased when the higher concentration of CD017 was used. The CP of PME could be dramatically reduced at the concentration of CD017 over 200 ppm. The maximum reduction of CP was obtained at 500 ppm of CD017 which decreased from 18.30°C to 17.50°C. However, the CP would be increased if the addition of CD017 was more than 1,000 ppm due to high amount of CD017 forming self-agglomerate. In addition, the PP of both IMME and PME could not be improved by using CD017 at any concentrations.

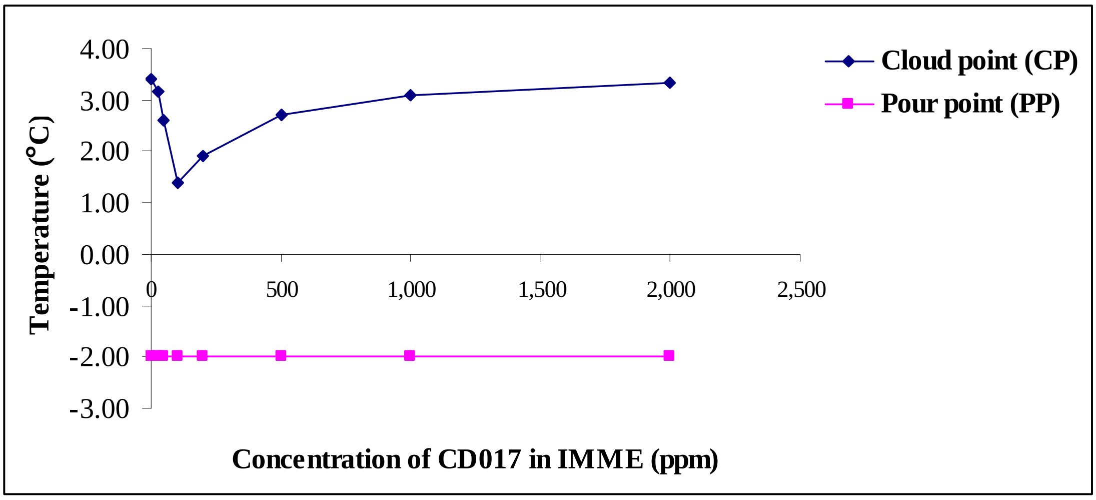

Figure 4.10 CP and PP of IMME with various concentrations of CD017.

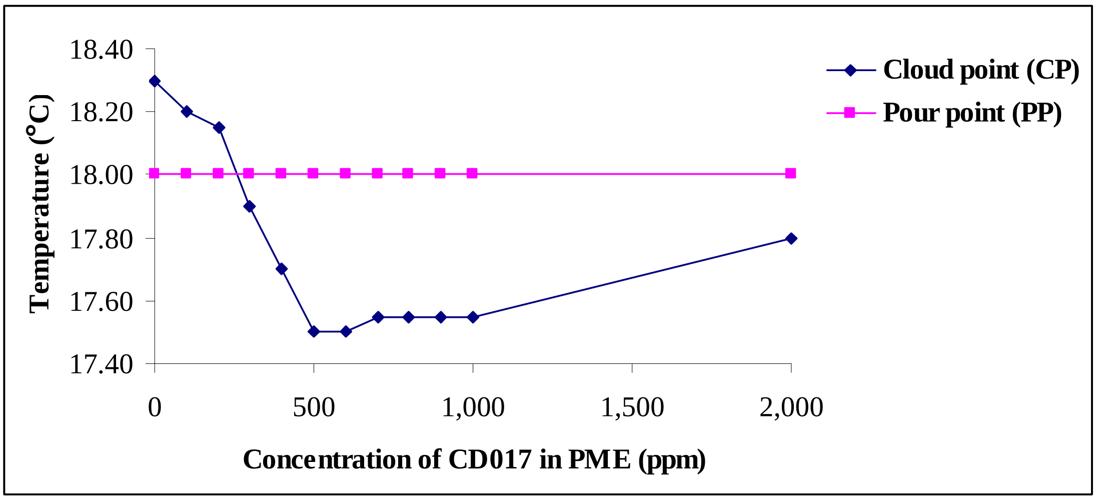

Figure 4.11 CP and PP of PME with various concentrations of CD017.

From Figure 4.12, the CP of diesel fuel was slightly increased when using the higher concentration of CD017. In contrast, the PP could be drastically reduced from -3.0°C to -32.0°C (ΔPP = 29.0°C) at 2,000 ppm of CD017.

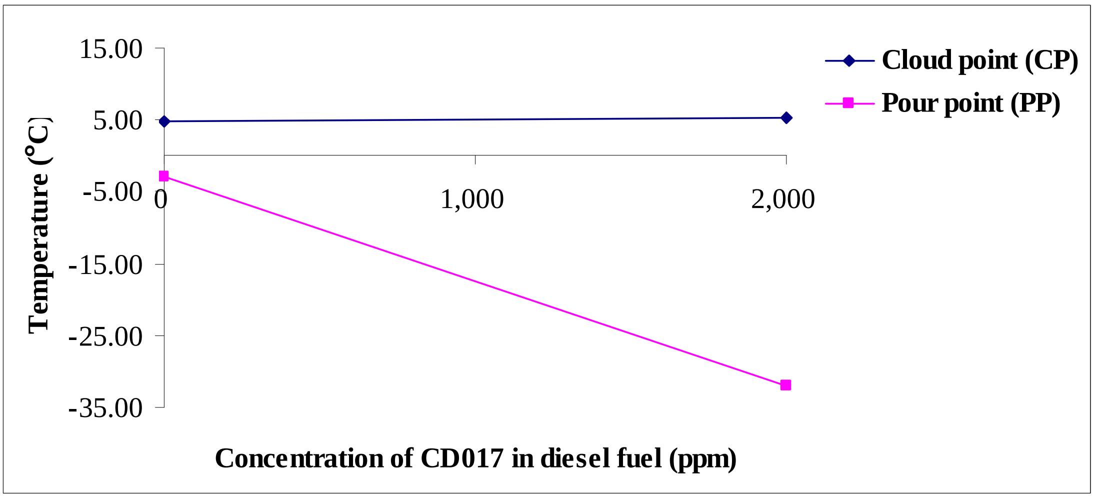

Figure 4.12 CP and PP of diesel fuel with various concentrations of CD017.

4.6.6 Using Zenith as PPDs

From Figures 4.13 and 4.14, the result showed that the cold flow property of IMME could not be improved by using Zenith. In contrast, the CP of PME was slightly decreased from 18.30°C to 17.90°C at 500 ppm of Zenith. The PP of both IME and PME could not be improved by using Zenith at any concentrations.

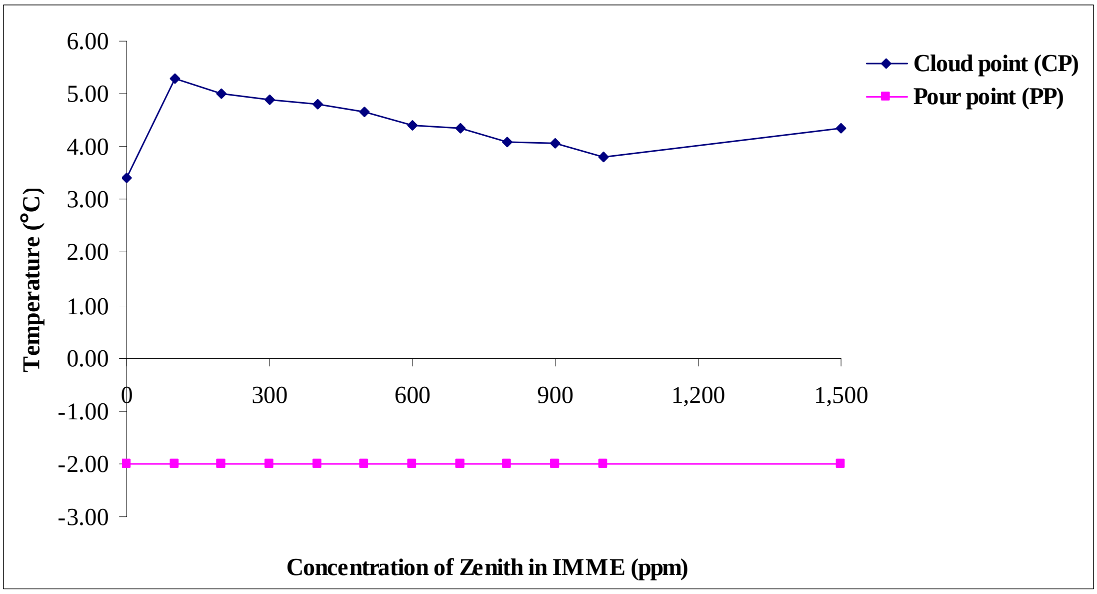

Figure 4.13 CP and PP of IMME with various concentrations of Zenith.

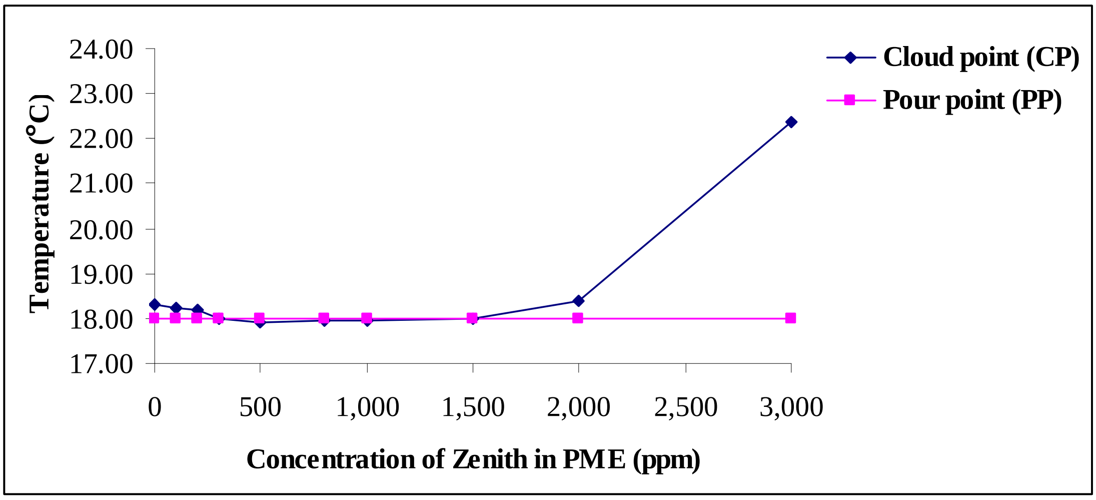

Figure 4.14 CP and PP of PME with various concentrations of Zenith.

From Figure 4.15, the CP of diesel fuel was increased when using the higher concentration of Zenith. At the concentration 10,000 ppm, the PP of diesel fuel was decreased from -3.0°C to -6.0°C (ΔPP = 3.0°C) and the PP was increased when the concentration of Zenith was higher than 10,000 ppm.

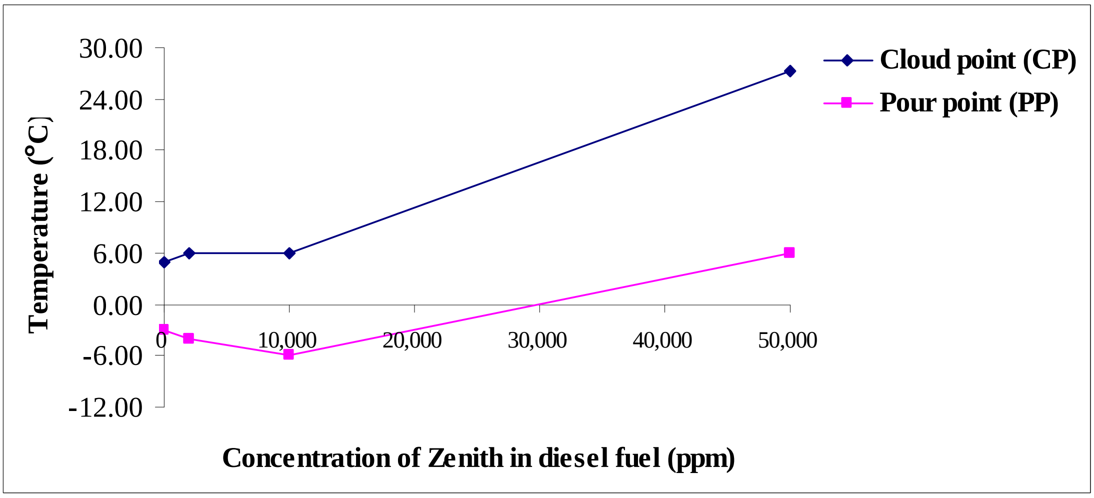

Figure 4.15 CP and PP of diesel fuel with various concentrations of Zenith.

4.6.7 Using Flozol 2251D as PPDs

From Figures 4.16 and 4.17, similarly to Zenith, the cold flow property of IMME could not be improved by using Flozol 2251D. On the other hand, the CP of PME was decreased from 18.30°C to 18.10°C at 300 ppm of Flozol 2251D. The PP of both IMME and PME could not be improved by using Flozol 2251D at any concentrations.

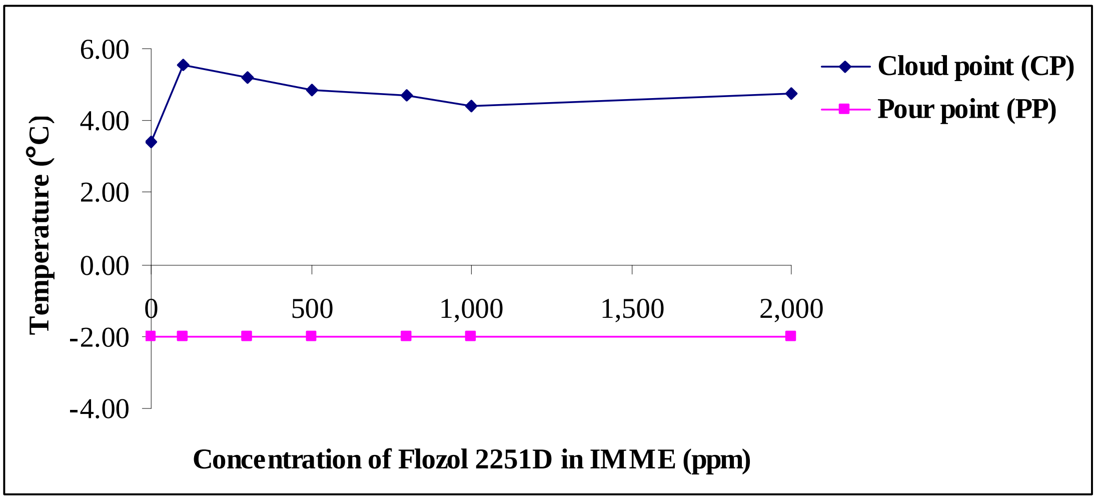

Figure 4.16 CP and PP of IMME with various concentrations of Flozol 2251D.

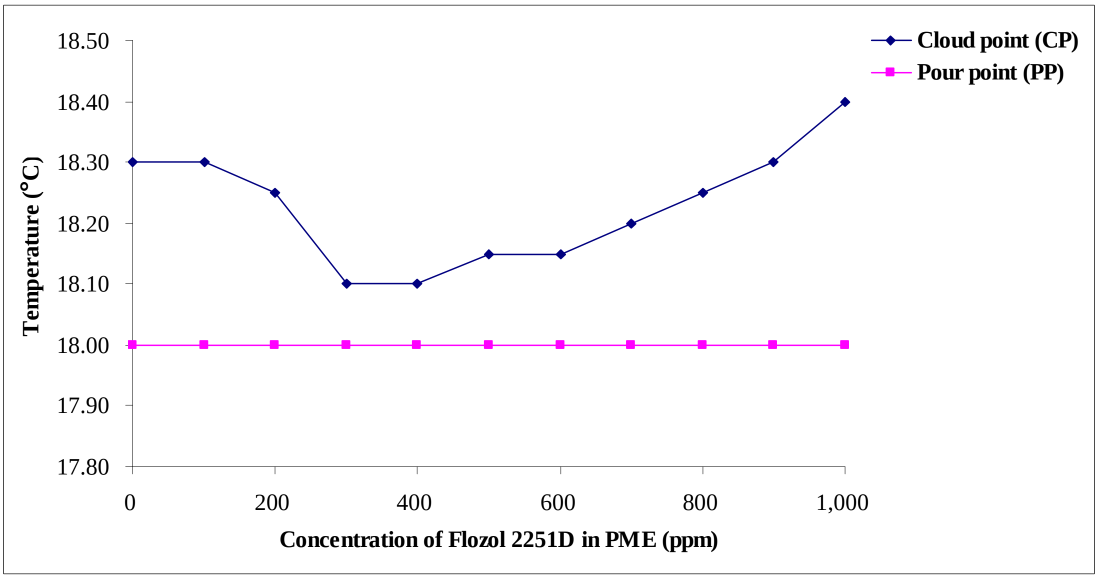

Figure 4.17 CP and PP of PME with various concentrations of Flozol 2251D.

From Figures 4.18, it could be seen that the cold flow property of diesel fuel could not be improved by using Flozol 2251D at any concentrations.

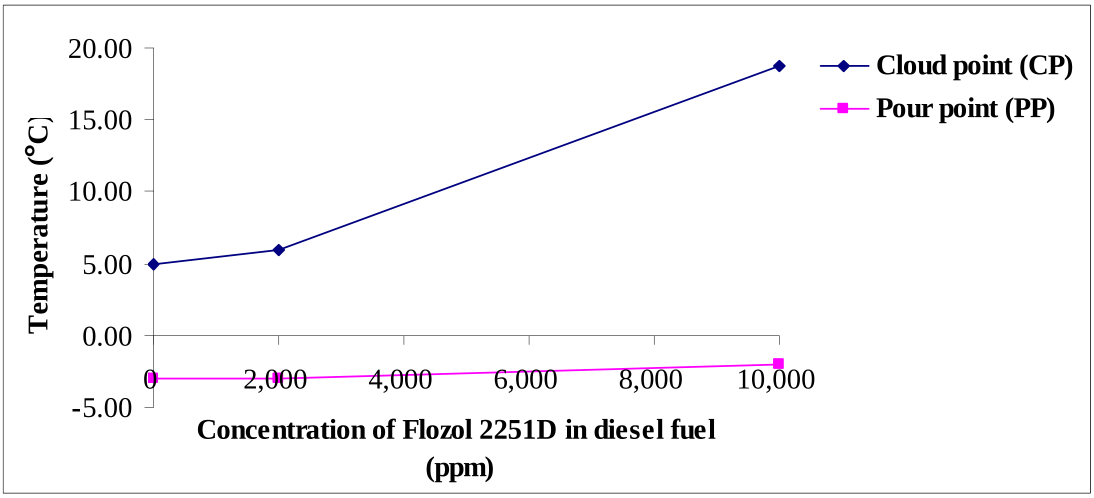

Figure 4.18 CP and PP of diesel fuel with various concentrations of Flozol 2251D.

4.6.8 Using Flozol 112 as PPDs

From Figures 4.19 and 4.20, it could be seen that the cold flow property of IMME and PME could not be improved by using Flozol 112 at any concentrations.

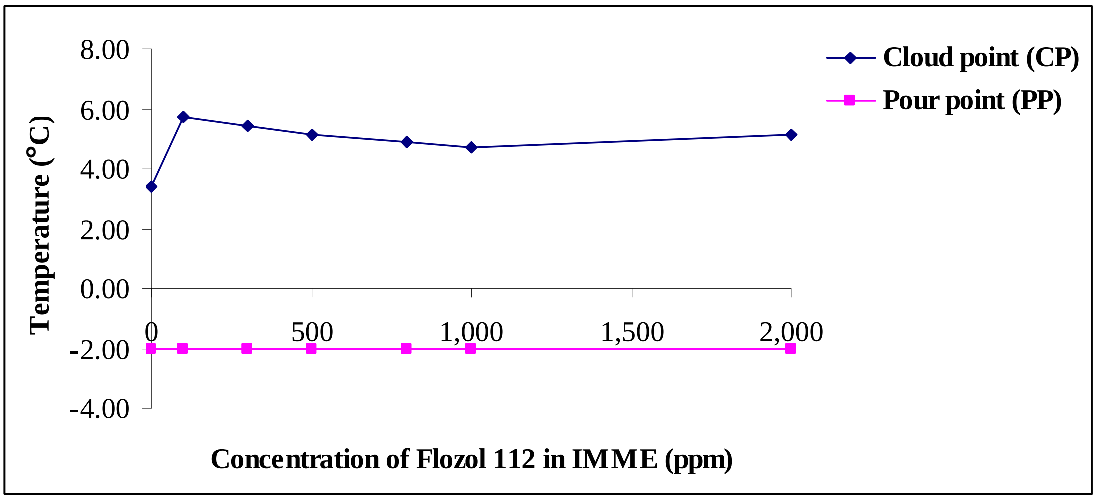

Figure 4.19 CP and PP of IMME with various concentrations of Flozol 112.

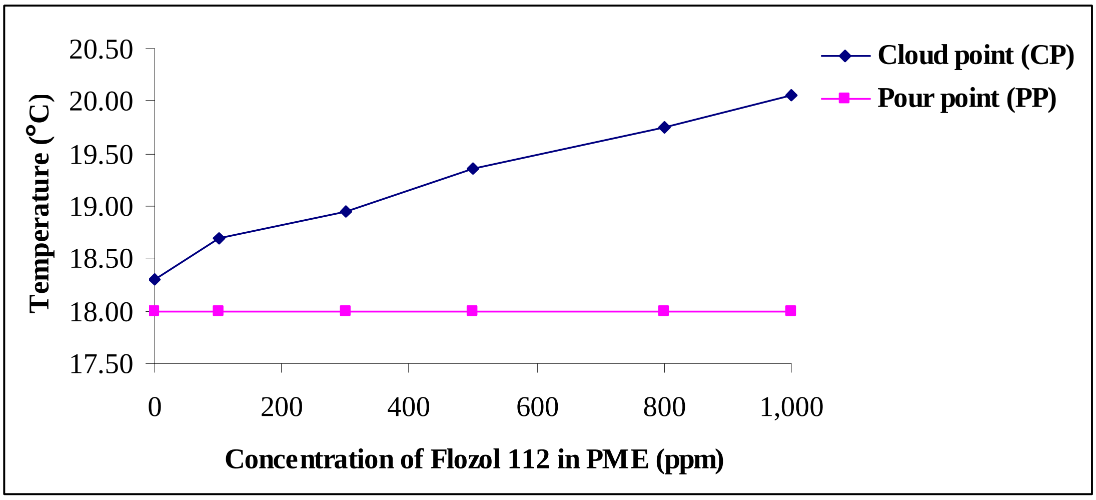

Figure 4.20 CP and PP of PME with various concentrations of Flozol 112.

From Figures 4.21, similarly to Flozol 2251D, the cold flow property of diesel fuel could not be improved by using Flozol 112.

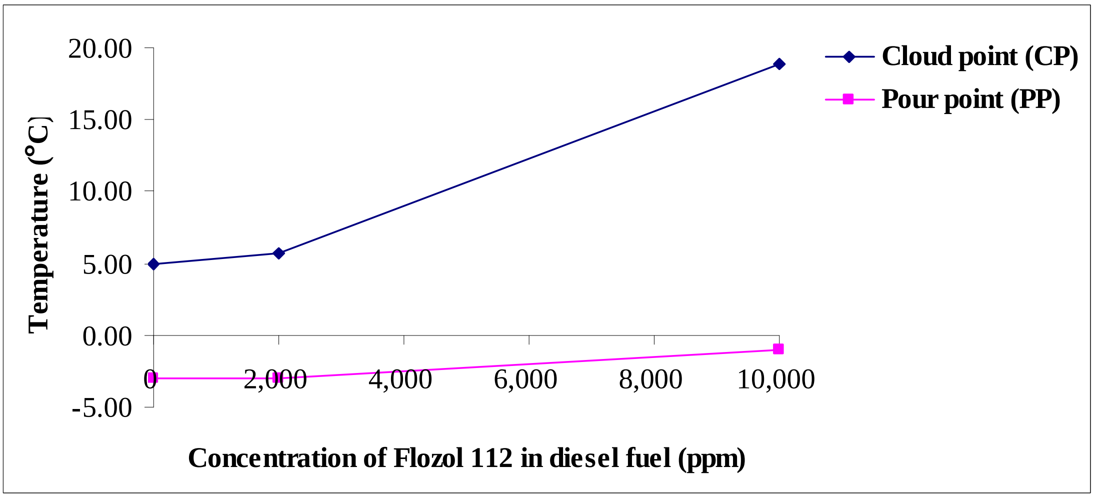

Figure 4.21 CP and PP of diesel fuel with various concentrations of Flozol 112.

4.6.9 Using kerosene as PPDs

From Figures 4.22 and 4.23, the CP and PP of IMME were decreased from 3.40°C to -0.55°C (ΔCP = 3.95°C) and from -2.0°C to -15.0°C (ΔPP = 13.0°C) when using 500,000 ppm of kerosene. At the same concentration as IMME, the CP and PP of PME were also decreased from 18.30°C to 4.75°C (ΔCP = 13.55°C) and from

18.0°C to 5.0°C (ΔPP = 13.0°C). It could be seen that the cold flow property of IMME and PME could be improved by adding kerosene at the higher concentration due to the lowest CP of kerosene among of these commercial additives.

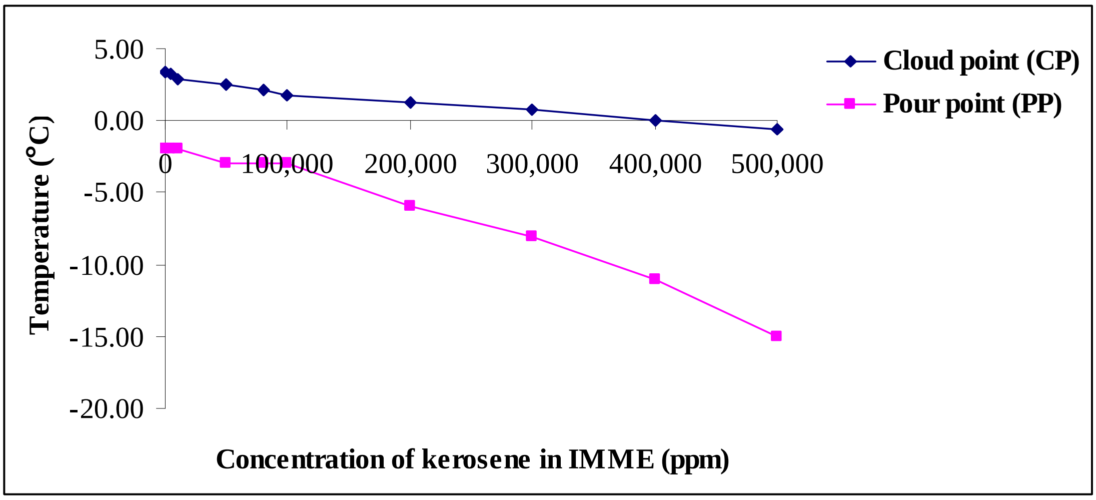

Figure 4.22 CP and PP of IMME with various concentrations of kerosene.

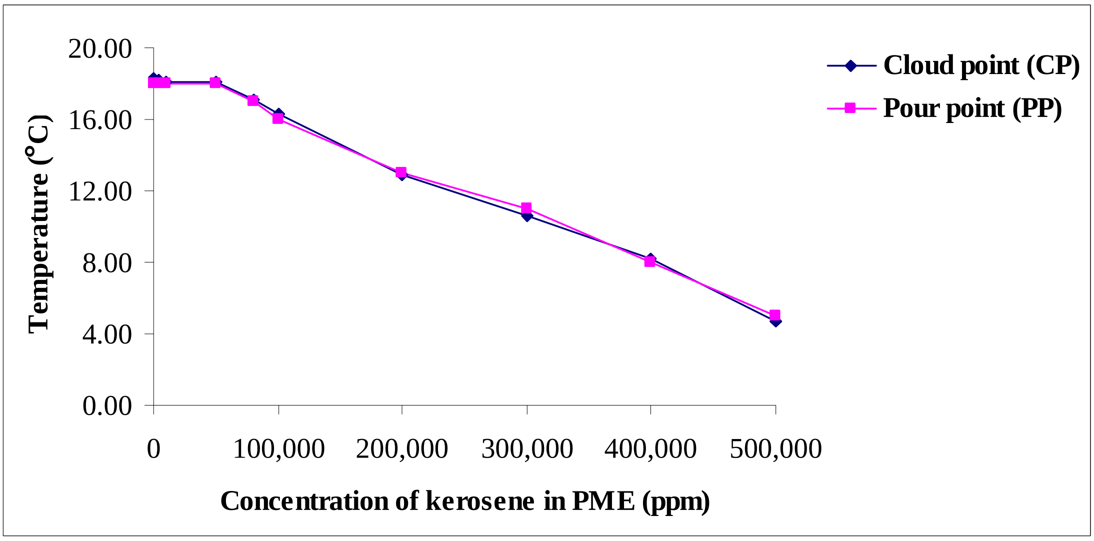

Figure 4.23 CP and PP of PME with various concentrations of kerosene.

For synthesized PPDs, IPL gave the best result on improving cold flow property of IMME and PME. At 500,000 ppm of IPL, the CP and PP of IMME were reduced by 8.70±1.0°C and 9.0±1.0°C, respectively. At the same concentration as IMME, the CP and PP of PME were also reduced by 12.55±1.0°C and 12.0±1.0°C, respectively. It could be concluded that, IPL had a greater effect on palm oil than

IMME because of PME contains less amount of short chain fatty acids. Furthermore, the branched chain of isopropyl moiety will hinder the packing of wax crystals to avoid the solidification of oil.

For commercial additives, kerosene gave the best result on improving cold flow property of IMME and PME due to its CP & PP (< -50.0°C). At 500,000 ppm of kerosene, the CP and PP of IMME were reduced by 3.95±1.0°C and 13.0±1.0°C, respectively. At the same concentration as IMME, the CP and PP of PME were also reduced by 13.55±1.0°C and 13.0±1.0°C, respectively.

CHAPTER V

CONCLUSION AND SUGGESTION

5.1 Conclusion

This research aimed to improve the cold flow property of biodiesel from *Irvingia malayana* Oliv. ex A. Benn. (IM) seeds by using Pour Point Depressant (PPDs). The IM seeds was chosen to be a novel source of biodiesel as its high yield (76% of dry weight basis). It was mainly consisted of 97% of saturated fatty acids especially lauric acid (C12:0) and myristic acid (C14:0) which displayed higher cloud point (CP) and pour point (PP) leading to crystallize at low temperature. The methyl ester of IM oil (IMME) was synthesized via transesterfication using based-catalyzed process. Four synthesized PPDs which were methyl laurate (ML), methyl stearate (MS), *i*-propyl laurate (IPL) and *i*-propyl stearate (IPS) and five commercial additives which were CD017, Zenith, Flozol 2251D, Flozol 112 and kerosene were used to improve cold flow property of methyl esters of IM oil (IMME) and palm oil (PME). Among of these additives, IPL gave the best result on improving cold flow property of IMME and PME. At 500,000 ppm of IPL, the CP and PP of IMME were reduced by 8.70±1.0°C and 9.0±1.0°C, respectively. The CP and PP of PME were also reduced by 12.55±1.0°C and 12.0±1.0°C, respectively at the same concentration as IMME. It could be concluded that, IPL had a greater effect on palm oil than IMME because of PME contains less amount of short chain fatty acids. In addition, the cold flow property could be effected by the types of hydrocarbon chain. At same concentration of IPL and ML, the branched chain alcohol gave the best result on improving cold flow property by which the CP and PP of IMME were reduced by 1.55±1.0°C (17.82%) and 4.0±1.0°C (44.44%), respectively. The CP and PP of PME were also reduced by 2.30±1.0°C (18.33%) and 2.0±1.0°C (16.67%), respectively. The branched chain of isopropyl moiety will hinder the packing of wax crystals to avoid the solidification of oil. On the other hand, the cold flow property of IMME could not be improved by using MS and IPS because of the molecular weight of MS and IPS were higher than that of IMME. For commercial additives, kerosene gave the best result on reducing CP and PP of IMME and PME due to CP & PP of kerosene was below -50.0°C.

5.2 Suggestion

- PPDs should be synthesized with long branched chain alcohol such as tert-butanol and 2-butanol etc. to hinder the solidification of oil.

REFERENCES

[1] Zlatica, J.P. The production of biodiesel from waste frying oils: A comparison of different purification steps. Fuel 87 (2008): 3522–3528.

[2] Haiying, T., Steven, O.S. and Simon, K.Y. Fuel properties and precipitate formation at low temperature in soy-, cottonseed-, and poultry fat-based biodiesel blends. Fuel 87 (2008): 3006-3017.

[3] Chen, B., Sun, Y., Fang, J., Wang, J. and Wu, J. Cold flow properties and crystal morphologies of biodiesel blends. Chemistry and Technology of Fuels and Oils 46 (2010): 52-57.

[4] Bandelier, J., Chunhieng, T., Olle, M. and Montet, D. Original study of the biochemical and oil composition of the Cambodia nut *Irvingia malayana*. Journal of Agricultural and Food Chemistry 50 (2002): 1478-1482.

[5] Knothe, G. Dependence of biodiesel fuel properties on the structure of fatty acid alkyl esters. Fuel Processing Technology 86 (2005): 1059-1070.

[6] Kleinova, A., Paligova, J., Vrbova, M., Mikulec, J. and Cvengros, J. Cold flow properties of fatty esters. Process Safety and Environmental Protection 85 (2007): 390–395.

[7] EPPO Department Operation Centre. Ministry of Energy, Thailand. Energy Statistics [Online]. 2003. Available from : http://www.eppo.go.th [2009, August 19]

[8] Pioch, D., Lozano, P., Rasoanantoandro, M.C., Graille, J., Geneste, P. and Guida, A. Biofuels from catalytic cracking of tropical vegetable oils. Oleagineux 48 (1993): 289-291.

[9] Arie van der Winden. Biodiesel Handbook: (2004), NREL/SR-510-36240.

[10] Knothe, G., Dunn, R.O. and Bagby, M.O. Biodiesel: The use of vegetable oils and their derivatives as alternative diesel fuels. U.S. Department of Agriculture [Online]. 2005. Available from : http://www.biodiesel.org [2009, August 19]

[11] Srivastava, A. and Prasad, R. Triglycerides-based diesel fuels. Renewable and Sustainable Energy Reviews 4 (2000): 111–133.

[12] Agarwal, A.K. Biofuels (alcohols and biodiesel) applications as fuels for internal combustion engines. Program of Energy and Combustion Science 33 (2007): 233-271.

[13] Korbitz, W. Biodiesel production in Europe and North America, an encouraging prospect. Renewable Energy 16 (1999): 1708-183.

[14] Phulkerd, P. Preparation of 1,3-Dioxolane derivatives from glycerol in biodiesel production Master’s Thesis, Department of Chemistry, Faculty of Science, Chulalongkorn University, 2006.

[15] Pramanik, K. Properties and use of *Jatropha curcas* oil and diesel fuel blends in compression ignition engine. Renewable Energy 28 (2003): 239–248.

[16] Schuchardt, U., Sercheli, R. and Matheus, R. Transesterification of Vegetable Oils: a Review. Journal of Brazil Chemistry Society 9 (1998): 199-210.

[17] Meher, L.C., Vidya, S.D. and Naik, S.N. Technical aspects of biodiesel production by transesterification: a review. Renewable and Sustainable Energy Reviews 33 (2000): 10248-10268.

[18] Dorado, M.P., Ballesteros, E., Almeida, J.A., Schellet, C., Lohrlein, H.P. and Krause, R. An alkali-catalyzed transesterification process for high free fatty acid oils. Trans ASAE 45 (2002): 525–529.

[19] Komers, K., Skopal, F., Stloukal, R. and Machek, J. Kinetics and mechanism of the KOH-catalyzed methanolysis of rapeseed oil for biodiesel production. Journal of Europe Lipid Science and Technology 104 (2002): 728–37.

[20] Jeong, G.T., Park, D.H., Kang, C.H., Lee, W.T., Sunwoo, C.S. and Yoon, C.H. Production of biodiesel fuel by transesterification of rapeseed oil. Applied of Biochemistry and Biotechnology 113–116 (2004): 747–58.

[21] Ma, F., Clements, L.D. and Hanna, M.A. The effect of catalyst, free fatty acids, and water on transesterification of beef tallow. Transformation American Society Agriculture Engineer 41 (1998): 1261–4.

[22] Demirbas, A. Importance of biodiesel as transportation fuel. Energy Policy 35 (2007): 4661-4670.

[23] Madras, G., Kolluru, C. and Kumar, R. Synthesis of biodiesel in supercritical Fluids. Fuel 83 (2004): 2029-2033.

[24] Freedman, B., Pryde, E.H. and Mounts, T.L. Variables affecting the yields of fatty esters from transesterified vegetable oils. Journal of American Oil Chemistry Society 61 (1984): 1638–1643.

[25] Ma, F., Clements, L.D. and Hanna, M.A. The effect of mixing on transesterification of beef tallow. Bioresource Technology 69 (1999): 289–93.

[26] Tyson, K.S. Biodiesel Handling and Use Guidelines National Renewable Energy Laboratory, Department of Energy, CO.USA, 2001.

[27] ประกาศกรมธุรกิจพลังงาน เรื่อง กำหนดลักษณะและคุณภาพของไบโอดีเซลประเภทเมทิลเอสเทอร์ของกรดไขมัน. ราชกิจจานุเบกษา (2548), 122 (ตอนพิเศษ 70 ง).

[28] Purnanand, V.B., Nishikant, V.D. and Shashikant, B.T. Improving the low temperature properties of biodiesel fuel. Renewable Energy 34 (2009): 794-800.

[29] Soriano, Jr.N., Migo, V.P. and Mastsumura, M. Ozonized vegetable oil as pour point depressant for neat biodiesel. Fuel 85 (2006): 25-31.

[30] Al-Sabagh, A.M., Noor El-Din, M.R., Morsi, R.E. and Elsabee, M.Z. Styrene-maleic anhydride copolymer esters as flow improvers of waxy crude oil. Journal of Petroleum Science and Engineering 65 (2009): 139-146.

[31] Hemant, P.S., Kiranbala, M.O. and Bharambe, D.P. Performance-based designing of wax crystal growth inhibitors. Energy and Fuels 22 (2008): 3930-3938.

[32] Chuang-Wei, C., Leon, G.S. and Galen, J.S. Impact of cold flow improvers on soybean biodiesel blend. Biomass and Bioenergy 27 (2004): 485-491.

[33] Kumar, S., Gupta, A.K. and Naik, S. Conversion of non-edible oil into biodiesel. Journal of Science and Industrial Research 62 (2003): 124-132.

[34] Meher, L.C. and Naik, S. Optimization of alkali-catalyzed transesterification of Karanja oil for production of biodiesel. Bioresource Technology 97 (2005): 1392-1397.

[35] Nascimento, R.S.V., Soares, V.L.P., Albainante, S. and Barreto, L.R. Effect of ester-additives on the crystallization temperature of methyl hexadecanoate. Journal of Thermal Analysis and Calorimetry 79 (2005): 249-254.

[36] Smith, P.C., Ngothai, Y., Nguyen, Q.D. and O'Neill, B.K. Alkoxylation of biodiesel and its impact on low-temperature properties. Fuel 88 (2009): 605-612.

APPENDICES

APPENDIX A

^{1}H-NMR SPECTRA, GC CHROMATOGRAMS AND IR SPECTRA

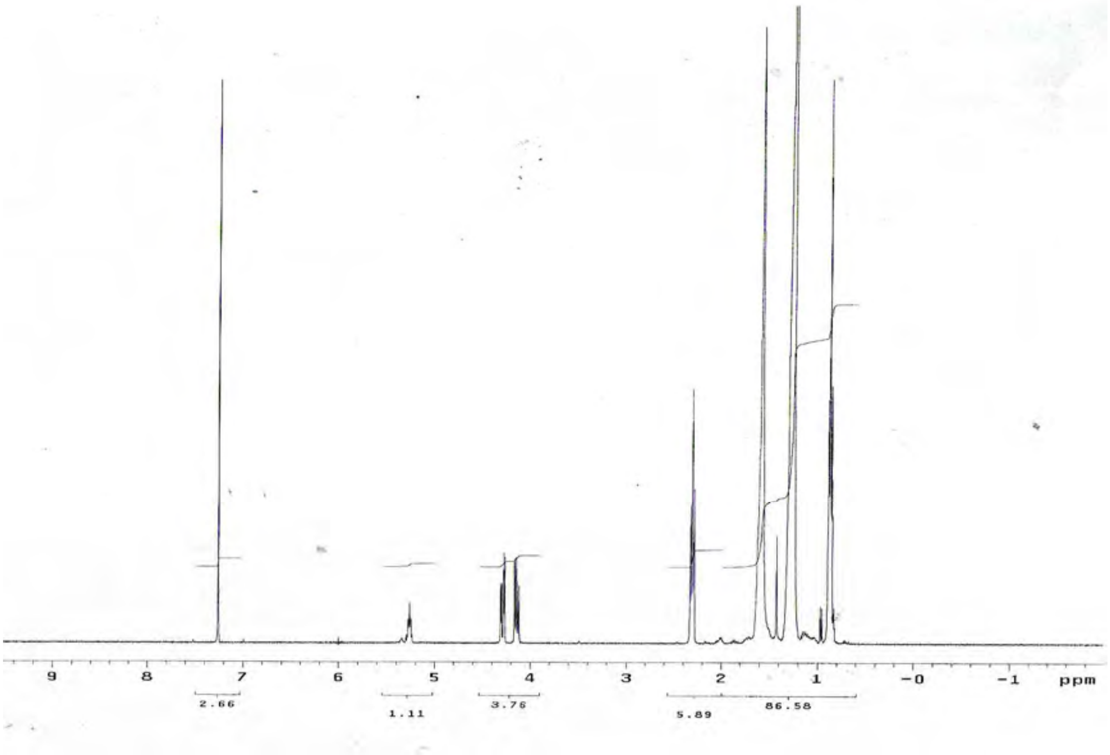

Figure A1 ^{1}H-NMR spectrum of IM oil.

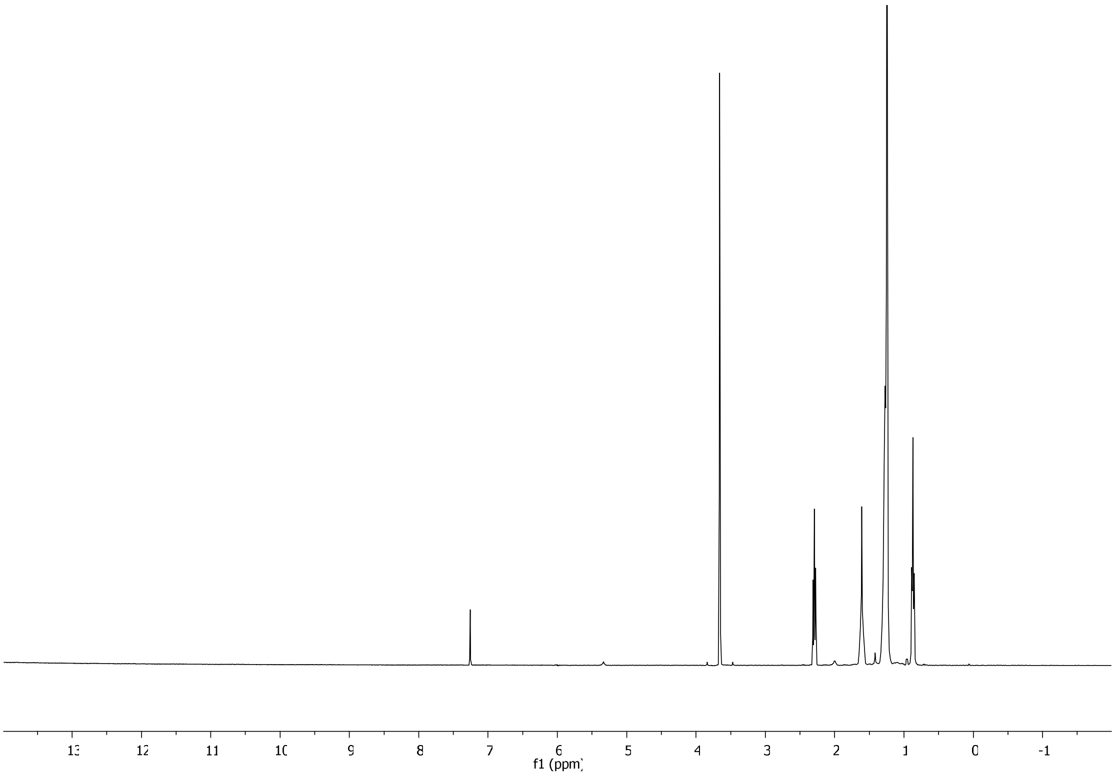

Figure A2 ^{1}H-NMR spectrum of IMME.

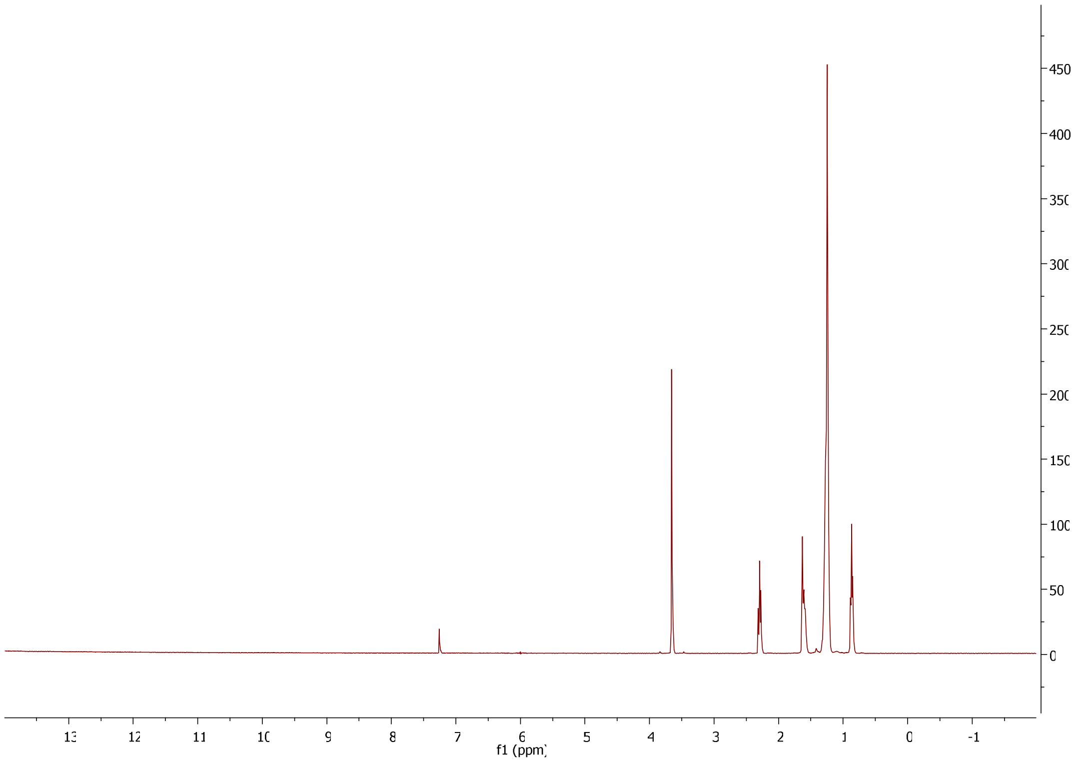

Figure A3 ^{1}H-NMR spectrum of ML.

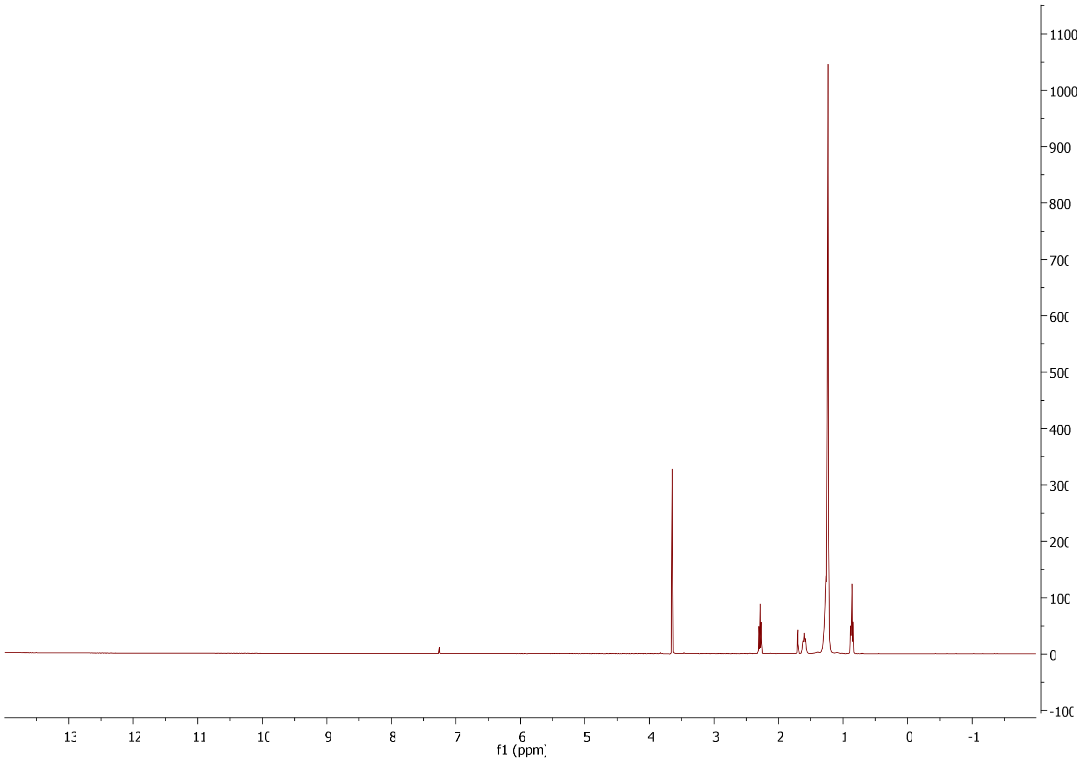

Figure A4 ^{1}H-NMR spectrum of MS.

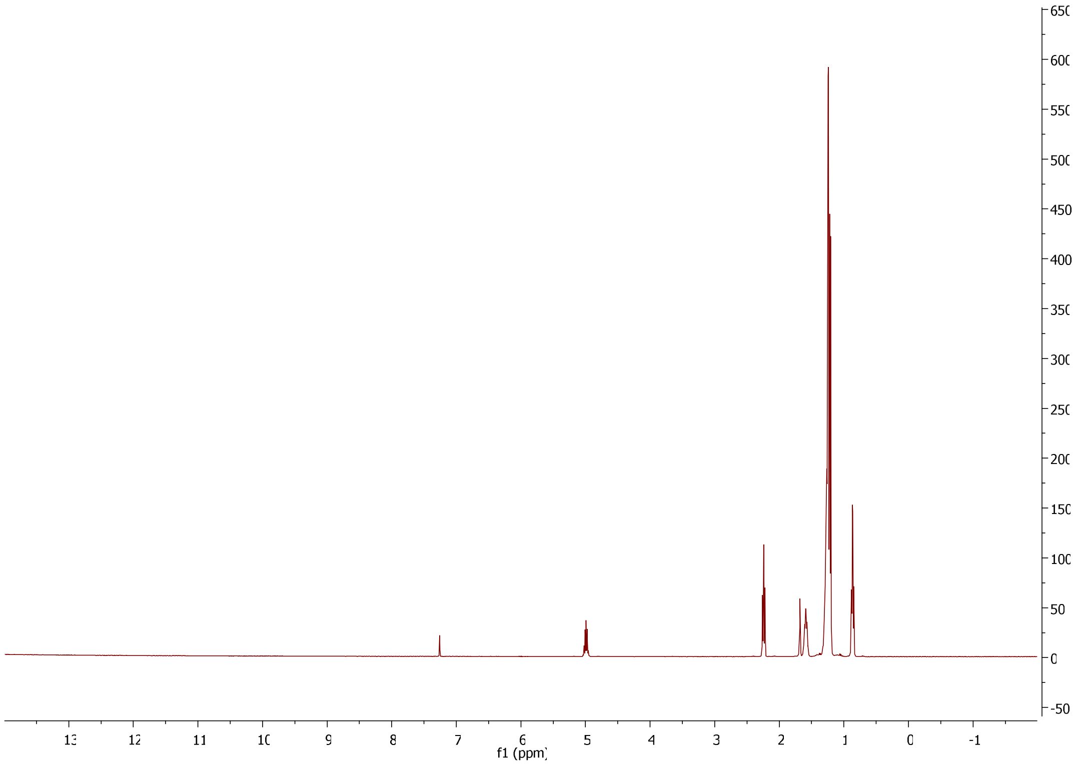

Figure A5 ^{1}H-NMR spectrum of IPL.

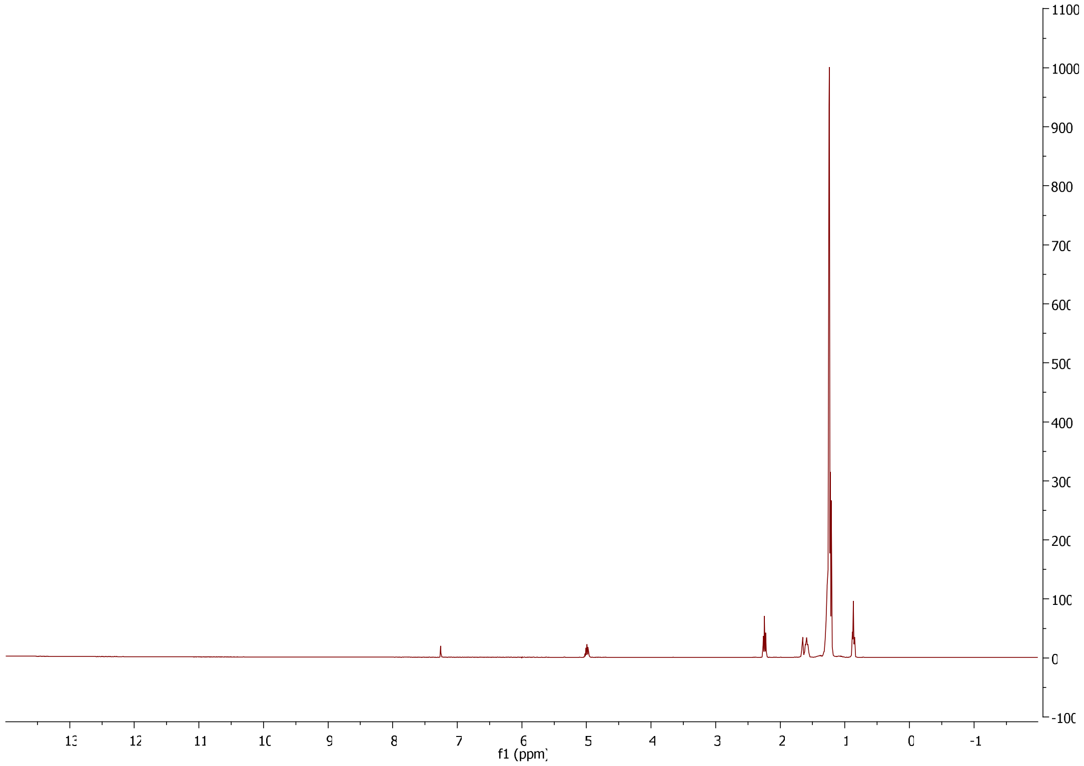

Figure A6 ^{1}H-NMR spectrum of IPS.

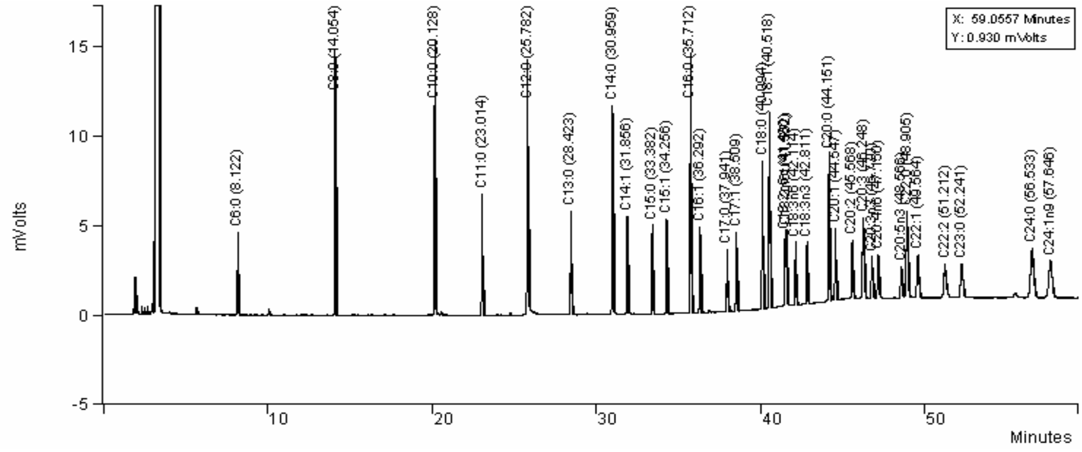

Identification (Peak Name)	Retention time (min)
C6:0 (Caproic)	8.122
C8:0 (Caprylic)	14.054
C10:0 (Capric)	20.128
C11:0 (Undecanoic)	23.014
C12:0 (Lauric)	25.782
C13:0 (Tridecanoic)	28.423
C14:0 (Myristic)	30.959
C14:1 (Myristoleic)	31.856
C15:0 (Pentadecanoic)	33.382
C15:1 (cis-10-Pentadecenoic)	34.256
C16:0 (Palmitic)	35.712
C16:1 (Palmitoleic)	36.292
C17:0 (Heptadecanoic) (Internal standard)	37.941
C17:1 (cis-10-Heptadecenoic)	38.509
C18:0 (Stearic)	40.094
C18:1n9c (Oleic)	40.518
C18:1n9t (Elaidic)	40.612
C18:2n6c (Linoleic)	41.480
C18:2n6t (Linolelaidic)	41.552
C18:3n6 (γ-Linolenic)	42.114
C18:3n3 (α-Linolenic)	42.811
C20:0 (Arachidic)	44.151
C20:1n9 (cis-11-Eicosenoic)	44.547
C20:2 (cis-11,14-Eicosadienoic)	45.568
C20:3n6 (cis-8,11,14-Eicosatrienoic)	46.248
C20:3n3 (cis-11,14,17-Eicosatrienoic)	46.770
C20:4n6 (Arachidonic)	47.150
C20:5n3 (cis-5,8,11,14,17-Eicosapentaenoic)	48.566
C22:0 (Behenic)	48.905
C22:1n9 (Erucic)	49.564
C22:2 (cis-13,16-Docosadienoic)	51.212
C23:0 (Tricosanoic)	52.241
C24:0 (Lignoceric)	56.533
C24:1n9 (Nervonic)	57.646

Figure A7 GC chromatogram of 37 FAMEs standard.

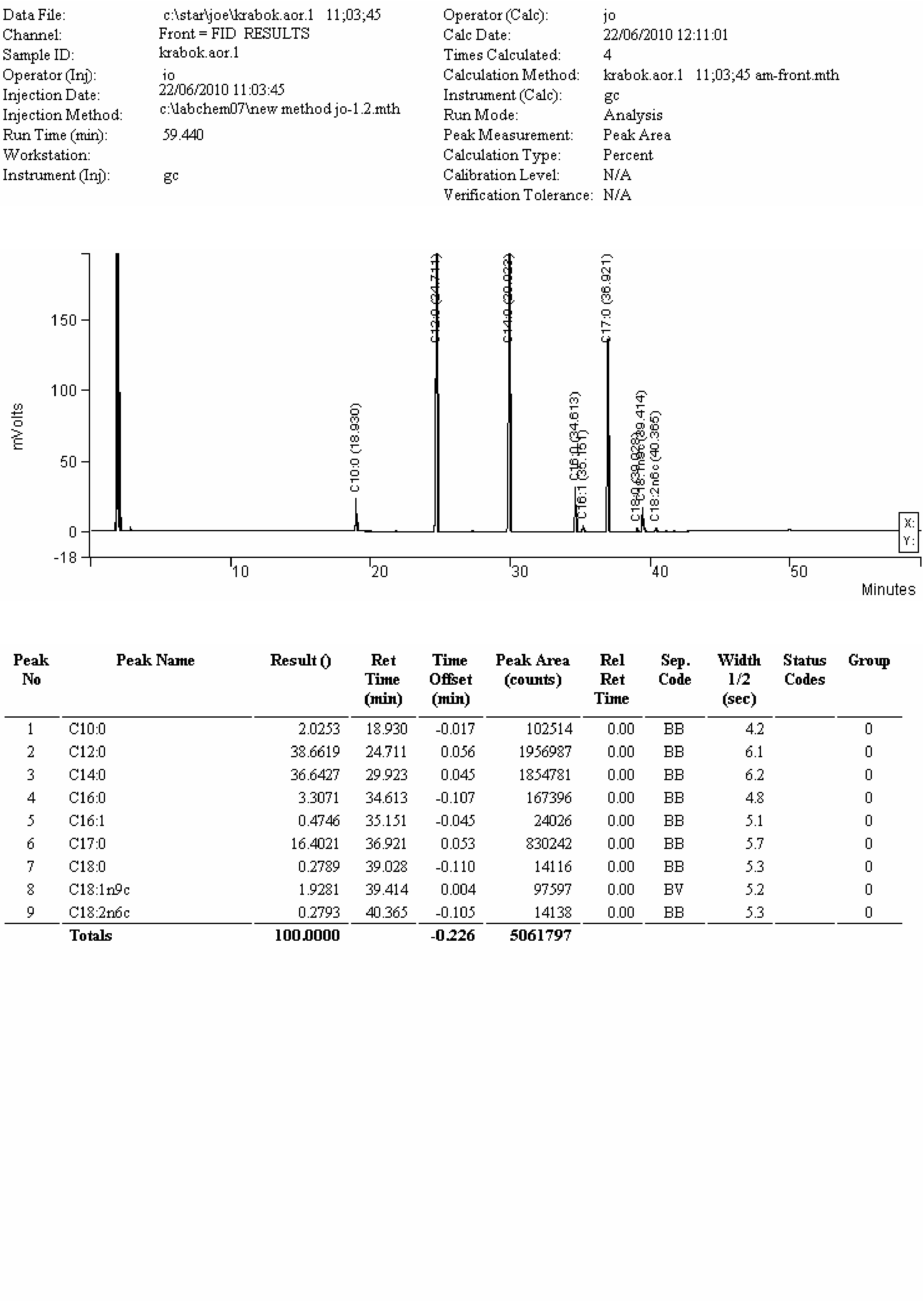

Data File: c:\star\joe\krabok.aor.1 11;03;45
Channel: Front = FID RESULTS
Sample ID: krabok.aor.1
Operator (Inj): jo
Injection Date: 22/06/2010 11:03:45
Injection Method: c:\labchem07\new method jo-1.2.mth
Run Time (min): 59.440
Workstation:
Instrument (Inj): gc

Operator (Calc): jo
Calc Date: 22/06/2010 12:11:01
Times Calculated: 4
Calculation Method: krabok.aor.1 11;03;45 am-front.mth
Instrument (Calc): gc
Run Mode: Analysis
Peak Measurement: Peak Area
Calculation Type: Percent
Calibration Level: N/A
Verification Tolerance: N/A

Peak No	Peak Name	Result ()	Ret Time (min)	Time Offset (min)	Peak Area (counts)	Rel Ret Time	Sep. Code	Width 1/2 (sec)	Status Codes	Group
1	C10:0	2.0253	18.930	-0.017	102514	0.00	BB	4.2		0
2	C12:0	38.6619	24.711	0.056	1956987	0.00	BB	6.1		0
3	C14:0	36.6427	29.923	0.045	1854781	0.00	BB	6.2		0
4	C16:0	3.3071	34.613	-0.107	167396	0.00	BB	4.8		0
5	C16:1	0.4746	35.151	-0.045	24026	0.00	BB	5.1		0
6	C17:0	16.4021	36.921	0.053	830242	0.00	BB	5.7		0
7	C18:0	0.2789	39.028	-0.110	14116	0.00	BB	5.3		0
8	C18:1n9c	1.9281	39.414	0.004	97597	0.00	BV	5.2		0
9	C18:2n6c	0.2793	40.365	-0.105	14138	0.00	BB	5.3		0
	Totals	**100.0000**		**-0.226**	**5061797**					

Figure A8 GC chromatogram of IMME.
]

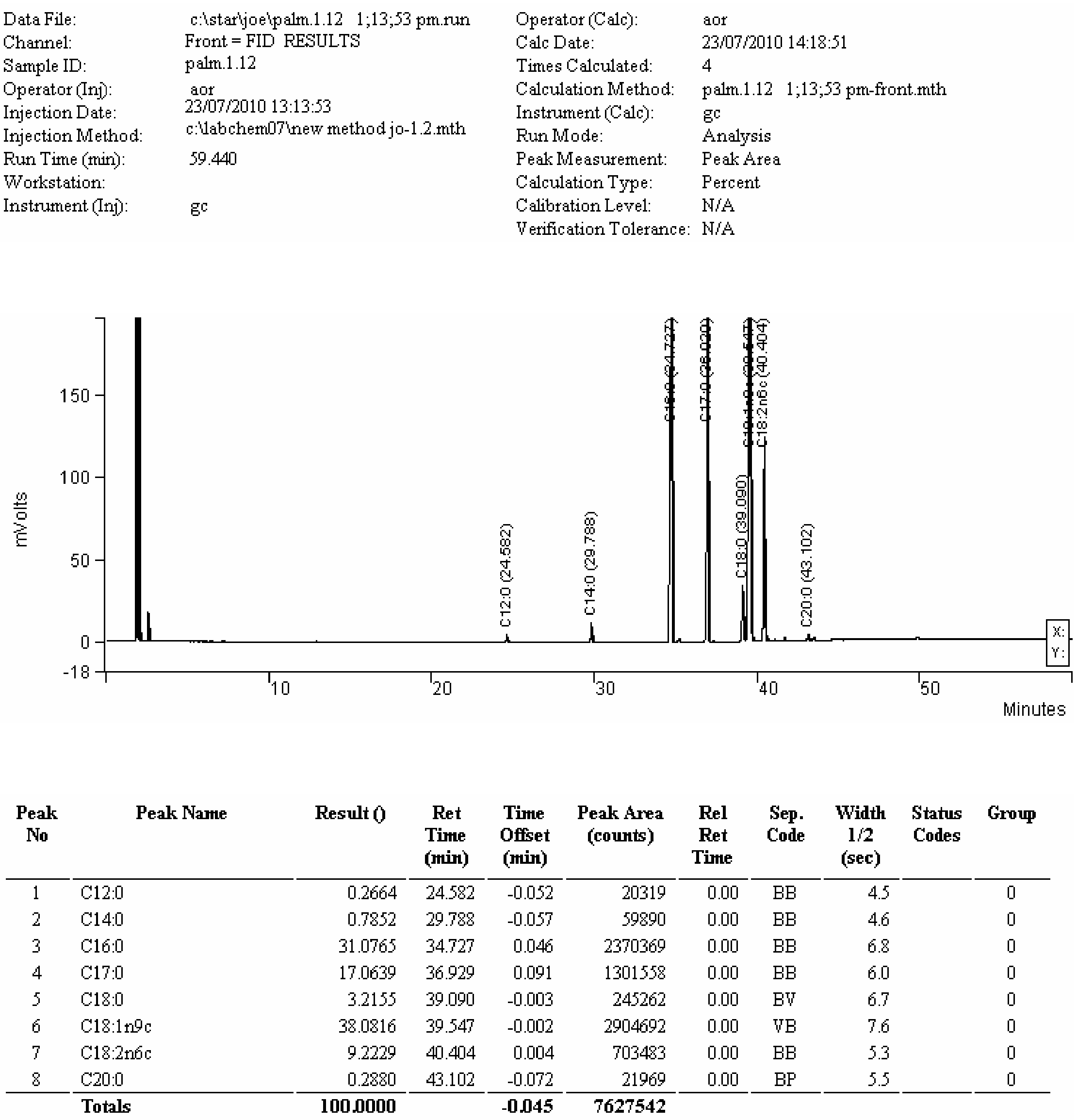

Data File: c:\star\joe\palm.1.12 1;13;53 pm.run
Channel: Front = FID RESULTS
Sample ID: palm.1.12
Operator (Inj): aor
Injection Date: 23/07/2010 13:13:53
Injection Method: c:\labchem07\new method jo-1.2.mth
Run Time (min): 59.440
Workstation:
Instrument (Inj): gc

Operator (Calc): aor
Calc Date: 23/07/2010 14:18:51
Times Calculated: 4
Calculation Method: palm.1.12 1;13;53 pm-front.mth
Instrument (Calc): gc
Run Mode: Analysis
Peak Measurement: Peak Area
Calculation Type: Percent
Calibration Level: N/A
Verification Tolerance: N/A

Peak No	Peak Name	Result ()	Ret Time (min)	Time Offset (min)	Peak Area (counts)	Rel Ret Time	Sep. Code	Width 1/2 (sec)	Status Codes	Group
1	C12:0	0.2664	24.582	-0.052	20319	0.00	BB	4.5		0
2	C14:0	0.7852	29.788	-0.057	59890	0.00	BB	4.6		0
3	C16:0	31.0765	34.727	0.046	2370369	0.00	BB	6.8		0
4	C17:0	17.0639	36.929	0.091	1301558	0.00	BB	6.0		0
5	C18:0	3.2155	39.090	-0.003	245262	0.00	BV	6.7		0
6	C18:1n9c	38.0816	39.547	-0.002	2904692	0.00	VB	7.6		0
7	C18:2n6c	9.2229	40.404	0.004	703483	0.00	BB	5.3		0
8	C20:0	0.2880	43.102	-0.072	21969	0.00	BP	5.5		0
	Totals	**100.0000**		**-0.045**	**7627542**					

Figure A9 GC chromatogram of PME.

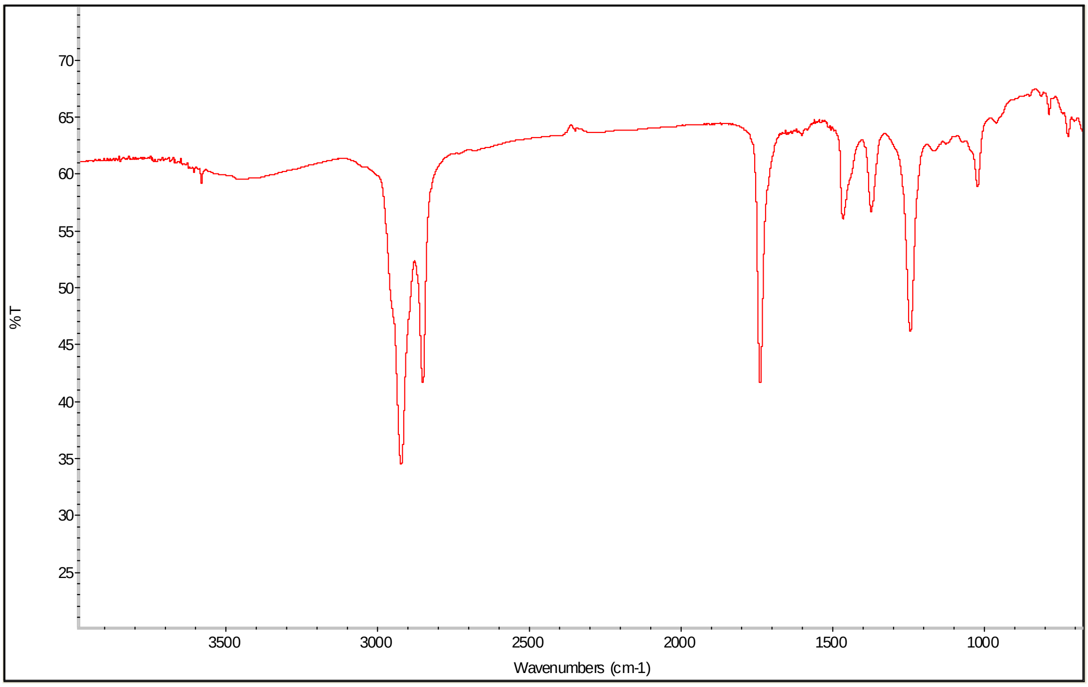

Figure A10 IR spectrum of CD017.

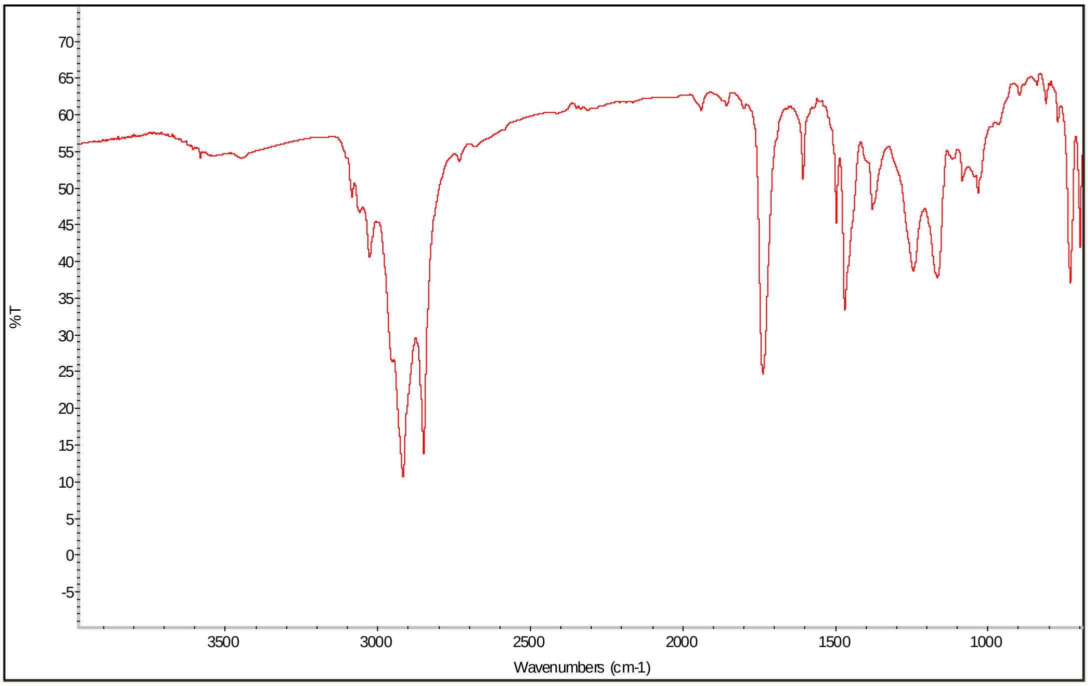

Figure A11 IR spectrum of Zenith.

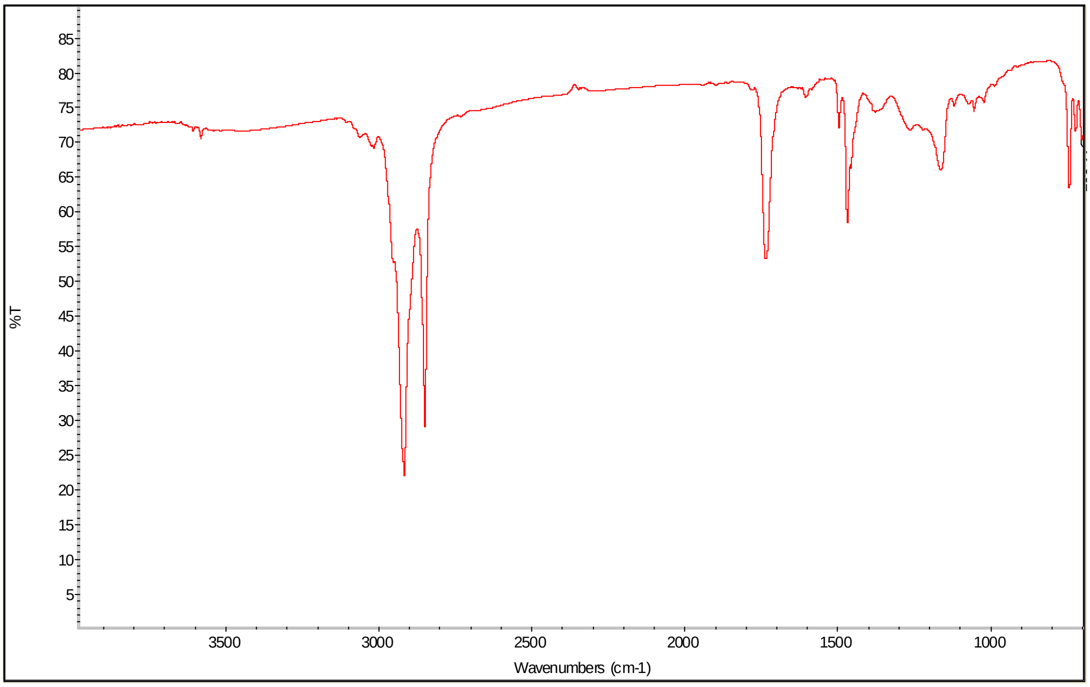

Figure A12 IR spectrum of Flozol 2251D.

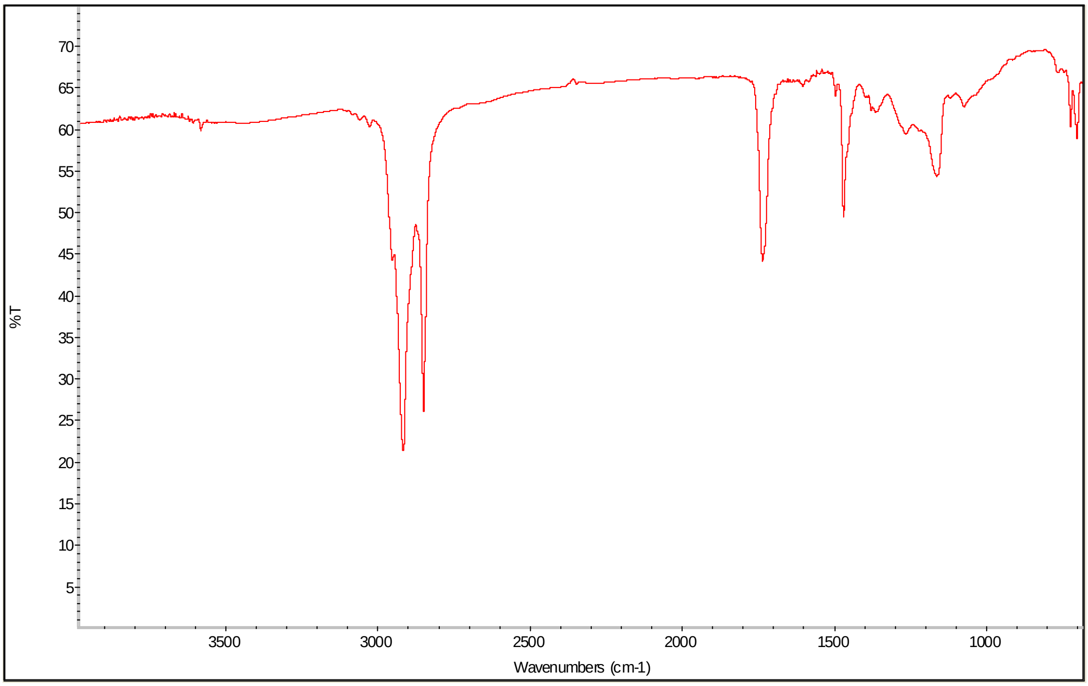

Figure A13 IR spectrum of Flozol 112.

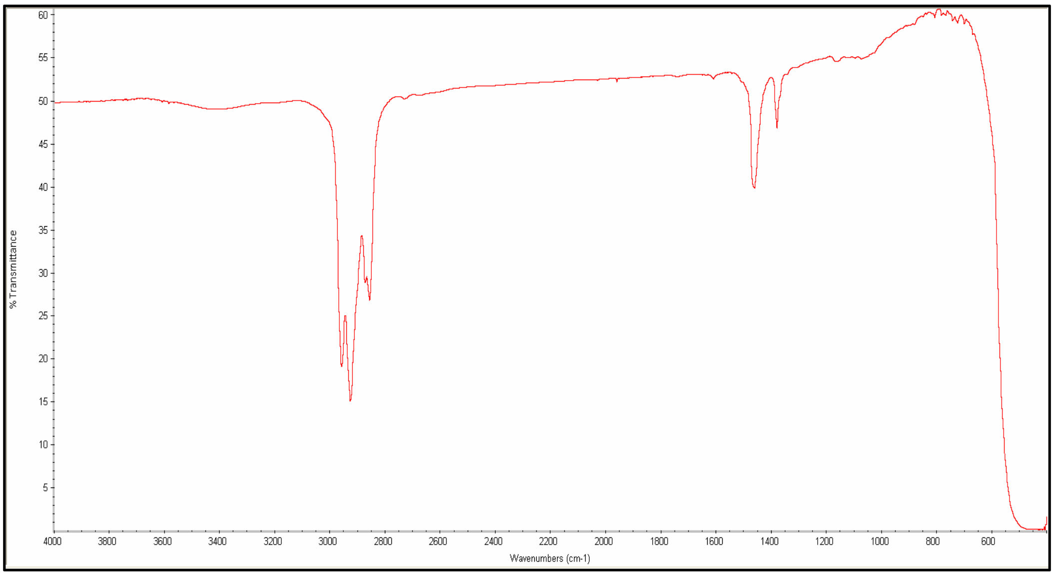

Figure 14 IR spectrum of kerosene.

APPENDIX B

VALUES OF CLOUD POINT AND POUR POINT OF METHYL ESTER OF IM OIL (IMME) AND PALM OIL (PME)

Table B1 Values of CP and PP of IMME using ML as PPDs.

Conc. (ppm)	**CP (°C)**			**PP (°C)**		
	1	2	CP_{ave}	1	2	PP_{ave}
0	3.4	3.4	3.40	-2.0	-2.0	-2.0
10,000	3.4	3.2	3.30	-2.0	-2.0	-2.0
20,000	3.2	3.1	3.15	-2.0	-2.0	-2.0
30,000	2.8	3.0	2.90	-2.0	-2.0	-2.0
40,000	2.7	2.7	2.70	-2.0	-2.0	-2.0
50,000	2.5	2.7	2.60	-2.0	-2.0	-2.0
60,000	2.3	2.5	2.40	-3.0	-3.0	-3.0
70,000	2.3	2.4	2.35	-3.0	-3.0	-3.0
80,000	2.0	2.2	2.10	-3.0	-3.0	-3.0
90,000	1.9	2.2	2.05	-3.0	-3.0	-3.0
100,000	1.9	1.6	1.75	-3.0	-3.0	-3.0
300,000	-1.2	-0.9	-1.05	-5.0	-5.0	-5.0
500,000	-3.9	-3.6	-3.75	-7.0	-7.0	-7.0

Table B2 Values of CP and PP of PME using ML as PPDs.

Conc. (ppm)	**CP (°C)**			**PP (°C)**		
	1	2	CP_{ave}	1	2	PP_{ave}
0	18.3	18.3	18.30	18.0	18.0	18.0
10,000	18.3	18.2	18.25	18.0	18.0	18.0
20,000	18.1	18.1	18.10	18.0	18.0	18.0
30,000	18.0	18.1	18.05	18.0	18.0	18.0
40,000	17.9	18.0	17.95	18.0	18.0	18.0
50,000	17.8	17.8	17.80	18.0	18.0	18.0
60,000	17.4	17.5	17.45	17.0	17.0	17.0
70,000	17.3	17.5	17.40	17.0	17.0	17.0
80,000	17.3	17.3	17.30	17.0	17.0	17.0
90,000	17.3	17.2	17.25	17.0	17.0	17.0
100,000	17.1	17.2	17.15	17.0	17.0	17.0
300,000	13.3	13.5	13.40	13.0	13.0	13.0
500,000	7.9	8.2	8.05	8.0	8.0	8.0

Table B3 Values of CP and PP of IMME using MS as PPDs.

Conc. (ppm)	**CP (°C)**			**PP (°C)**		
	1	2	CP$_{ave}$	1	2	PP$_{ave}$
0	3.4	3.4	3.40	-2.0	-2.0	-2.0
10,000	4.4	4.7	4.55	-2.0	-2.0	-2.0
20,000	4.8	4.8	4.80	-2.0	-2.0	-2.0
30,000	5.1	5.3	5.20	-1.0	-1.0	-1.0
40,000	5.2	5.4	5.30	-1.0	-1.0	-1.0
50,000	5.5	5.3	5.40	0.0	0.0	0.0
60,000	5.6	5.6	5.60	0.0	0.0	0.0
70,000	5.7	6.0	5.85	1.0	1.0	1.0
80,000	6.3	6.1	6.20	1.0	1.0	1.0
90,000	6.3	6.6	6.45	2.0	2.0	2.0
100,000	6.7	6.4	6.55	2.0	2.0	2.0
300,000	13.6	13.3	13.45	12.0	12.0	12.0
500,000	-^{a}	-^{a}	-^{a}	-^{a}	-^{a}	-^{a}

Table B4 Values of CP and PP of PME using MS as PPDs.

Conc. (ppm)	**CP (°C)**			**PP (°C)**		
	1	2	CP$_{ave}$	1	2	PP$_{ave}$
0	18.3	18.3	18.30	18.0	18.0	18.0
10,000	18.2	18.3	18.25	18.0	18.0	18.0
20,000	18.2	18.2	18.20	18.0	18.0	18.0
30,000	17.8	17.9	17.85	17.0	17.0	17.0
40,000	17.9	17.8	17.85	17.0	17.0	17.0
50,000	18.1	18.1	18.10	17.0	17.0	17.0
60,000	18.3	18.4	18.35	17.0	17.0	17.0
70,000	18.5	18.7	18.60	17.0	17.0	17.0
80,000	18.8	18.9	18.85	18.0	18.0	18.0
90,000	19.1	19.1	19.10	18.0	18.0	18.0
100,000	19.3	19.1	19.20	18.0	18.0	18.0
300,000	23.6	23.4	23.50	22.0	22.0	22.0
500,000	-^{a}	-^{a}	-^{a}	-^{a}	-^{a}	-^{a}

****** -^{a} = *not detected*

Table B5 Values of CP and PP of IMME using IPL as PPDs.

Conc. (ppm)	**CP (°C)**			**PP (°C)**		
	1	2	CP_{ave}	1	2	PP_{ave}
0	3.4	3.4	3.40	-2.0	-2.0	-2.0
10,000	3.3	3.1	3.20	-2.0	-2.0	-2.0
20,000	3.1	2.8	2.95	-2.0	-2.0	-2.0
30,000	2.9	2.8	2.85	-2.0	-2.0	-2.0
40,000	2.5	2.7	2.60	-2.0	-2.0	-2.0
50,000	2.4	2.6	2.50	-2.0	-2.0	-2.0
60,000	2.1	2.3	2.20	-3.0	-3.0	-3.0
70,000	2.1	2.1	2.10	-3.0	-3.0	-3.0
80,000	1.8	2.0	1.90	-3.0	-3.0	-3.0
90,000	1.5	1.8	1.65	-3.0	-3.0	-3.0
100,000	1.2	1.5	1.35	-3.0	-3.0	-3.0
300,000	-1.9	-2.0	-1.95	-7.0	-7.0	-7.0
500,000	-5.4	-5.2	-5.30	-11.0	-11.0	-11.0

Table B6 Values of CP and PP of PME using IPL as PPDs.

Conc. (ppm)	**CP (°C)**			**PP (°C)**		
	1	2	CP_{ave}	1	2	PP_{ave}
0	18.3	18.3	18.30	18.0	18.0	18.0
10,000	18.1	18.3	18.20	18.0	18.0	18.0
20,000	17.9	18.2	18.05	18.0	18.0	18.0
30,000	17.9	17.9	17.90	18.0	18.0	18.0
40,000	17.6	17.9	17.75	18.0	18.0	18.0
50,000	17.7	17.5	17.60	17.0	17.0	17.0
60,000	17.5	17.4	17.45	17.0	17.0	17.0
70,000	17.4	17.4	17.40	17.0	17.0	17.0
80,000	17.2	17.4	17.30	17.0	17.0	17.0
90,000	17.0	17.3	17.15	17.0	17.0	17.0
100,000	17.1	17.0	17.05	17.0	17.0	17.0
300,000	12.1	12.2	12.15	12.0	12.0	12.0
500,000	5.8	5.7	5.75	6.0	6.0	6.0

Table B7 Values of CP and PP of IMME using IPS as PPDs.

Conc. (ppm)	**CP (°C)**			**PP (°C)**		
	1	2	CP_{ave}	1	2	PP_{ave}
0	3.4	3.4	3.40	-2.0	-2.0	-2.0
10,000	3.6	3.8	3.70	-2.0	-2.0	-2.0
20,000	4.0	3.8	3.90	-2.0	-2.0	-2.0
30,000	4.2	4.3	4.25	-2.0	-2.0	-2.0
40,000	4.3	4.6	4.45	-2.0	-2.0	-2.0
50,000	4.5	4.7	4.60	-2.0	-2.0	-2.0
60,000	4.9	5.0	4.95	-1.0	-1.0	-1.0
70,000	5.2	5.2	5.20	-1.0	-1.0	-1.0
80,000	5.4	5.1	5.25	-1.0	-1.0	-1.0
90,000	5.4	5.6	5.50	-1.0	-1.0	-1.0
100,000	5.9	5.7	5.80	-1.0	-1.0	-1.0
300,000	8.9	8.6	8.75	6.0	6.0	6.0
500,000	14.3	14.2	14.25	13.0	13.0	13.0

Table B8 Values of CP and PP of PME using IPS as PPDs.

Conc. (ppm)	**CP (°C)**			**PP (°C)**		
	1	2	CP_{ave}	1	2	PP_{ave}
0	18.3	18.3	18.30	18.0	18.0	18.0
10,000	18.0	18.1	18.05	18.0	18.0	18.0
20,000	17.7	17.8	17.75	17.0	17.0	17.0
30,000	17.5	17.4	17.45	16.0	16.0	16.0
40,000	17.3	17.5	17.40	16.0	16.0	16.0
50,000	17.5	17.5	17.50	16.0	16.0	16.0
60,000	17.5	17.6	17.55	16.0	16.0	16.0
70,000	17.7	17.7	17.70	16.0	16.0	16.0
80,000	17.9	17.9	17.90	17.0	17.0	17.0
90,000	18.0	17.9	17.95	17.0	17.0	17.0
100,000	18.0	18.1	18.05	17.0	17.0	17.0
300,000	19.9	19.7	19.80	17.0	17.0	17.0
500,000	21.9	21.8	21.85	20.0	20.0	20.0

Table B9 Values of CP and PP of IMME using CD017 as PPDs.

Conc. (ppm)	**CP (°C)**			**PP (°C)**		
	1	2	CP_{ave}	1	2	PP_{ave}
0	3.4	3.4	3.40	-2.0	-2.0	-2.0
25	3.2	3.1	3.15	-2.0	-2.0	-2.0
50	2.6	2.6	2.60	-2.0	-2.0	-2.0
100	1.3	1.5	1.40	-2.0	-2.0	-2.0
200	1.9	1.9	1.90	-2.0	-2.0	-2.0
500	2.8	2.9	2.70	-2.0	-2.0	-2.0
1,000	3.1	3.1	3.10	-2.0	-2.0	-2.0
2,000	3.3	3.4	3.35	-2.0	-2.0	-2.0

Table B10 Values of CP and PP of PME using CD017 as PPDs.

Conc. (ppm)	**CP (°C)**			**PP (°C)**		
	1	2	CP_{ave}	1	2	PP_{ave}
0	18.3	18.3	18.30	18.0	18.0	18.0
100	18.2	18.2	18.20	18.0	18.0	18.0
200	18.2	18.1	18.15	18.0	18.0	18.0
300	18.0	17.8	17.90	18.0	18.0	18.0
400	17.7	17.7	17.70	18.0	18.0	18.0
500	17.5	17.5	17.50	18.0	18.0	18.0
600	17.5	17.5	17.50	18.0	18.0	18.0
700	17.5	17.6	17.55	18.0	18.0	18.0
800	17.5	17.6	17.55	18.0	18.0	18.0
900	17.6	17.5	17.55	18.0	18.0	18.0
1,000	17.6	17.5	17.55	18.0	18.0	18.0
2,000	17.8	17.8	17.80	18.0	18.0	18.0

Table B11 Values of CP and PP of diesel fuel using CD017 as PPDs.

Conc. (ppm)	**CP (°C)**			**PP (°C)**		
	1	2	CP_{ave}	1	2	PP_{ave}
0	4.9	4.9	4.90	-3.0	-3.0	-3.0
2,000	5.1	5.3	5.20	-32.0	-32.0	-32.0

Table B12 Values of CP and PP of IMME using Zenith as PPDs.

Conc. (ppm)	**CP (°C)**			**PP (°C)**		
	1	2	CP_{ave}	1	2	PP_{ave}
0	3.4	3.4	3.40	-2.0	-2.0	-2.0
100	5.2	5.4	5.30	-2.0	-2.0	-2.0
200	5.0	5.0	5.00	-2.0	-2.0	-2.0
300	4.8	5.0	4.90	-2.0	-2.0	-2.0
400	4.9	4.7	4.80	-2.0	-2.0	-2.0
500	4.6	4.7	4.65	-2.0	-2.0	-2.0
600	4.3	4.5	4.40	-2.0	-2.0	-2.0
700	4.5	4.2	4.35	-2.0	-2.0	-2.0
800	4.2	4.0	4.10	-2.0	-2.0	-2.0
900	3.9	4.2	4.05	-2.0	-2.0	-2.0
1,000	3.8	3.8	3.80	-2.0	-2.0	-2.0
1,500	4.2	4.5	4.35	-2.0	-2.0	-2.0

Table B13 Values of CP and PP of PME using Zenith as PPDs.

Conc. (ppm)	**CP (°C)**			**PP (°C)**		
	1	2	CP_{ave}	1	2	PP_{ave}
0	18.3	18.3	18.30	18.0	18.0	18.0
100	18.3	18.2	18.25	18.0	18.0	18.0
200	18.2	18.2	18.20	18.0	18.0	18.0
300	18.0	18.0	18.00	18.0	18.0	18.0
500	17.9	17.9	17.90	18.0	18.0	18.0
800	17.9	18.0	17.95	18.0	18.0	18.0
1,000	17.8	18.1	17.95	18.0	18.0	18.0
1,500	18.1	17.9	18.00	18.0	18.0	18.0
2,000	18.5	18.3	18.40	18.0	18.0	18.0
3,000	22.3	22.4	22.35	18.0	18.0	18.0

Table B14 Values of CP and PP of diesel fuel using Zenith as PPDs.

Conc. (ppm)	**CP (°C)**			**PP (°C)**		
	1	2	CP_{ave}	1	2	PP_{ave}
0	4.9	4.9	4.90	-3.0	-3.0	-3.0
2,000	5.8	6.0	5.90	-4.0	-4.0	-4.0
10,000	6.0	6.0	6.00	-6.0	-6.0	-6.0
50,000	27.2	27.4	27.3	6.0	6.0	6.0

Table B15 Values of CP and PP of IMME using Flozol 2251D as PPDs.

Conc. (ppm)	CP (°C)			PP (°C)		
	1	2	CP_{ave}	1	2	PP_{ave}
0	3.4	3.4	3.40	-2.0	-2.0	-2.0
100	5.7	5.4	5.55	-2.0	-2.0	-2.0
300	5.3	5.1	5.20	-2.0	-2.0	-2.0
500	4.8	4.9	4.85	-2.0	-2.0	-2.0
800	4.7	4.7	4.70	-2.0	-2.0	-2.0
1,000	4.3	4.5	4.40	-2.0	-2.0	-2.0
2,000	4.8	4.7	4.75	-2.0	-2.0	-2.0

Table B16 Values of CP and PP of PME using Flozol 2251D as PPDs.

Conc. (ppm)	CP (°C)			PP (°C)		
	1	2	CP_{ave}	1	2	PP_{ave}
0	18.3	18.3	18.30	18.0	18.0	18.0
100	18.3	18.3	18.30	18.0	18.0	18.0
200	18.2	18.3	18.25	18.0	18.0	18.0
300	18.1	18.1	18.10	18.0	18.0	18.0
400	18.1	18.1	18.10	18.0	18.0	18.0
500	18.1	18.2	18.15	18.0	18.0	18.0
600	18.2	18.1	18.15	18.0	18.0	18.0
700	18.2	18.2	18.20	18.0	18.0	18.0
800	18.3	18.2	18.25	18.0	18.0	18.0
900	18.3	18.3	18.30	18.0	18.0	18.0
1,000	18.3	18.5	18.40	18.0	18.0	18.0

Table B17 Values of CP and PP of diesel fuel using Flozol 2251D as PPDs.

Conc. (ppm)	CP (°C)			PP (°C)		
	1	2	CP_{ave}	1	2	PP_{ave}
0	4.9	4.9	4.90	-3.0	-3.0	-3.0
2,000	5.9	5.9	5.90	-3.0	-3.0	-3.0
10,000	18.6	18.8	18.70	-2.0	-2.0	-2.0

Table B18 Values of CP and PP of IMME using Flozol 112 as PPDs.

Conc. (ppm)	**CP (°C)**			**PP (°C)**		
	1	2	CP_{ave}	1	2	PP_{ave}
0	3.4	3.4	3.40	-2.0	-2.0	-2.0
100	5.8	5.7	5.75	-2.0	-2.0	-2.0
300	5.5	5.4	5.45	-2.0	-2.0	-2.0
500	5.1	5.2	5.15	-2.0	-2.0	-2.0
800	4.8	5.0	4.90	-2.0	-2.0	-2.0
1,000	4.7	4.7	4.70	-2.0	-2.0	-2.0
2,000	5.0	5.3	5.15	-2.0	-2.0	-2.0

Table B19 Values of CP and PP of PME using Flozol 112 as PPDs.

Conc. (ppm)	**CP (°C)**			**PP (°C)**		
	1	2	CP_{ave}	1	2	PP_{ave}
0	18.3	18.3	18.30	18.0	18.0	18.0
100	18.6	18.8	18.70	18.0	18.0	18.0
300	19.0	18.9	18.95	18.0	18.0	18.0
500	19.3	19.4	19.35	18.0	18.0	18.0
800	19.6	19.9	19.75	18.0	18.0	18.0
1,000	20.1	20.0	20.05	18.0	18.0	18.0

Table B20 Values of CP and PP of diesel fuel using Flozol 112 as PPDs.

Conc. (ppm)	**CP (°C)**			**PP (°C)**		
	1	2	CP_{ave}	1	2	PP_{ave}
0	4.9	4.9	4.90	-3.0	-3.0	-3.0
2,000	5.6	5.8	5.70	-3.0	-3.0	-3.0
10,000	18.9	18.9	18.90	-1.0	-1.0	-1.0

Table B21 Values of CP and PP of IMME using kerosene as PPDs.

Conc. (ppm)	**CP (°C)**			**PP (°C)**		
	1	2	CP_{ave}	1	2	PP_{ave}
0	3.4	3.4	3.40	-2.0	-2.0	-2.0
5,000	3.4	3.2	3.30	-2.0	-2.0	-2.0
10,000	3.0	2.7	2.85	-2.0	-2.0	-2.0
50,000	2.6	2.4	2.50	-3.0	-3.0	-3.0
80,000	2.0	2.3	2.15	-3.0	-3.0	-3.0
100,000	1.9	1.6	1.75	-3.0	-3.0	-3.0
200,000	1.4	1.1	1.25	-6.0	-6.0	-6.0
300,000	0.9	0.6	0.75	-8.0	-8.0	-8.0
400,000	0.2	-0.1	0.05	-11.0	-11.0	-11.0
500,000	-0.7	-0.4	-0.55	-15.0	-15.0	-15.0

Table B22 Values of CP and PP of PME using kerosene as PPDs.

Conc. (ppm)	**CP (°C)**			**PP (°C)**		
	1	2	CP_{ave}	1	2	PP_{ave}
0	18.3	18.3	18.30	18.0	18.0	18.0
5,000	18.2	18.3	18.25	18.0	18.0	18.0
10,000	18.2	18.1	18.15	18.0	18.0	18.0
50,000	18.1	18.1	18.10	18.0	18.0	18.0
80,000	17.0	17.2	17.10	17.0	17.0	17.0
100,000	16.2	16.4	16.30	16.0	16.0	16.0
200,000	13.1	12.8	12.95	13.0	13.0	13.0
300,000	10.5	10.8	10.65	11.0	11.0	11.0
400,000	8.3	8.2	8.25	8.0	8.0	8.0
500,000	4.9	4.6	4.75	5.0	5.0	5.0

APPENDIX C

CALCULATIONS

1. Calculated % ester content of IMME from GC

The % ester content of methyl ester of IM oil (IMME) was calculated as follow:

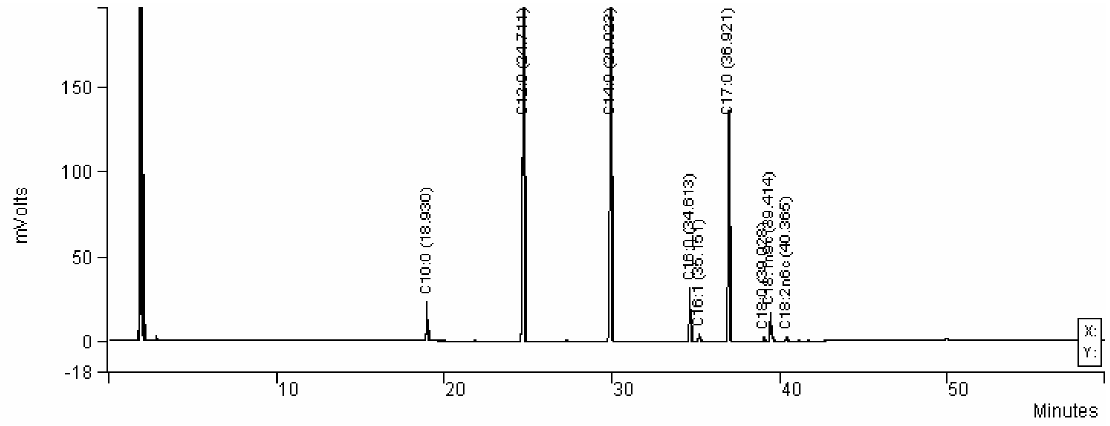

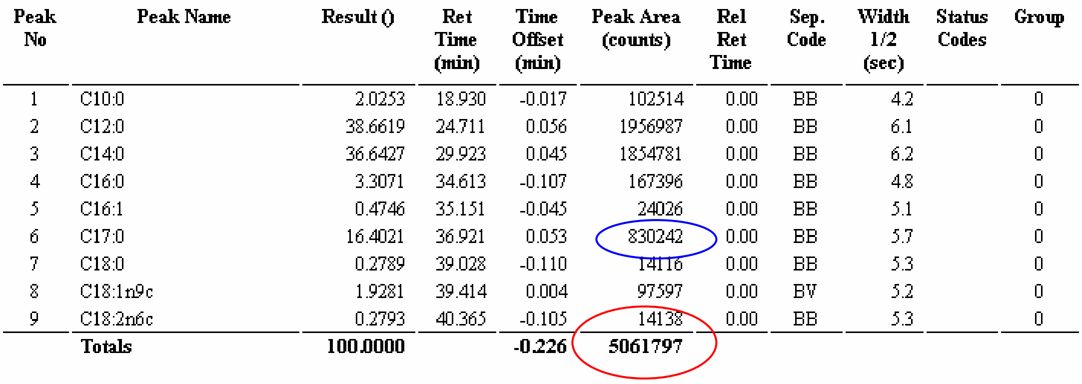

Peak No	Peak Name	Result ()	Ret Time (min)	Time Offset (min)	Peak Area (counts)	Rel Ret Time	Sep. Code	Width 1/2 (sec)	Status Codes	Group
1	C10:0	2.0253	18.930	-0.017	102514	0.00	BB	4.2		0
2	C12:0	38.6619	24.711	0.056	1956987	0.00	BB	6.1		0
3	C14:0	36.6427	29.923	0.045	1854781	0.00	BB	6.2		0
4	C16:0	3.3071	34.613	-0.107	167396	0.00	BB	4.8		0
5	C16:1	0.4746	35.151	-0.045	24026	0.00	BB	5.1		0
6	C17:0	16.4021	36.921	0.053	830242	0.00	BB	5.7		0
7	C18:0	0.2789	39.028	-0.110	14116	0.00	BB	5.3		0
8	C18:1n9c	1.9281	39.414	0.004	97597	0.00	BV	5.2		0
9	C18:2n6c	0.2793	40.365	-0.105	14138	0.00	BB	5.3		0
	Totals	**100.0000**		**-0.226**	**5061797**					

$$C = \frac{(\sum A - Ai)}{Ai} \times \frac{(Ci \times Vi)}{m} \times 100$$

C = Methyl ester content

$\sum A$ = Total area of fatty acid methyl esters

Ai = Area of methyl heptadecanoate

Ci = Concentration of methyl heptadecanoate solution

Vi = Volume of methyl heptadecanoate solution

m = Mass of the sample

$$\text{C of IMME} = \frac{(5061797 - 830242)}{830242} \times \frac{(10.026 \times 5)}{265.80} \times 100$$

$$= 96.13\%$$

2. % precision from GC

Methyl sterate (250 mg) was dissolved in heptadecanoic solution (5 ml) (500 mg heptadecanoate dissolved in heptane (50 ml)) and 1 µl of solution was injected in to GC using 1:100 split ratios. The GC condition for the determination of methyl ester was set as 3.2.2.4. Methyl heptadecanoate was used as an internal standard. The methyl ester content of biodiesel was calculated by the following equation:

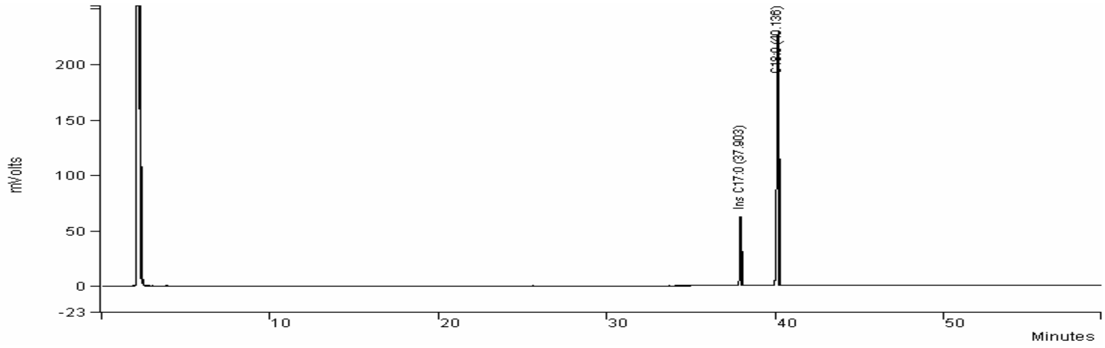

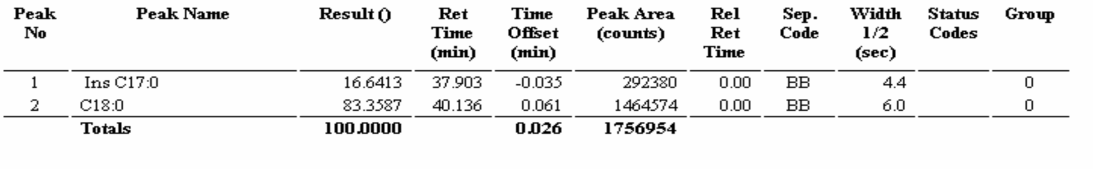

Peak No	Peak Name	Result ()	Ret Time (min)	Time Offset (min)	Peak Area (counts)	Rel Ret Time	Sep. Code	Width 1/2 (sec)	Status Codes	Group
1	Ins C17:0	16.6413	37.903	-0.035	292380	0.00	BB	4.4		0
2	C18:0	83.3587	40.136	0.061	1464574	0.00	BB	6.0		0
	Totals	**100.0000**		**0.026**	**1756954**					

$$\text{C of Methyl Stearate} = \frac{(\sum A - Ai)}{Ai} \times \frac{(Ci \times Vi)}{m} \times 100$$

$$= \frac{(1756954-292380)}{292380} \times \frac{(10.0346 \times 5)}{254.45} \times 100$$

$$= 98.77\ \%$$

$$\%\ \text{precision} = 98.77 \times \text{purity of C18 } (99.5\%)$$

$$= 99.26\ \%$$

3. Calculated % ester content of IMME from ^{1}H-NMR spectrum

The % ester content of methyl ester of IM oil (IMME) was calculated as follow:

$$\boxed{\%\ \text{Ester content} = [(2I_{OCH3}) / (3I_{CH2})] \times 100}$$

I_{OCH3} = Integration value of the protons of the methyl esters, appear at δ 3.7 ppm

I_{CH2} = Integration value of the methylene protons, appear at δ 2.3 ppm

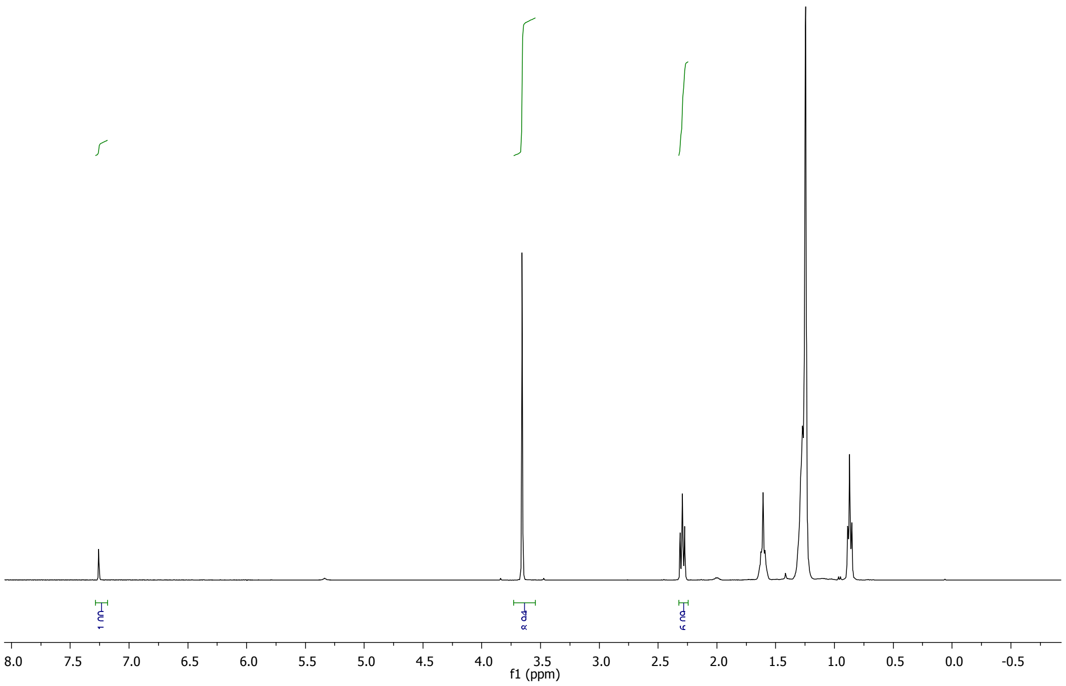

$$\%\ \text{Ester content of IMME} = [(2 \times 8.94) / (3 \times 6.09)] \times 100$$

$$= 97.87\ \%$$

4. Calculated % conversion of PPDs from ^{1}H-NMR spectrum

4.1 The % conversion of ML and MS were calculated as follow:

$$\boxed{\%\ \text{Conversion} = [(2I_{OCH3}) / (3I_{CH2})] \times 100}$$

I_{OCH3} = Integration value of the protons of the methyl esters, appear at δ 3.7 ppm

I_{CH2} = Integration value of the methylene protons, appear at δ 2.3 ppm

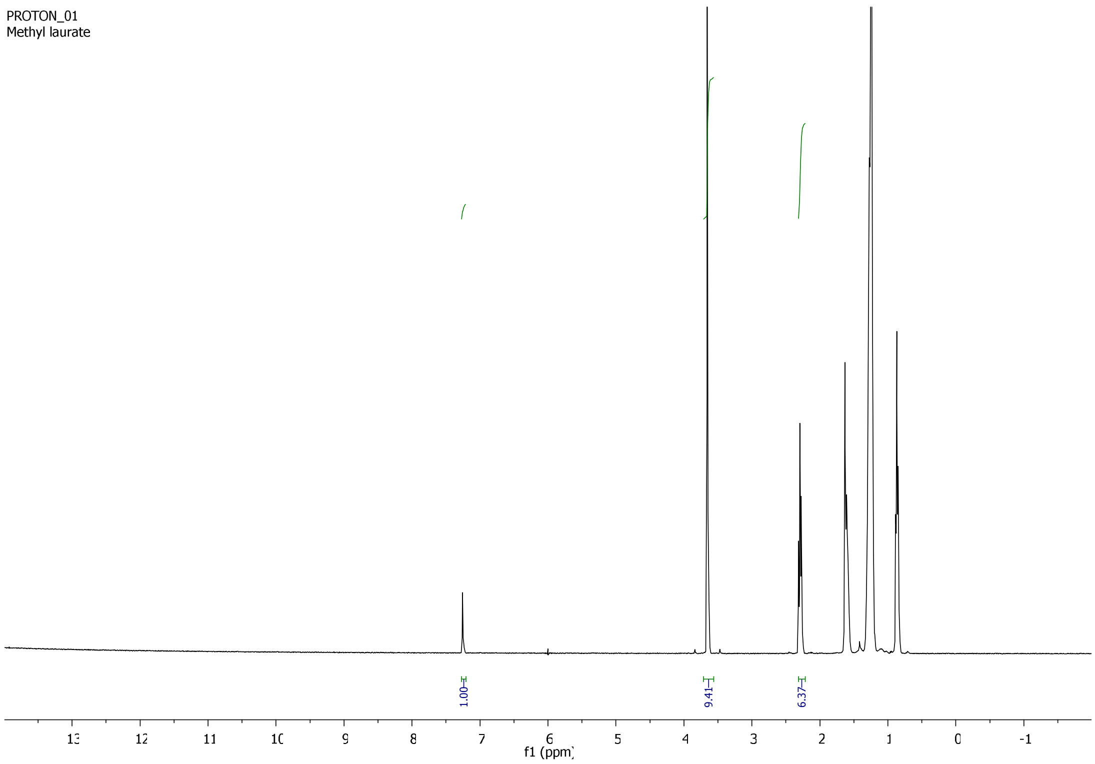

% Conversion of ML = [(2 × 9.41) / (3 × 6.37)] × 100

= 98.48 %

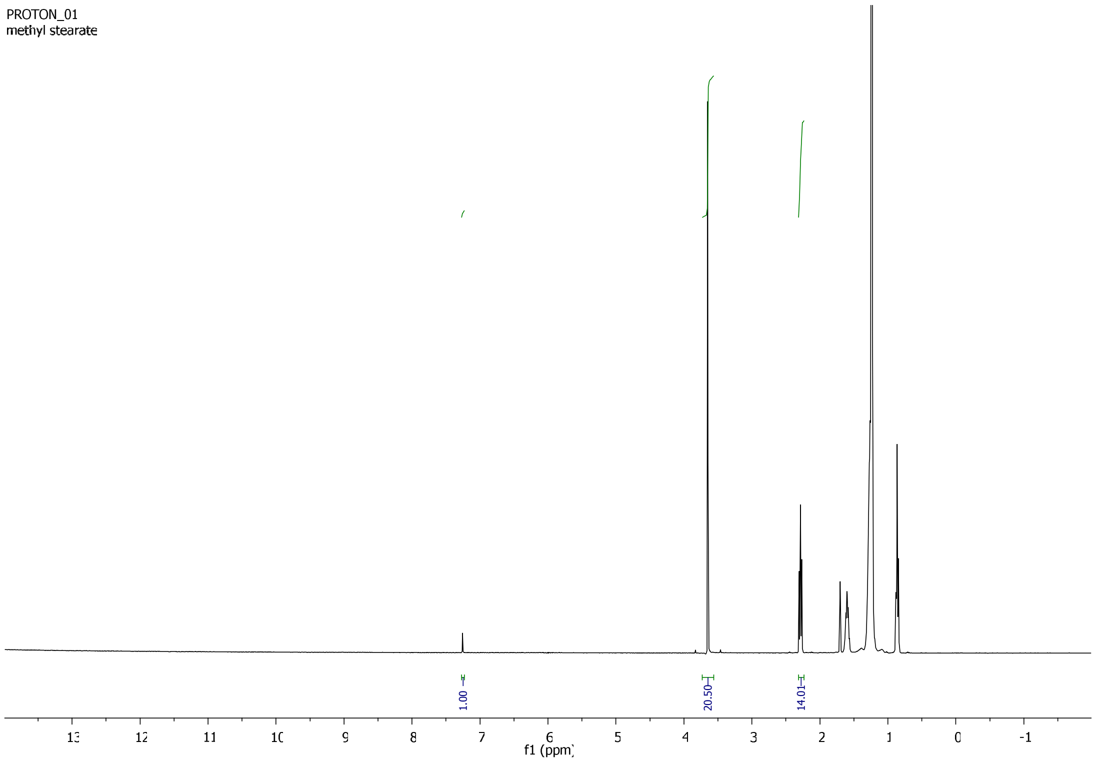

% Conversion of MS = [(2 × 20.50) / (3 × 14.01)] × 100

= 97.55 %

4.2 The % conversion of IPL and IPS were calculated as follow:

$$\boxed{\%\ \text{Conversion} \quad = \quad [(2I_{O\underline{CH}(CH3)2} / I_{CH2}] \times 100}$$

$I_{O\underline{CH}(CH3)2}$ = Integration value of the protons of the *i*-propyl esters, appear at δ 5.0 ppm

I_{CH2} = Integration value of the methylene protons, appear at δ 2.3 ppm

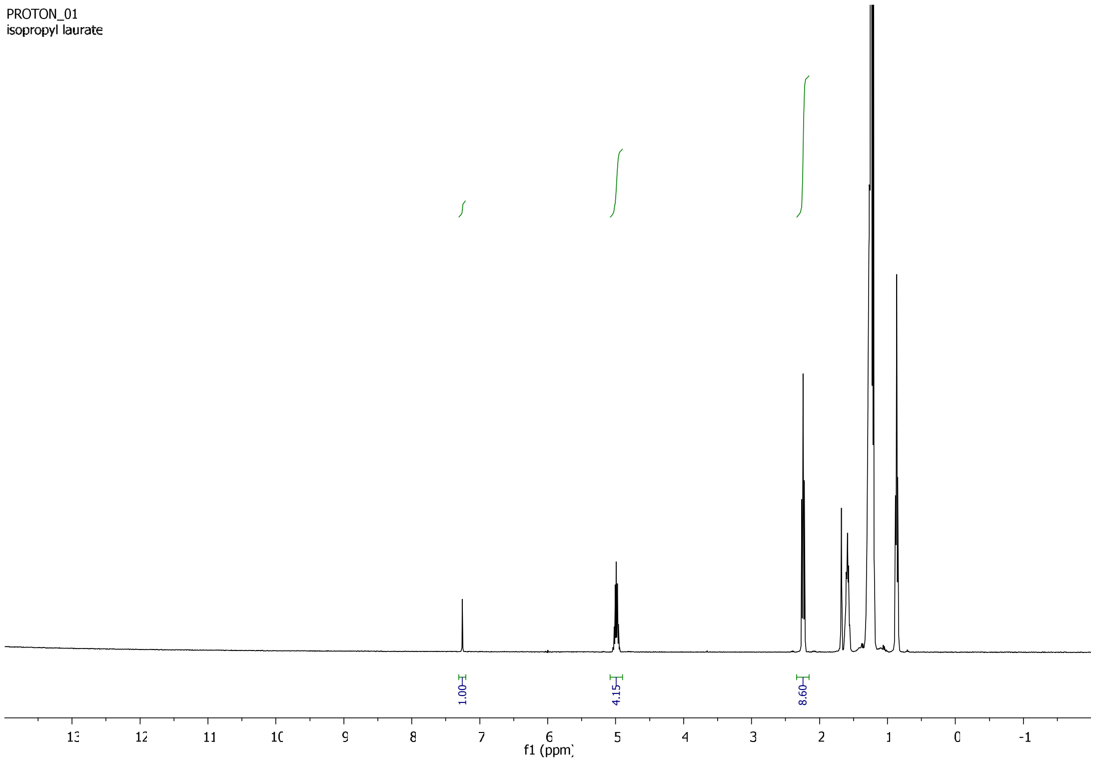

% Conversion of IPL = [(2 × 4.15) / (1 × 8.60)] × 100

= 96.51 %

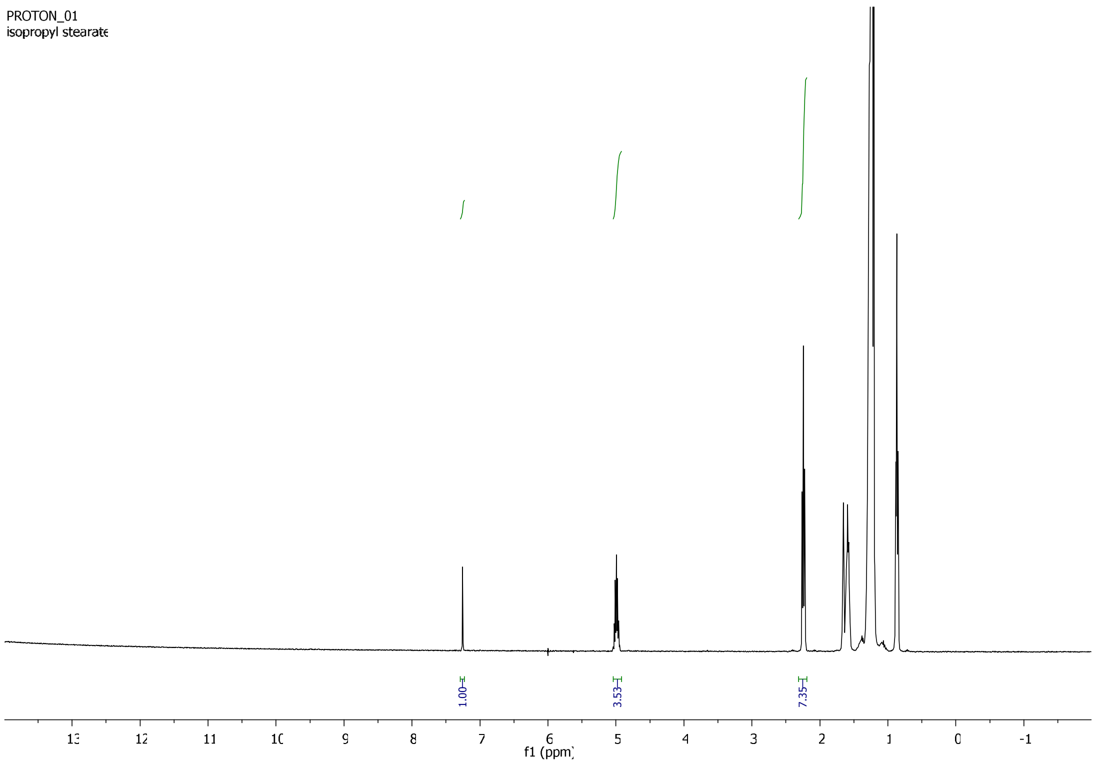

% Conversion of IPS = [(2 × 3.53) / (1 × 7.35)] × 100

= 96.05 %

5. Determine the % free fatty acid (ASTM D5555)

Reagent

1. Ethanol
2. Phenolphthalein
3. 0.25 N NaOH

To the 250 ml of Erlenmeyer flask, oil sample (1 g), ethanol (75 ml) and 2ml of 1% phenolphthalein were added. The mixture was subject to titrate with 0.25 N sodium hydroxide solutions until the pink color was occurred. The ml of alkali solution used was recorded.

The percentage of free fatty acid (FFA) was calculated as follows:

% FFA = (ml of alkali x N x 28.2) / weight of sample
N = normality of alkaline solution
ml of alkali = ml of sodium hydroxide solution

Table C1 Value of free fatty acid containing in IM oil

Sample	Weight of sample (g)	Volume of titrant (ml)	Concentration of NaOH (N)	% FFA
IM oil	1.0311	0.40	0.2273	2.49
	1.0295	0.40	0.2273	

6. Determination of the Saponification number (ASTM D5558)

<u>Reagent</u>

1. Phenolphthalein
2. Alcoholic KOH solution
3. 0.5 N HCl

To the 250 ml of Erlenmeyer flask, oil sample (1 g), alcoholic potassium hydroxide (25 ml) and 1 ml of 1% phenolphthalein were added. The mixture was subject to titrate with 0.5 N of hydrochloric acid until the pink color has disappeared. Prepare a blank determination and carried out same with the sample. The ml of acid solution used was recorded.

The saponification number (SN) was calculated as follows:

SN = $56.1 \times N \times (A - B)$ / weight of sample
A = titration of blank
B = titration of sample
N = normality of hydrochloric acid solution
Alcoholic KOH = 40 g of potassium hydroxide
dissolved in 1 L of ethanol

Table C2 Saponification number of IM oil

Sample	Weight of sample (g)	Volume of titrant (ml)	Volume of blank (ml)	SN
IM oil	1.0233	24.10	32.80	237.92 [a]
	1.0179	24.10	32.80	

Remark : a = 0.4975 N

7. Determination of the Iodine value (ASTM D5554)

Reagent

1. KOH solution
2. Wijs solution
3. CCl_4
4. 0.1 N $Na_2S_2O_3$
5. Starch

To the 500 ml of Glass-Stopper flask, oil sample (0.1 g), carbon tetra chloride (20 ml) and Wijs solution (25 ml) were added. Store the flasks in a dark place for 30 min. From storage, removed the flasks and add 20 ml of KI solution followed by 100 ml of distilled water. The mixture was subject to titrate with 0.1 N of sodium thiosulfate until the yellow color has almost disappeared, add 2 ml of starch indicator solution, and continued the titration until the blue color has just disappeared. Prepare a blank determination and carried out same with the sample. The ml of sodium thiosulfate used was recorded.

The iodine value (IV) was calculated as follows:

Iodine value = $(B - S) \times N \times 12.69$ / weight of sample
B = titration of blank
S = titration of sample
N = normality of $Na_2S_2O_3$ solution

Table C3 Iodine value of IM oil

Sample	Weight of sample (g)	Volume of titrant (ml)	Volume of blank (ml)	IV
IM oil	0.1002	47.00	47.40	5.22[a]
	0.1010	47.00	47.40	

Remark : a = 0.1035 N

8. Determination of the acid value (ASTM D974)

Reagent

1. p-naphtholbenzein indicator solution
2. 0.1 M Alcoholic KOH solution
3. Titration solvent (250 ml toluene + 250 ml isopropyl alcohol)

To the 250 ml of Erlenmeyer flask, oil sample (2 g), titration solvent (25 ml) and 0.125 ml of 1% p-naphtholbenzein indicator solution were added. The mixture was subject to titrate with 0.1 M of alcoholic KOH until the green color was occured. Prepare a blank determination and carried out same with the sample. The ml of acid solution used was recorded.

The acid value was calculated as follows:

Acid value = $[(A - B) \times N \times 56.1]$ / weight of sample
A = titration of sample
B = titration of blank
N = normality of alcoholic KOH solution
Alcoholic KOH = 0.6 g of potassium hydroxide
dissolved in 100 ml of isopropyl alcohol

Table C4 Acid values of IMME, PME and PPDs

Sample	Weight of sample (g)	Volume of titrant (ml)	Volume of blank (ml)	AV
IMME	2.0030	0.10	0.05	0.14 [a]
	2.0008	0.10	0.05	
PME	2.0006	0.20	0.05	0.42 [a]
	2.0019	0.20	0.05	
ML	2.0015	0.05	0.05	0.00 [a]
	2.0022	0.05	0.05	
MS	2.0006	0.05	0.05	0.00 [a]
	2.0011	0.05	0.05	
IPL	2.0019	0.05	0.05	0.00 [a]
	2.0007	0.05	0.05	
IPS	2.0018	0.05	0.05	0.00 [a]
	2.0032	0.05	0.05	

Remark : a = 0.1035 N

VITA

Miss Doungkamol Panlek was born on October 14, 1985 in Lopburi, Thailand. She graduated at Pibul Witthayalai School in 2003. She received the Bachelor Degree of Engineering in Petrochemicals and Polymeric Materials, Silpakorn University in 2007. She continued her Master study in Program of Petrochemistry and Polymer Science, Faculty of Science, Chulalongkom University in 2007 and completed the program in 2010.

Conference

26-27 August 2010 “Improving cold flow property of biodiesel from *Irvingia malayana* Oliv. ex A. Benn. seeds”

GMSTEC 2010: International Conference for a Sustainable Greater Mekong Subregion

King Mongkut’s University of Technology Thonburi